



УДК 57.072

THE OSTEOLOGY OF *AZHDARCHO LANCICOLLIS* NESSOV, 1984 (PTEROSAURIA, AZHDARCHIDAE) FROM THE LATE CRETACEOUS OF UZBEKISTAN

A.O. Averianov

Zoological Institute of the Russian Academy of Sciences, Universitetskaya Emb. 1, 199034 Saint Petersburg, Russia;
e-mail: lepus@zin.ru

ABSTRACT

The osteology of the azhdarchid pterosaur *Azhdarcho lancicollis* Nesso, 1984 from the Late Cretaceous (Turonian) of Uzbekistan is described in detail based on more than 200 bone fragments representing several skull bones, cervical and dorsal vertebrae, pectoral girdle, and limb bones. *Azhdarcho lancicollis* is characterized by relatively short dentary symphysis and hyperelongated middle cervical vertebrae. The relative length of the cervicals is expressed by the formula $I+II < III < IV < V > VI > VII > VIII > IX$. The osteology in all azhdarchids is remarkable uniform but *Azhdarcho* can be distinguished from all other known azhdarchid genera. The phylogenetic analysis showed that the Turonian *Azhdarcho* and the Santonian *Bakonydraco* occupy a phylogenetic position basal to the Campanian *Zhejiangopterus* and the Maastrichtian *Quetzalcoatlus*.

Key words: Azhdarchidae, *Azhdarcho*, Late Cretaceous, osteology, Pterosauria, Uzbekistan

ОСТЕОЛОГИЯ *AZHDARCHO LANCICOLLIS* NESSOV, 1984 (PTEROSAURIA, AZHDARCHIDAE) ИЗ ПОЗДНЕГО МЕЛА УЗБЕКИСТАНА

А.О. Аверьянов

Зоологический институт Российской академии наук, Университетская наб. 1, 199034 Санкт-Петербург, Россия;
e-mail: lepus@zin.ru

РЕЗЮМЕ

Детально описана остеология аждархидного птерозавра *Azhdarcho lancicollis* Nesso, 1984 из позднего мела (турон) Узбекистана на основе более 200 костных фрагментов различных костей черепа, шейных и грудных позвонков, костей плечевого пояса и конечностей. *Azhdarcho lancicollis* характеризуется сравнительно коротким симфизом зубных костей и сильно удлинёнными средними шейными позвонками. Относительная длина шейных позвонков выражается формулой $I+II < III < IV < V > VI > VII > VIII > IX$. Остеология всех аждархид удивительно однообразна, однако *Azhdarcho* можно отличить по некоторым остеологическим признакам от других родов семейства. По результатам филогенетического анализа туронский *Azhdarcho* и сантонский *Bakonydraco* являются более базальными таксонами относительно кампанского *Zhejiangopterus* и маастрихтского *Quetzalcoatlus*.

Ключевые слова: Azhdarchidae, *Azhdarcho*, поздний мел, остеология, Pterosauria, Узбекистан

INTRODUCTION

Azhdarchidae is a group of Cretaceous pterosaurs that included the largest known flying creatures with wing span reaching at least 10 m and possibly 12 m (Witton and Naish 2008). Azhdarchidae had a world-wide distribution and was the last group of pterosaurs surviving until the Maastrichtian. Mostly because of the enormous size of some azhdarchids this group is familiar to the general public with the Maastrichtian *Quetzalcoatlus* from North America being one of the most famous extinct animals. In spite of this public interest to azhdarchids, the scientific knowledge of this group is limited. The first fossils referable to Azhdarchidae, including lower jaw and humerus fragments, were described in XIX century from the Campanian of Austria and attributed to *Ornithocheirus bunzeli* Seeley, 1881 (Bunzel 1871; Seeley 1881; Wellnhofer 1980). A rather complete humerus and other wing elements from the Turonian of Czech Republic described as *Cretornis hlavaci* Fritsch, 1881 may also belong to an azhdarchid (Fritsch 1881, 1883, 1905). Some pterosaur bones found in XIX century in the Albian Cambridge Greensand of England were attributed to Azhdarchidae by Nesson (1991a), but this group is not currently listed for the pterosaur fauna of this locality (Unwin 2001; Barrett et al. 2008).

The first cervical vertebra fragment of an azhdarchid was found in 1911 by Russian geologist Khimenkov in the Campanian of Penza Province of Central Russia and later described as *Ornithostoma orientalis* Bogolubov, 1914 (Nesson and Yarkov 1989; Averianov 2008). The next discovery was an incomplete giant cervical vertebra exceeding 50 cm in length from the Maastrichtian of Jordan described by Arambourg (1954, 1959). The morphology of this vertebra was so unusual that Arambourg mistook it for the wing metacarpal bone. The animal was described as *Titanopteryx philadelphiae* Arambourg, 1959 but the generic name was found to be preoccupied and later replaced by *Arambourgiania* Nesson in Nesson et Yarkov, 1989. A similar long vertebra from the Maastrichtian of Wyoming, USA, was figured by Estes (1964: fig. 70), but still was not recognized as a cervical vertebra.

The next described azhdarchid taxon was *Quetzalcoatlus northropi* Lawson, 1975b from the Maastrichtian Texas, USA. Lawson (1975a) reported on three partial pterosaur skeletons, the large specimen with estimated wing-span of 15.5 m (~10 m in more recent

estimate; Witton and Naish 2008), and two smaller specimens about half the size of the former. Both forms were found in different localities separated by 40 km but was believed to represent the same species by Lawson. The large specimen included only articulated wing skeleton while the smaller specimens contained also elongated cervical vertebrae similar to those of "*Titanopteryx*." The name *Quetzalcoatlus northropi* appeared in a subsequent publication (Lawson 1975b) and was based on the large specimen. The smaller form is now considered as a separate taxon designated as *Quetzalcoatlus* sp. (Kellner and Langston 1996).

A distinct group of Late Cretaceous pterosaurs with hyperelongated middle cervical vertebrae, including *Quetzalcoatlus* and "*Titanopteryx*," was almost simultaneously recognized by Nesson (1984) and Padian (1984, 1986). *Azhdarcho* Nesson, 1984 from the Turonian of Uzbekistan becomes the type genus for this group, the family Azhdarchidae. The original material of *Azhdarcho lancicollis* Nesson, 1984 included fragmented jaws, cervical vertebrae, notarium, radius, and femur. Some more specimens of *A. lancicollis* were figured but not described in subsequent publications (Nesson 1986, 1988, 1995, 1997; Bakhurina and Unwin 1995; Unwin and Bakhurina 2000; Averianov and Atabekyan 2005).

Now azhdarchid pterosaurs are known from the Aptian of Brazil, Albian of Oregon and Texas (USA), Cenomanian of Uzbekistan and Morocco, Turonian of Uzbekistan, Kazakhstan, Armenia, and Czech Republic, Turonian – Santonian of Mongolia, Santonian of Tajikistan and Hungary, Santonian – Campanian of Kazakhstan, Campanian of China, Japan, Russia, Austria, Spain, Montana and Delaware (USA), and Alberta (Canada), Campanian – Maastrichtian of France, Senegal, and New Zealand, Maastrichtian of Jordan, Rumania, France, Spain, Morocco, Texas, Wyoming and Montana (USA), and Australia (Bunzel 1871; Seeley 1881; Fritsch 1883, 1905; Bogolubov 1914; Gilmore 1928; Arambourg 1954, 1959; Estes 1964; Russell 1972; Lawson 1975a, b; Wellnhofer 1980; Baird and Galton 1981; Langston 1981; Currie and Russell 1982; Monteillet et al. 1982; Nesson 1984, 1990, 1991a–c, 1997; Padian 1984; Wiffen and Molnar 1988; Nesson and Yarkov 1989; Bennett and Long 1991; Murry et al. 1991; Padian and Smith 1992; Cai and Wei 1994; Bakhurina and Unwin 1995; Currie and Jacobsen 1995; Padian et al. 1995; Chitoku 1996; Frey and Martill 1996; Kellner and Langston 1996; Buffetaut et al. 1997, 2002, 2003; Steel et al. 1997; Unwin

and Lü 1997; Unwin et al. 1997; Martill et al. 1998; Buffetaut 1999, 2001; Company et al. 1999; Martill and Frey 1999; Wellnhofer and Buffetaut 1999; Ikegami et al. 2000; Unwin and Bakhurina 2000; McGowen et al. 2002; Pereda Suberbiola et al. 2003; Averianov 2004, 2007, 2008; Averianov and Atabekyan 2005; Averianov et al. 2005, 2008; Godfrey and Currie 2005; Ősi et al. 2005; Henderson and Peterson 2006; Barrett et al. 2008; Watabe et al. 2009).

Although the list of azhdarchid records presented above is extensive, majority of findings are isolated and fragmented bones. Several more or less complete skeletons are known only for *Zhejiangopterus linhaiensis* Cai et Wei, 1994 from the Campanian of China, but detailed study of these specimens is limited by poor bone preservation (Cai and Wei 1994; Unwin and Lü 1997). The best three dimensional (although somewhat crushed) cranial and postcranial materials known for Azhdarchidae are that for *Quetzalcoatlus* sp. from the Maastrichtian of Texas, USA, but only cranial part of this collection has been described so far (Kellner and Langston 1996). Relatively complete articulated skeletal fragments are known for *Montanazhdarcho minor* Padian et al., 1995 from the Campanian of Montana, USA, and *Phosphatodraco mauritanicus* Pereda Suberbiola et al., 2003 from the Maastrichtian of Morocco (McGowen et al. 2002; Pereda Suberbiola et al. 2003). An extensive collection of well preserved azhdarchid postcranial elements has been accumulated recently from the Campanian of Alberta, Canada (Godfrey and Currie 2005). Another important collection is fragmentary but exceptionally well preserved bones of *Azhdarcho lancicollis* from the Turonian of Uzbekistan. Majority of postcranial elements are represented there but cranial materials are scarce. The part of this collection gathered by Nessov in 1977–1994 was the basis of his study of azhdarchid morphology, systematics, palaeoecology, and taphonomy (Nessov 1984, 1990, 1991a–c). This collection was significantly enriched by a joint Uzbek-Russian-British-American-Canadian expedition (URBAC) worked in Uzbekistan in 1997–2006 (Archibald et al. 1998). Now the collection includes more than two hundred registered specimens and several hundreds uncatalogued bone fragments. The aim of this study is to present a detailed osteological description of all skeletal elements referable to *A. lancicollis*.

Measurements. Vertebrae: ACH, anterior height of centrum (with hypapophysis); ACW, anterior

width of centrum; ANW, anterior width of neural arch (between lateral margins of prezygapophyses); CL, centrum length; PCH, posterior height of centrum; PCW, posterior centrum width; PNW, posterior width of neural arch (between lateral margins of postzygapophyses).

Limb bones: L, length; PW, maximum width of proximal end; DW, maximum width of distal end. All measurements are in mm.

Institutional abbreviations. CCMGE, Chernyshev's Central Museum of Geological Exploration, Saint Petersburg, Russia; ZIN PH, Paleoherpological Collection, Zoological Institute of the Russian Academy of Sciences, Saint Petersburg, Russia; ZIN PO, Paleornithological Collection, Zoological Institute of the Russian Academy of Sciences, Saint Petersburg, Russia.

Locality indexes. CBI, Central [Kyzylkum Desert], Bissekty Formation, locality index used by Nessov for localities within the middle and upper parts of the Bissekty Formation. CDZH, Central [Kyzylkum Desert], Dzharakuduk, locality index used by Nessov for localities within the lower part of the Bissekty Formation.

GEOGRAPHIC AND GEOLOGIC SETTING

All specimens attributed to *Azhdarcho lancicollis* come from the type horizon and locality, the Bissekty Formation at Dzharakuduk. The locality consists of about 15 km long escarpment exposed some 100 m of the Cretaceous deposits (Fig. 1). The Dzharakuduk escarpment is situated ~27 km South-West of Mynbulak settlement and ~80 km West of Uchkuduk city in Central Kyzylkum Desert (Navoi Viloyat of Uzbekistan; Fig. 1C). This and more western Itemir escarpments form the northern wall of the Itemir-Dzharakuduk depression (Fig. 1D). At Itemir the older part of the Cretaceous section is exposed (Fig. 1A). At Dzharakuduk the fluvial Bissekty formation is intercalated between the marine strata of Dzheirantui and Aitym formations containing orthostratigraphic taxa of invertebrates. The Cretaceous strata of Itemir-Dzharakuduk depression was studied by Russian geologists who determined the age of what is now Bissekty Formation as late Turonian (Pyatkov et al. 1967), Coniacian – Santonian (Sochava 1968), or late Turonian to Coniacian (Martinson 1969; Nessov 1997; Nessov et al. 1998).

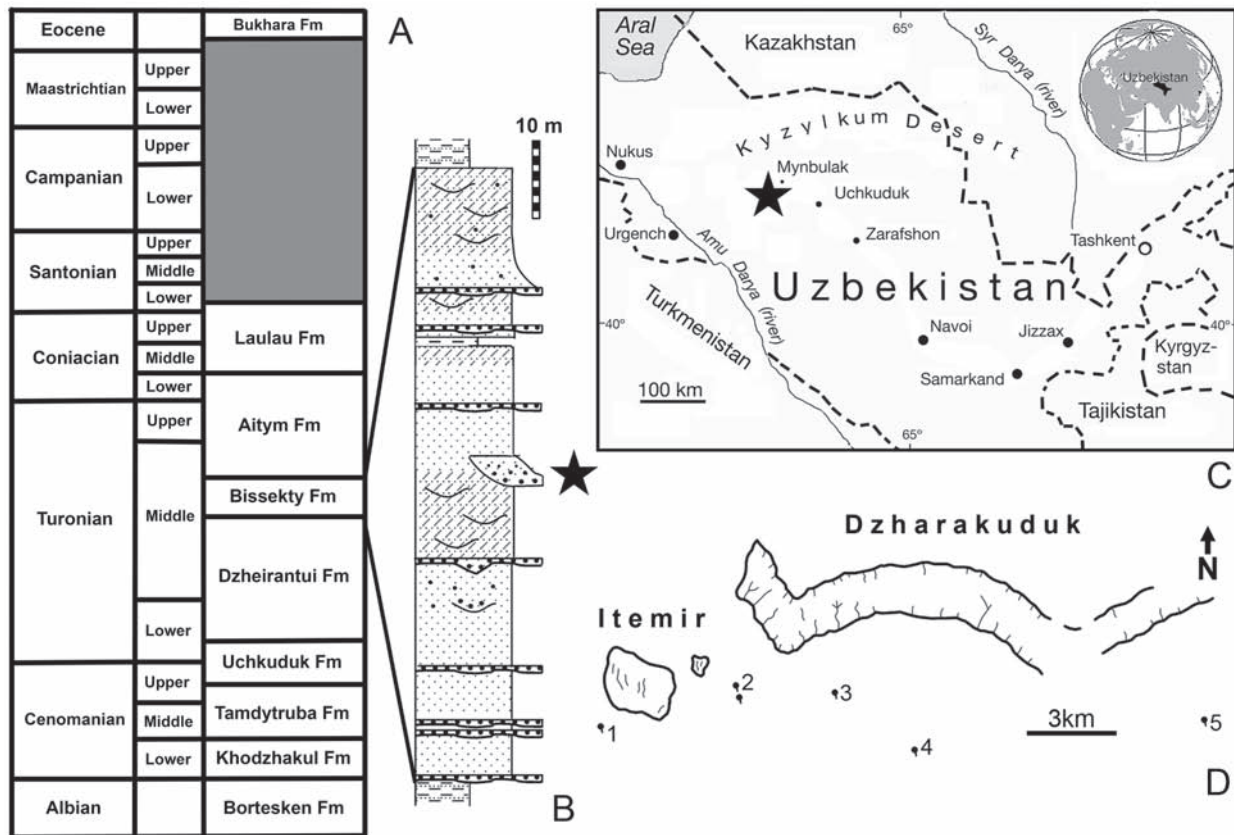


Fig. 1. Stratigraphic and geographic setting for Dzharakuduk locality, Kyzylkum Desert, Uzbekistan. Stratigraphic scheme of the Cretaceous deposits (A) and section of the Bissekty Formation (B) at Itemir-Dzharakuduk depression are modified from unpublished work by C. King and colleagues. Asterisk in B denotes position of the CBI-14 site, one of the most productive for microvertebrates and *Azhdarcho lancicollis* remains. Map of Uzbekistan (C) with the position of the Itemir-Dzharakuduk depression marked by asterisk and sketch of the Itemir-Dzharakuduk escarpments (D) are modified from Averianov and Sues (2007): 1 – Itemir well; 2 – Dzharakuduk wells; 3 – Kul’beke well; 4 – Bissekty well; 5 – Khodzhakhmet well.

A more recent biostratigraphic study of Cretaceous deposits of Kyzylkum Desert was done by members of URBAC expeditions (King, Ward, and Morris, unpublished data; Archibald et al. 1998; Redman and Leighton 2009) who restricted the age of the Bissekty Formation to middle Turonian (Fig. 1A).

Except pterosaurs, Bissekty Formation produced numerous remains of about 80 taxa of various fishes, amphibians, turtles, plesiosaurs, lizards, crocodiles, dinosaurs, birds, and mammals (see reviews in Nessov 1995, 1997; Archibald et al. 1998; Archibald and Averianov 2005). This is arguably one of the most diverse fauna of Cretaceous vertebrates known in the world.

SYSTEMATICS

Pterosauria Kaup, 1834

Azhdarchoidea Nessov, 1984

Azhdarchidae Nessov, 1984

Azhdarcho Nessov, 1984

Azhdarcho Nessov 1984: 48.

Type species. *Azhdarcho lancicollis* Nessov, 1984.

Differential diagnosis. Differs from *Bennettazhia* Nessov, 1991 from the Albian of Oregon, USA, by tapering deltopectoral crest of the humerus. Differs from *Bakonydraco* Ósi et al., 2005 from the Santo-

nian of Hungary by dentary symphysis which is not sinusoid in dorsal profile and lack a median ridge on the triturating surface. Differs from *Aralazhdarcho* Averianov, 2007 from the Santonian – Campanian of Kazakhstan by well developed pneumatic foramina lateral to the neural canal in middle cervical vertebrae and concave ventral surface of the atlas-axis. Differs from *Volgadraco* Averianov et al., 2008 from the Campanian of Central Russia by having shorter mandibular symphysis with more numerous and regular vascular foramina. Differs from *Montanazhdarcho* Padian et al., 1995 from the Campanian of Montana, USA, by lack of a distinct pneumatic foramen on the distal surface of the distal epiphysis of radius and humerus. Differs from *Phosphatodraco* Pereda Suberbiola et al., 2003 from the Maastrichtian of Morocco by proportionally shorter cervical VIII, which is only about 30% of the length of cervical V (more than 50% in *Phosphatodraco*). Differs from *Quetzalcoatlus* Lawson, 1975 from the Maastrichtian of Texas, USA by much shorter rostrum and by having a pneumatic foramen on the anterior side of ulna between the cotyles. Differs from *Arambourgiania* Nessov, 1989 by the cervical V which is less elongated (CL/ANW ratio is 4.2 compared with 6.9 in *Arambourgiania*), has cotyles and condyles wider than high, additional anterior pneumatic foramen dorsal to the neural canal, and rudimentary vertebrocostal sulcus at the anterior end, by the lateral crests do not approaching the crest-like neural spine, and by lack of the prominent ventral crest posterior to the hypapophysis.

Comments. Originally *Azhdarcho* was grouped with *Quetzalcoatlus* and *Arambourgiania* and diagnosed by “neural spine in the middle of tubular cervical vertebrae has the form of a weak crest, which is not approached by the lateral crests” (Nessov 1984: 48). Unwin and Bakhurina (2000: 427) commented that “it is not clear that this feature distinguishes *Azhdarcho* from other pterosaurs ...” However, this character indeed distinguishes *Azhdarcho* from *Arambourgiania* at least. Later, Nessov (1991a: 21) provided a much expanded diagnosis of *Azhdarcho* (ignored in the review by Unwin and Bakhurina [2000]). Some of the characters mentioned in the diagnosis of *Azhdarcho*, according to Nessov (1991), are now found to be common for Azhdarchidae (third pneumatic foramen dorsal to the neural canal in middle cervical vertebrae, proximal pneumatic foramen on ventral side of the humerus, asymmetrical sternocoracoid joint, fourth wing finger phalanx subtriangular in cross-section,

low angle between neck and shaft of the femur, slit-like proximal pneumatic foramen on the femur). The morphology of the ventral end of dorsal ribs with two additional processes is a peculiar character of *Azhdarcho* but dorsal ribs are not known or described for other azhdarchids and this character may have a broader distribution within the group. Nessov (1991) mentioned in the diagnosis a synsacrum consisting of four vertebrae. This is based on misidentification of the specimen actually belonging to a theropod dinosaur (Averianov 2008). The remaining characters cited by Nessov in the diagnosis of *Azhdarcho* are difficult to evaluate because of poor knowledge of other azhdarchid taxa.

Zhejiangopterus from the Campanian of China is represented by several rather complete and articulated skeletons but poor preservation of individual bones precludes its detailed description (Cai and Wei 1994; Unwin and Lü 1997). Differences between *Zhejiangopterus* and *Azhdarcho* are not clear. It is also difficult to compare *Azhdarcho* with *Hatzegopteryx* from the Maastrichtian of Romania (Buffetaut et al. 2002, 2003). The only skeletal elements known for both these taxa are a humerus and quadrate condyle. The humerus of *Hatzegopteryx* is poorly preserved and not particularly diagnostic. The quadrate condyle of *Hatzegopteryx* is markedly different from that structure in *Azhdarcho* and *Quetzalcoatlus* (Kellner and Langston 1996). In *Hatzegopteryx*, the quadrate is described as “helical”, but the lateral and medial condyles are separated by a groove, while in *Pteranodon*, with the helical craniomandibular joint they are separated by a ridge (Wellnhofer 1980; Bennett 2001). Furthermore, in contrast with *Azhdarcho* and *Quetzalcoatlus*, in *Hatzegopteryx* the condyles are rounded, less separated, and oriented not perpendicular to the skull axis. A better knowledge of the cranial anatomy of azhdarchids and other pterosaurs is needed to evaluate these differences.

Nessov (1984: 49) referred to *Azhdarcho* sp. a middle cervical vertebra from the Maastrichtian of Wyoming, USA (Estes 1964: fig. 70). Lawson (1975) noted the close similarity of this specimen with *Quetzalcoatlus*. This specimen cannot be identified beyond Azhdarchidae indet. Nessov (1997: 131) also cited *Azhdarcho* sp. nov. for the Santonian of Tajikistan but it is not clear on what materials this identification has been based. Currently *Azhdarcho* is a monotypic genus.

***Azhdarcho lancicollis* Nessov, 1984**

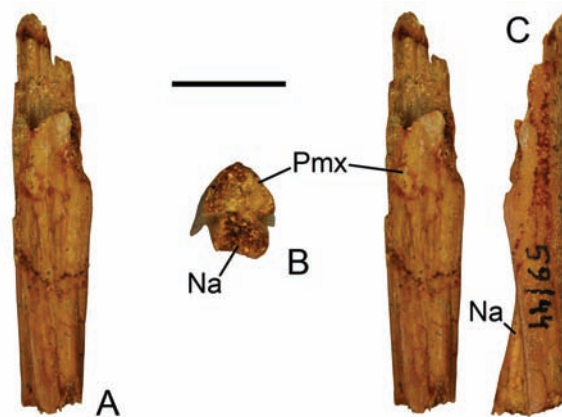
(Figs 2–37)

Azhdarcho imparidens Nessov 1981: 92 [nomen nudum].cf. *Nyctosaurus* [sp.]: Nessov 1981: 92.*Azhdarcho lancicollis* Nessov 1984: 49, pl. 7, figs 1–11; Nessov 1986: pl. 2, fig. 1; Nessov and Yarkov 1989: pl. 2, figs 2–8; Bakhurina and Unwin 1995: fig. 13; Nessov 1995: pl. 1, fig. 18; Nessov 1997: pl. 14, figs 1–13, 15, pl. 15, figs 1–5, 7–12, 14–17, pl. 16, figs 1, 2; Unwin and Bakhurina 2000: fig. 21.8; Averianov and Atabekyan 2005: fig. 2f–j; Averianov 2008: 334, pl. 1, figs 5–7.

Aves indet.: Nessov 1984: pl. 8, fig. 6; Nessov 1988: pl. 1, fig. 1.

Holotype. CCMGE 1/11915, anterior part of the neck vertebra (CBI-17, 1980).**Type locality and horizon.** Dzharakuduk, Central Kyzylkum Desert, Uzbekistan. Bissekty Formation, Late Cretaceous, middle-late Turonian.**Diagnosis.** As for the genus.**DESCRIPTION****Skull fragments****Material.** Fragment of fused premaxillae and nasals: ZIN PH 59/44 (CBI-14, 2004). Quadrate condyle fragments: ZIN PH 184/44, right (CBI-4, 1989); ZIN PH 185/44, left (CBI-5a, 1989); ZIN PH 186/44, left (CBI-14, 1980).**Description.** ZIN PH 59/44 is a fragment of fused premaxillae and nasals that formed the roof of the nasoantorbital fenestra (Fig. 2). No suture between the two bones is recognizable. The fragment is triangular in cross-section. The height of premaxillae and nasals is gradually increasing respectively anteriorly and posteriorly. The minimal height of the fragment is at the anterior end of confluent nasals. Anterior to the nasals, the ventral surface of premaxillae is concave with a distinct median ridge. The ventral edges of premaxillae are very sharp and in posterior part separated from nasals by a groove. The premaxillae are hollow at the anterior end and both bones are filled by a delicate bone tissue at the posterior end. The posterior deepening of the nasals may indicate presence of a nasal process, but this is not certain.

The quadrate condyle is known from three fragmentary specimens among which ZIN PH 184/44 is the most complete (Fig. 3). The lateral wall of the quadrate is a thin plate with flattened lateral surface. The condyle is placed on the transverse bar of the

**Fig. 2.** ZIN PH 59/44, fragment of fused premaxillae and nasals that formed the roof of the nasoantorbital fenestra of *Azhdarcho lancicollis*, in ventral (A, stereopair), posterior (B), and lateral (C) views.*Abbreviations:* Na – nasal; Pmx – premaxilla. Scale bar = 1 cm.bone which is perpendicular to the lateral wall. The width of this bar is rapidly decreasing dorsally and the posterior side of the bar is convex. The lateral and medial condyles are triangular in ventral view. They overlap by about one third of their transverse width. The lateral condyle is somewhat larger, with pointed posterior angle, while the posterior angle in the medial condyle is rounded. The articulation surface of both condyles is slightly concave. The thickened medial edge of the lateral condyle which is oblique to the condyle long axis is corresponding to the oblique median ridge of *Pteranodon* with helical jaw joint (Wellnhofer 1980: fig. 6b; Bennett 2001: fig. 4A). There is a slight transverse groove anterior to the articular surfaces of the condyles. The posterior and lateral surfaces of the fragment are sculptured by short ridges some of which could be scars for muscle attachment. The quadratojugal was likely fused to the quadrate and the vertical ridge on the angle between lateral and posterior sides of the fragment may represent the boundary between two bones.**Comparison.** ZIN PH 59/44 is similar to the roof of nasoantorbital fenestra in *Pteranodon* (Bennett 2001: figs 7, 10). It similarly narrow and have a ventral median ridge as in *Quetzalcoatlus* (Kellner and Langston 2006: figs 2B and 3B, C), but in the latter taxon the anterior end of nasals is at the posterior end of sagittal crest. In *Azhdarcho* either the nasals extend more anteriorly, anterior to the sagittal crest, or the sagittal crest was not present in this region dorsal to the nasoantorbital fenestra.

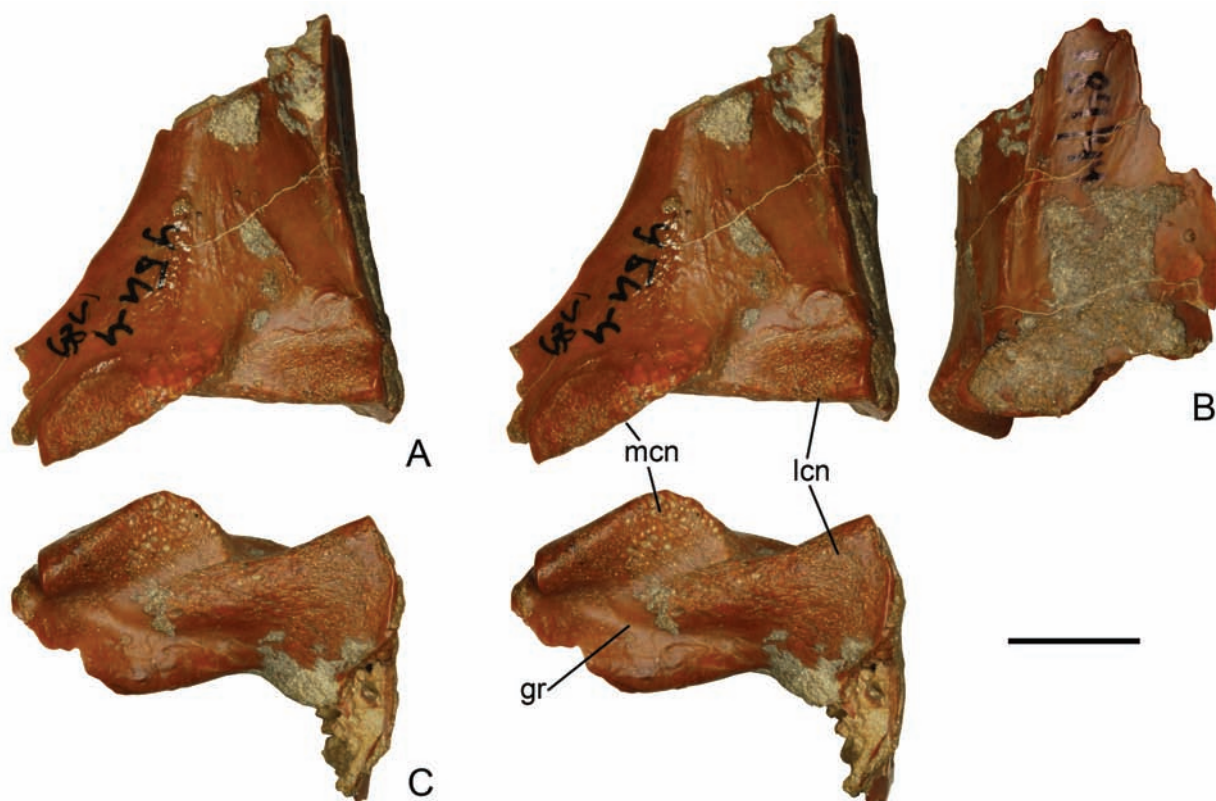


Fig. 3. ZIN PH 184/44, right quadrate condyle of *Azhdarcho lancicollis*, in posterior (A, stereopair), lateral (B), and ventral (C, stereopair) views.

Abbreviations: gr – groove; lcn – lateral condyle; mcn – medial condyle. Scale bar = 1 cm.

The quadrate condyle of *Azhdarcho* is similar to that of *Quetzalcoatlus* in posterior view (Kellner and Langston 2006; fig. 4A), the only view in which quadrate of *Quetzalcoatlus* has been illustrated. However, the description of quadrate condyles provided by Kellner and Langston (1996: 226) is different from what we see in *Azhdarcho*. Without firsthand comparison of the specimens it is not possible to evaluate these differences. For comparison with the quadrate in *Hatzegopteryx* see comments following the generic diagnosis.

Jaw fragments

Material. ZIN PH 112/44 (CBI-16, 1989), fragment of fused maxillae and premaxillae. Anterior premaxillary fragments: ZIN PH 85/44 (CBI-14, 2004); ZIN PH 114/44 (CBI-14, 2004). Anterior dentary fragments: ZIN PO 3471 (CBI-17, 1984); ZIN PH 115/44 (CBI-14, 2004); ZIN PH 116/44 (CBI-5a,

1987). Unidentified rostrum fragments: CCMGE 17/11915 (CBI-17, 1980); CCMGE 18/11915 (CD-ZH-17a, 1980); ZIN PH 113/44 (CBI-14, 2004); ZIN PH 117/44 (CBI-50, 1987); ZIN PH 118/44 (CBI-4, 1987); ZIN PH 119/44 (CBI-14, 1985); ZIN PO 4548 (CBI-14, 1985); ZIN PO 5216 (CBI-14, 1984); ZIN PO 5217 (CBI-14, 1984).

Description. ZIN PH 112/44 is a fragment of fused maxillae and premaxillae anterior to the nasoantorbital fenestra (Fig. 4). It is triangular in cross-section with the dorsal crest becoming narrower posteriorly. The dorsal profile is convex and the posterior end of the fragment is 2.5 times higher than the anterior end. The ventral surface is transversely slightly convex, with sharp lateral edges. The rostrum is tapering anteriorly, with the anterior end 1.7 times narrower than the posterior end of the fragment. The bone surface, where preserved, is smooth. The bone structure is cancellous.

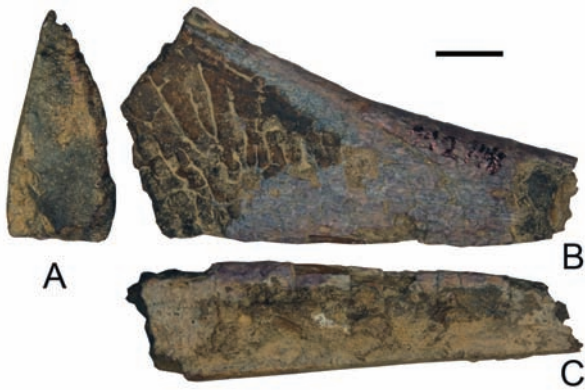


Fig. 4. ZIN PH 112/44, fragment of fused maxillae and premaxillae anterior to the nasoantorbital fenestra of *Azhdarcho lancicollis*, in posterior (A), lateral (B), and ventral (C) views. Scale bar = 1 cm.

Anterior jaw fragments are perhaps the most common remains of *Azhdarcho* in Dzharakuduk. Only more complete or previously catalogued specimens are listed in the material. Some specimens are very tiny, with maximum width ~1.3 mm (ZIN PH 113/44); these may belong to embryonic or recently hatched individuals. Rostra are triangular in cross-section tapering towards the very sharp anterior end. The triturating surface is flat or slightly concave and depressed between the sharp lateral edges. On triturating surface there is a series of parallel slit-like vascular foramina placed close to the lateral edges. In two specimens (ZIN PH 118 and 119/44) there are two lines of small circular foramina at the each lateral edge in posterior part which transforms to typical single line of slit-like foramina in anterior part. A line of three to five slit-like foramina is present on the lateral sides of rostra. In small juvenile specimens anterior of these vascular foramina could be large.

The upper jaw rostra are formed by fused premaxillae (Fig. 5A, B). They have dorsal and ventral profile straight in posterior part, while at the anterior end ventral and dorsal profiles become slightly convex and concave respectively. In this anterior portion of the upper rostrum there is a weak median ridge on the triturating surface. The lower jaw rostrum is formed by fused dentaries and has a shape complementary to that of the upper rostrum: at the anterior end the dorsal profile is slightly concave and the ventral profile is convex (Fig. 5C, D). More posteriorly both profiles are straight. The median ridge is absent. A strong median ridge is present in ZIN PH 117/44, but it is not clear if this upper or lower rostrum fragment.

Comparison. ZIN PH 112/44 is more similar to the anterior rostrum of *Tupuxuara* than *Quetzalcoatlus* (Kellner and Langston 1996: fig. 3B; Witton 2009: fig. 3D) in having concave rather than straight dorsal profile. This might suggest that a relatively high sagittal crest may be present in *Azhdarcho* dorsal to the anterior and of the antorbital fenestra, but possible not dorsal to the posterior end, as evident from the ZIN PH 59/44 described in previous section. A bone fragment from the Cenomanian of Morocco similar to ZIN PH 112/44 has been interpreted as mandibular symphysis and referred to Tapejaridae (Wellnhofer and Buffetaut 1999: fig. 5; Kellner 2004: fig. 6). More likely, this specimen is also the azhdarchid upper jaw fragment.

The rostrum fragment from the Cenomanian of Morocco identified as anterior end of premaxilla of ?Pteranodontidae (Wellnhofer and Buffetaut 1999: fig. 2) is similar in shape and cross-section to the rostrum fragments of *Azhdarcho* and may belong to a member of Azhdarchidae rather than Pteranodontidae. It has double row of vascular foramina on occlusal surface and single row on lateral surface. On the occlusal surface the foramina are confined to the anterior half of the fragment and lack posteriorly. The angle between the occlusal and opposite sides is ~12°, similar to the condition in *Azhdarcho*. Another rostrum fragment from the same locality, interpreted as anterior fragment of premaxilla of ?Azhdarchidae (Wellnhofer and Buffetaut 1999: fig. 4), differs from the rostra of *Azhdarcho* by a more acute angle be-



Fig. 5. Rostrum fragments of *Azhdarcho lancicollis*: A, B – ZIN PH 85/44, premaxillary symphysis, in lateral (A) and ventral (B) views; C, D – ZIN PO 3471, dentary symphysis, in dorsal (C) and lateral (D) views. Scale bar = 1 cm.

tween the occlusal and opposite side ($\sim 8^\circ$), by fewer and less regular vascular foramina, and by wineglass cross-section.

All more or less complete rostrum fragments of *Azhdarcho* are short, suggesting that the rostrum and mandibular symphysis were distinctly shorter than those of *Quetzalcoatlus* and more approximating condition of *Tupuxuara*, *Zhejiangopterus*, or *Bakonydraco* (Kellner and Langston 1996; Unwin and Lü 1997; Ősi et al. 2005; Witton 2009). The dentary symphysis of *Azhdarcho* is generally similar to that of *Bakonydraco* (Ősi et al. 2005: fig. 2), except that in the latter taxon the dorsal profile is sinusoid while in *Azhdarcho* it is gently concave. In *Bakonydraco* also there is a median ridge on the triturating surface of dentary symphysis. In *Azhdarcho* a similar but more anteriorly situated ridge is present on the premaxillary symphysis but not on dentary symphysis. In *Volgadraco* the dentary symphysis is relatively longer and has fewer vascular foramina (Averianov et al. 2008: pl. 5, fig. 1). The rostral vascular foramina are not described and not visible in published illustrations of *Quetzalcoatlus* (Kellner and Langston 1996). It is not clear if these were really absent or not recognizable due to the specific bone preservation in that taxon.

A relatively long rostrum fragment without vascular foramina similar to the rostrum of *Volgadraco* is known from the Campanian of Penza Province, Russia (Averianov 2007: pl. 8, fig. 3).

A jaw fragment with a double row of slit-like vascular foramina on the occlusal surface similar to the specimens of *Azhdarcho* has been described from the Campanian-Maastrichtian of Spain (Buffetaut 1999: fig. 1a).

Mandible fragment

Material. ZIN PH 120/44 (CBI-14), left mandibular fragment with glenoid fossa.

Description. ZIN PH 120/44 is a fragment of completely fused surangular and articular with a partially preserved glenoid fossa (Fig. 6). The lateral margin of the fragment is gently convex. The glenoid fossa extends into a medial bone projection and thus its width is about twice as large as the width of the surangular anterior to this projection. The glenoid fossa is divided by a sharp diagonal ridge into a lateral and medial cotyle. The lateral cotyle is bordered anteriorly by a transverse ridge. Its articular surface is convex and cone-like in dorsal view, with later-

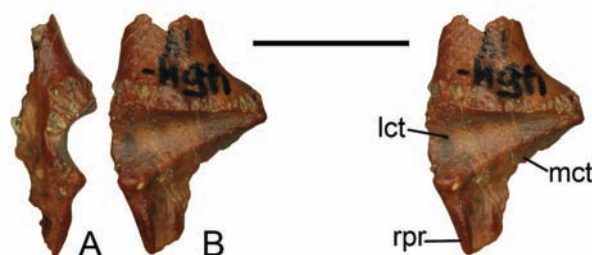


Fig. 6. ZIN PH 120/44, fragment of fused surangular and articular with a mandibular glenoid fossa of *Azhdarcho lancicollis*, in lateral (A) and dorsal (B, stereopair) views.

Abbreviations: lct – lateral cotyle; mct – medial cotyle; rpr – retroarticular process. Scale bar = 1 cm.

ally open base and medially pointed apex. The medial cotyle is only partially preserved. Apparently it was also cone-like and mirrored the lateral condyle having cone apex pointed laterally. On the retroarticular process there is a sharp ridge along the lateral margin.

Comparison. The glenoid fossa separated by a diagonal ridge into lateral and medial cotyles suggests presence in *Azhdarcho* of a helical jaw joint similar to that of *Pteranodon* (Wellnhofer 1980). Compared with the mandible of *Pteranodon* (Wellnhofer 1980: fig. 3c; Bennett 2001: fig. 4B) in ZIN PH 120/44 the medial projection of the glenoid is more developed. The same feature is also characteristic for *Bakonydraco* (Ősi et al. 2005: fig. 2A–D) and *Quetzalcoatlus* (Kellner and Langston 1996: fig. 4C, D). Also in azhdarchids the glenoid fossa seems to be shallower in lateral view compared with other pterodactyls (Kellner and Langston 1996).

Atlas and axis

Material. ZIN PH 105/44 (CBI-4, 1987); ZIN PH 106/44 (CBI-14, 1984); ZIN PH 107/44, neural arch (CBI-14, 1991); ZIN PH 108/44, centrum (CBI-, 2003); ZIN PH 109/44, centrum (CBI-17, 2003); ZIN PH 110/44, centrum (CBI-4v); ZIN PH 111/44, centrum (CBI-14, 1985); CCMGE 3/11915, centrum (CBI-14, 1980).

Description. The atlas-axis complex is known from several fragments and ZIN PH 105/44, a complete beautifully preserved specimen (Fig. 7A–E; ACH = 10.1; ACW = 13.8; CL = 24.7; PCH = 13.5; PCW = 20.1; PNW = 27.5). The atlas and axis are completely fused. The atlas intercentrum forms the spherical cotyle for articulation with the cranial

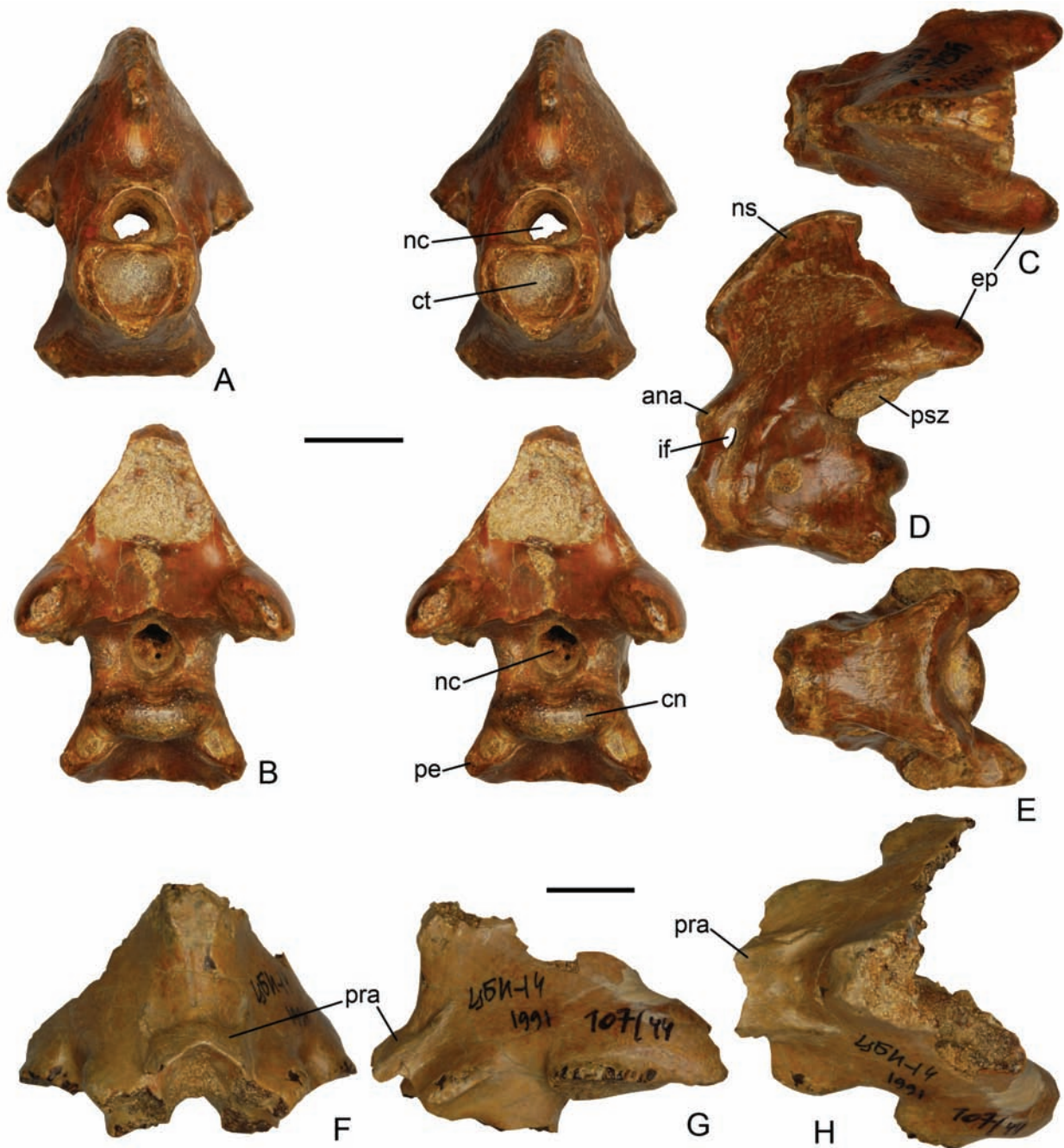


Fig. 7. Atlas-axis complex of *Azhdarcho lancicollis*: A–E – ZIN PH 105/44, atlas-axis, in anterior (A, stereopair), posterior (B, stereopair), dorsal (C), lateral (D), and ventral (E) views; F–H – ZIN PH 107/44, neural arch of atlas-axis with fused proatlas, in anterior (F), lateral (G), and dorsal (H) views.

Abbreviations: ana – atlantal neural arch; cn – condyle; ct – cotyle; ep – epipophysis; if – intervertebral foramen; nc – neural canal; ns – neural spine; pe – postexapophysis; pra – proatlas; psz – postzygapophysis. Scale bars = 1 cm.

condyle. There is a small hypapophysis on the ventral rim of the cotyle. The atlantal neural arch is short and ring-like. It is separated from the axis neural arch by a large oval intervertebral foramen for the spinal nerve. A distinct groove extends ventrally from this foramen demarcating the border between the atlas intercentrum and axis centrum. In a larger specimen ZIN PH 107/44 the proatlas is fused with the atlantal neural arch. It is a thin plate forming the roof of the neural canal (Fig. 7F–H).

The axis centrum is short, with the posterior width greater than the centrum length. The centrum is about 1.5 times wider posteriorly than anteriorly. The ventral and lateral sides of the axis centrum are convex. Approximately at the middle of the lateral side there is a pneumatic foramen. It varies in size, being relatively small in ZIN PH 105/44 and large in ZIN PH 106/44. The dorsoventrally narrow oval condyle is placed at the dorsal margin of the centrum confluent with the floor of the neural canal. The widest point of the postexapophyses is at the midheight of the centrum. The concave postexapophyseal articulation surfaces are laterally attached to the condyle. The posterior surface of the centrum beneath the condyle is about twice higher than the condyle and deeply concave.

The opening of the neural canal is subtriangular anteriorly and round posteriorly. It is relatively small, less in diameter than the cotyle. The neural arch is triangular in anterior/posterior and side views. The highest point of the neural arch is only little posterior to the centrum midline. On anterior side of the neural arch there is a marked incision between the atlantal neural arch and the neural spine. The dorsal surface of the neural arch is concave and slanted anteriorly. It is rugose suggesting powerful muscle attachment. A distinct muscle scar is present also on the lateral surface of the neural arch. At the bottom of the lateral surface of neural arch, between the spinal foramen and the postzygapophysis, there is a marked oblique ridge. A bump-like extension on this ridge is a possible rudiment of diapophysis. The postzygapophyseal articular surfaces are limited to the anterior ends of the postzygapophyses. These surfaces are large, oval, remarkable flat, and facing ventrally and slightly laterally. Posterior to the articular surfaces, the postzygapophyses are extended into relatively long and robust processes (epipophyses) that project posteriorly well beyond the axis centrum. The ends of the epipophyses bear strong sculpture on medial

and ventral sides suggesting muscle attachment. On the dorsal half of the posterior side of the neural arch there is a prominent depression not covered by a compact bone but revealing the cancellous bone structure. This depression was apparently housing a big intervertebral ligament. The posterior surface of the neural arch beneath this depression is separated into two parts by a transverse ridge extending between the posterior ends of the postzygapophyseal articular surfaces. The concave upper surface is facing mostly posteriorly while the flatter lower surface, dorsal to the neural canal, is facing mostly ventrally.

Comparison. The atlas-axis complex of *Azhdarcho* differs from that structure in Burkhant azhdarchid from the Cenomanian-Santonian of Mongolia (Watabe et al. 2009) in different shape of the axis neural arch. In Burkhant azhdarchid the dorsal margin of the axis neural spine is almost horizontal while it is slanted anteriorly in *Azhdarcho*. In the axis from Burkhant there is no anterior incision of the neural arch so that is so prominent in *Azhdarcho*. *Azhdarcho* lacks small foramina on the posterior side of the axis neural arch between the neural canal and postzygapophyses described for the Burkhant specimen (Watabe et al. 2009: fig. 6A). Such foramina are also present in *Pteranodon* (Bennett 2001: figs 34B and 35B), in which they are distinctly larger. The axial epipophyses in *Azhdarcho* are much longer and stronger than in Burkhant azhdarchid. But the most conspicuous difference between the atlas-axis complexes of *Azhdarcho* and Burkhant azhdarchid is the presence of the lateral pneumatic foramen in the former. The lateral pneumatic foramen is present on cervical vertebrae in most pterodactyloids (Howse 1986; Bennett 2001), but it is reduced in azhdarchids. In *Azhdarcho* it is present only in the axis. The absence of the lateral pneumatic foramen in the axis of Burkhant azhdarchid is certainly the derived feature. The atlas-axis is not known or described for other azhdarchids (Watabe et al. 2009).

The atlas and axis are fused in most pterodactyloids, except *Pterodactylus* (Wellnhofer 1970; Bennett et al. 2001). In *Pteranodon* there is no hypapophysis and the shape of neural arch is different, relatively taller and without an incision above the atlas (Bennett 2001: figs 33A and 34). For *Pteranodon* the spinal nerve foramen in atlas-axis complex is not described possible due to inadequate preservation of the specimens. *Pteranodon* is also different from azhdarchids and other pterodactyloids in having the atlantal neu-

ral arch not extending dorsally beyond the level of the floor of the neural canal and not contacting the axis neural arch (Bennett 2001; Watabe et al. 2009).

Bennett (2001: 41) pointed out that in *Azhdarcho* the atlantal neural halves do not meet dorsal to the neural canal. This is apparently not correct if the intervertebral foramen demarcates the border between the atlantal and axial neural arches. The dorsal border of the anterior opening of the neural canal is formed by atlas and also by proatlas in more grown specimens (see above).

In *Aralazhdarcho* the atlas-axis has the convex ventral surface (Averianov 2007: pl. 9, fig. 1), while it is concave in *Azhdarcho*.

Postaxial cervical vertebrae

Material. Cervical III: ZIN PH 131/44 (CBI-14, 2004); ZIN PH 132/44 (CBI-14, 1984); ZIN PH 133/44, anterior fragment (CBI-14, 1987); ZIN PH 134/44, anterior fragment (CBI-4); ZIN PH 135/44, posterior fragment (CBI-4v, 1979); ZIN PH 136/44, neural arch fragment (CBI-, 2006); ZIN PH 172/44, juvenile neural arch (CBI-14). Cervical IV: ZIN PH 144/44 (CBI-, 2003). Cervical V: CCMGE 1/11915, holotype, anterior fragment (CBI-17, 1980); ZIN PH 145/44, anterior fragment (CBI-14, 1984); ZIN PH 139/44, posterior fragment (CBI-41, 1984); ZIN PH 140/44, posterior fragment (CBI-5, 2006); ZIN PH 142/44, posterior fragment (CBI-41, 1985); ZIN PH 143/44, posterior fragment (CBI-41, 1984); CCMGE 4/11915, posterior fragment (CBI-17, 1980); ZIN PH 141/44, posterior fragment juvenile (CBI-14, 1985); ZIN PH 121/44, posterior fragment juvenile (CBI-56, 2006). Cervical VI: ZIN PH 147/44 (CBI-4e, 2003); ZIN PH 148/44 (CBI-14, 1989); CCMGE 5/11915, anterior fragment (CBI-4, 1980); CCMGE 6/11915, anterior fragment (CBI-14, 1980); ZIN PH 149/44, anterior fragment (CBI-5a, 1989); ZIN PH 150/44, anterior fragment (CBI-, 1985); ZIN PH 151/44, posterior fragment (CBI-5a); ZIN PH 152/44, posterior fragment (CBI-4, 1987); ZIN PH 146/44, posterior fragment (CBI-). Cervical VII: ZIN PH 138/44 (CBI-14, 1984). Cervical VIII: ZIN PH 137/44, centrum (CBI-17, 1991). Cervical IX: ZIN PH 122/44 (CBI-); ZIN PH 123/44, centrum (CBI-); ZIN PH 124/44, centrum (CBI-14, 1989); ZIN PH 125/44, centrum (CBI-5a, 1989); ZIN PH 126/44, centrum (CBI-, 1987); ZIN PH 127/44, centrum (CBI-17, 2004); ZIN PH 128/44, centrum

(CBI-5a, 1989); ZIN PH 129/44, centrum (CBI-14, 1984); ZIN PH 130/44, centrum (CBI-4e).

Description. All postaxial cervical vertebrae are known for *Azhdarcho*. All cervicals except IV, VII, and VIII are represented by several specimens. The cervical V is the longest and the cervical IX is the shortest in the series. The middle cervicals are hyperelongated with the centrum length to minimum centrum width ratio of 4.0 in cervical III, 4.5 in cervical IV, and 4.3 in cervical VI (unknown for cervical V). In spite of this elongation, the relative length of the cervicals is the same as in other, short-necked pterodactyls: I + II < III < IV < V > VI > VII > VIII > IX. The mid-cervicals can be easily distinguished by combination of the diagnostic features of the anterior end summarized in Table 1 (see also Fig. 8).

The centra are procoelous with large and wide intercentral articulation surfaces, anterior cotyle and posterior condyle, elaborated by additional post- and preexapophyseal articulations. The postexapophyseal articulation surfaces are placed on distinct processes lateral to the centrum condyle, the postexapophyses. In mid-cervicals the neural arch between the zygapophyses is confluent with the centrum into a common tube with oval cross-section (long axis horizontal). There is no pneumatic foramen on the lateral side of the vertebrae except cervical VIII. On the anterior and posterior sides of the neural arch there is two pneumatic foramina lateral to the neural canal. The size of these pneumatic foramina varies but usually they are smaller than the neural canal (larger in cervical VII). A third pneumatic foramen is present dorsal to the neural on the anterior side of V-VII cervicals (unknown for cervicals VIII and IX). The neural canal is small relative to the size of the centrum. The zygapophyses are widely separated and their articulation surfaces are placed lateral to the intercentral articulation surfaces. In all postaxial cervicals the prezygapophyses project anterior to the cotyle and postzygapophyses do not project posterior to the condyle. The orientation of pre- and postzygapophyseal articulation surfaces varies between the vertebrae. The neural spine is also variably developed, being most reduced in mid-cervicals. There are no free cervical ribs on either cervical. The parapophysis and diapophysis are extremely rudimentary and usually not recognizable as distinct structures. The parapophysis corresponds to the preexapophyseal lateral extension of the cotyle and the diapophysis is sometimes represented by a bump-like eminence at

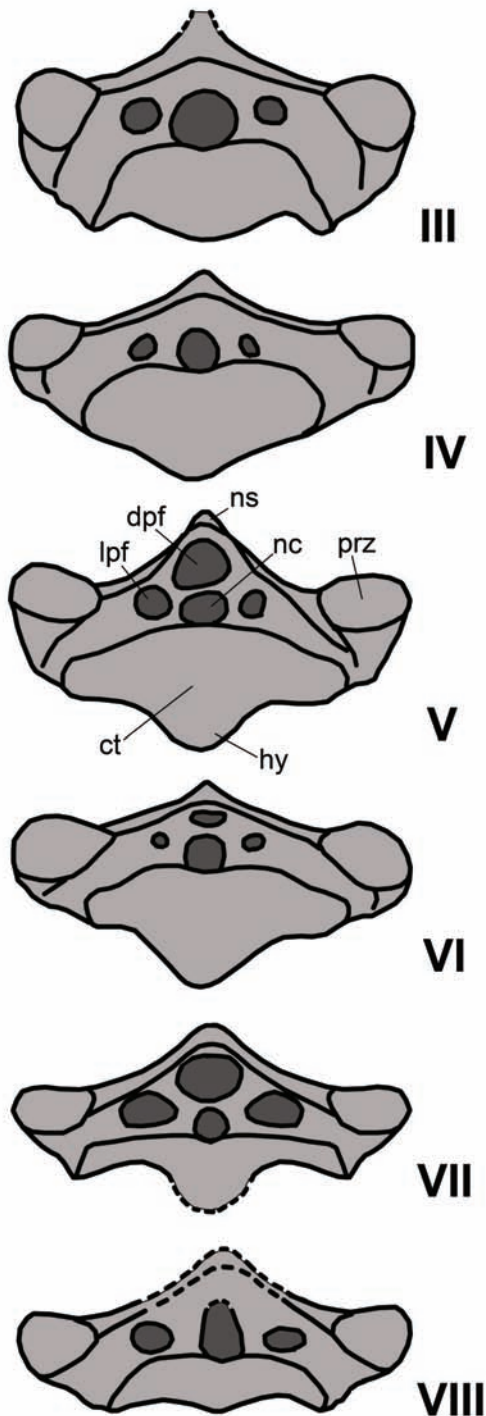


Fig. 8. Outlines of the cervical vertebrae III through VIII in anterior view scaled to the same width.

Abbreviations: ct – cotyle; dpf – dorsal pneumatic foramen; hy – hypapophysis; lpf – lateral pneumatic foramen; nc – neural canal; ns – neural spine; prz – prezygapophysis.

the base of the prezygapophysis. Between them usually there is a distinct vertebrocostal sulcus (= canal for housing of the vertebral artery). Sometimes this sulcus can be covered laterally by a short and thin bony wall representing the rudimentary cervical rib. The epiphyses are short ridges on the dorsal surface of the postzygapophyses.

The most complete cervical III is ZIN PH 131/44 (Fig. 9; ACH = 8.0; ACW = 20.0; ANW = 29.1; CL = 62.1; PCH = 11.7; PCW = 22.7; PNW = 28.0). Cervical III differs from other mid-cervical vertebrae by having unreduced neural spine extending between anterior and posterior margins of the neural arch. It is better preserved in neural arch fragments ZIN PH 136/44 and 172/44 where it higher than in cervicals IV and V. In cervical III the interzygapophyseal ridge on the lateral side of the neural arch is somewhat more pronounced than in other cervicals. In lateral view the cotyle is projecting only little ventral to the prezygapophyses while the condyle is completely ventral to the postzygapophyses. The centrum is ventrally convex in the middle and flat posteriorly, beneath the condyle and postexapophyses. The cotyle has a distinct dorsal incision at the base of the neural canal. The hypapophysis is small and does not project ventrally beyond the preexapophyseal surfaces. On the neural arch the lateral pneumatic foramina are more than twice smaller than the neural canal. The convex and elongated prezygapophyseal articulation surfaces are facing anterodorsally. The postzygapophyseal articulation surfaces are shorter, flatter, and facing posterovertrally. The condyle is high dorsoventrally, higher than the neural canal, with convex dorsal surface. The maximum lateral constriction of the vertebra is near the middle, little closer to the anterior end. ZIN PH 172/44 is a tiny neural arch of the cervical III with the total length of only about 17 mm. It is completely fused to the partially preserved centrum.

ZIN PH 144/44 is a complete but weathered cervical IV (Fig. 10; ACH = 11.2; ACW = 22.2; ANW = 36.0; CL = 83.6; PCH = 12.1). Cervical IV is more elongated than cervical III and has a greatly reduced neural spine which is separated into two short and low ridges confined to the anterior and posterior ends of the neural arch; the length of each ridge is only about 20% of the total length of the neural arch. The two ridges are connected by a line along the dorsal side of the neural arch. In this region the neural arch is confluent with the centrum and vertebra is oval in cross-section. In lateral view the ventral profile of the

Table 1. Diagnostic characters of the anterior end of the mid-cervical vertebrae in *Azhdarcho lancicollis*.

Character	Cervical					
	III	IV	V	VI	VII	VIII
Cotyle: higher than neural canal (A); lower than neural canal (B)	A	A	A	A	A	B
Cotyle maximum height (including hypapophysis): about one half of the maximum width (A); about one fourth of the maximum width (B)	A	A	A	A	B	B
Dorsal margin of cotyle: slightly concave (A); straight or slightly convex (B)	A	A	B	A	A	A
Hypapophysis: absent or very small (A); large (B)	A	B	B	B	B?	A
Lateral pneumatic foramina: smaller or subequal to neural canal (A); larger than neural canal (B)	A	A	A	A	B	A
Dorsal pneumatic foramen dorsal to the neural canal: absent (A); present (B)	A	A	B	B	B	?
Neural spine: large (A); absent or very small (B)	A	B	B	B	B?	?

centrum is convex in the middle in contrast with the concave profile in cervical III. The posterior part of the ventral centrum surface is flat or slightly convex. The cotyle has slightly concave dorsal margin. The hypapophysis is better developed than in cervical III, protruding ventrally beyond the preexapophyseal surfaces. The condyle is as high as in the cervical III. The articulation surfaces of the postzygapophyses are more steeply inclined than in any other cervical; they are almost subvertical. On the posterior side the lateral pneumatic foramina are as large as the neural canal in ZIN PH 144/44 (Fig. 10E). In contrast with cervical III, the maximum lateral constriction of the vertebra is closer to the posterior end.

Cervical V is known from several anterior and posterior fragments (Figs 11–12). It is certainly the most elongated vertebra in the series with extreme reduction of the neural spine. In anterior view cervical V is similar to cervicals IV and VI. The unique feature of cervical V is a concave dorsal margin of the cotyle. The dorsal pneumatic foramen is present, as in cervical VI (absent in cervical IV), and could be large, larger than the neural canal (Fig. 11A). The posterior end is similar to that of vertebra IV, but the postzygapophyseal articulation surfaces are more obliquely oriented. The condyle is higher than the neural canal and has a convex dorsal margin. Cervical V differs from other mid-cervicals by remarkable flat

ventral surface of the centrum beneath the condyle. The maximum lateral constriction of the vertebra is approximately at the middle.

Besides fragments, cervical VI is represented by two exquisitely preserved specimens, ZIN PH 148/44 and 147/44 (Fig. 13; ACW = 29.3; ANW = 45.6; CL = 99.3; PCH = 12.3 for ZIN PH 147/44). In anterior view cervical VI is similar to cervical V but could be easily distinguished by a concavity on the dorsal margin of the cotyle at the neural canal base. The dorsal pneumatic foramen is relatively large in ZIN PH 147/44, very small in ZIN PH 150/44, and absent in the smallest specimen ZIN PH 148/44. Cervical VI differs from cervicals IV and V by less reduced neural spine. It is also separated into two parts, but both parts are relatively longer and the posterior part is distinctly higher (it is incompletely preserved in all specimens). In lateral view cervical VI differs from cervical V by distinctly more concave ventral profile and the condyle placed much lower relative to the postzygapophyses. In posterior view it is different, besides the larger neural spine, also in much shallower condyle having a broad concavity along the dorsal margin (condyle high and dorsally convex in cervicals III–V). The ventral side of the centrum is convex between the postexapophyses (flat in cervical V). The neural canal is relatively larger than in cervical V and tear shaped. The lateral pneumatic

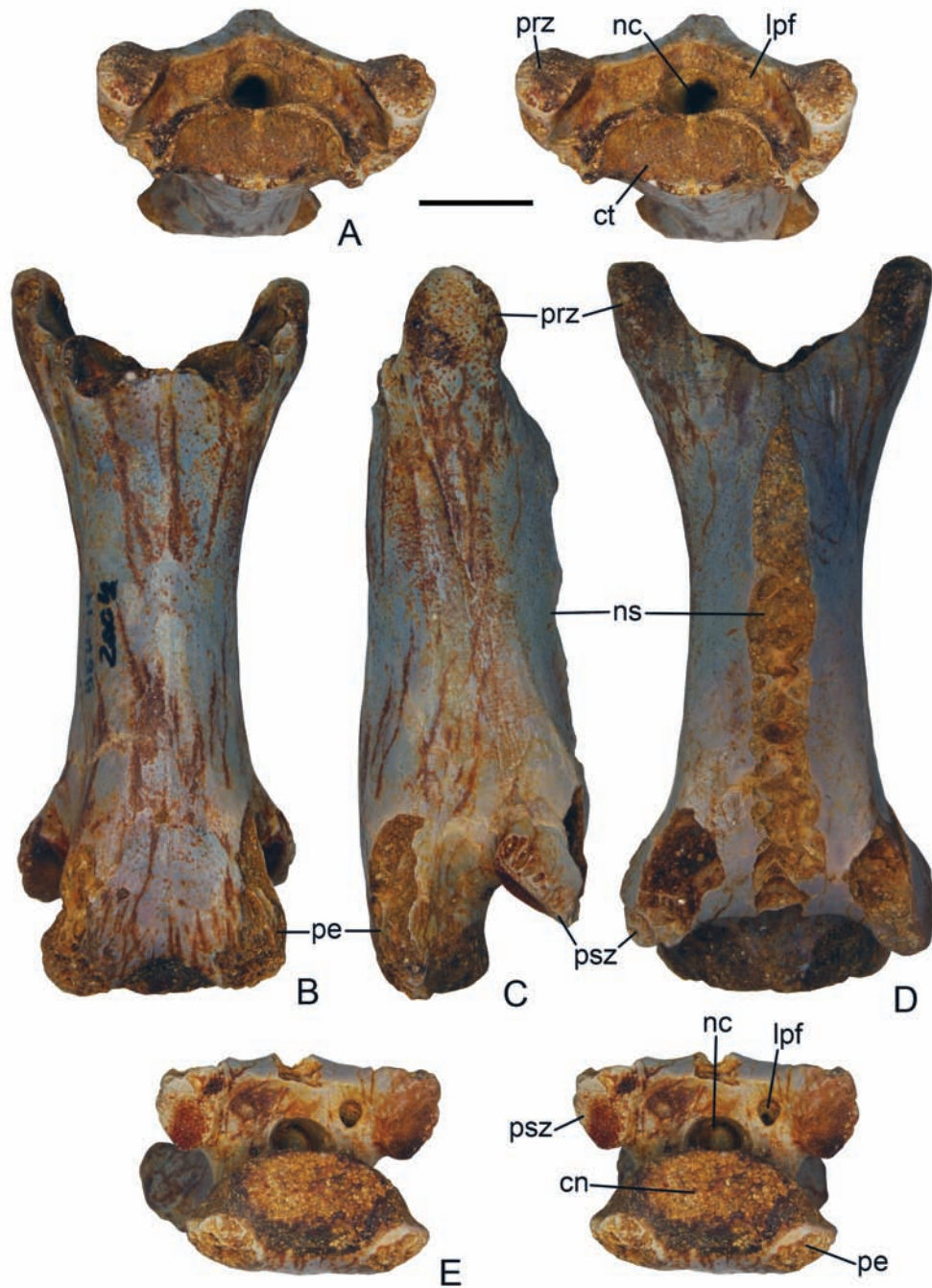


Fig. 9. ZIN PH 131/44, cervical III of *Azhdarcho lancicollis*, in anterior (A, stereopair), ventral (B), lateral (C), dorsal (D), and posterior (E, stereopair) views.

Abbreviations: cn – condyle; ct – cotyle; lpf – lateral pneumatic foramen; nc – neural canal; ns – neural spine; pe – postexapophysis; prz – prezygapophysis; psz – postzygapophysis. Scale bar = 1 cm.



Fig. 10. ZIN PH 144/44, cervical IV of *Azhdarcho lancicollis*, in anterior (A, stereopair), dorsal (B), lateral (C), ventral (D), and posterior (E, stereopair) views.

Abbreviations: cn – condyle; ct – cotyle; lpf – lateral pneumatic foramen; nc – neural canal; ns – neural spine; pe – postexapophysis; prz – prezygapophysis; psz – postzygapophysis. Scale bar = 1 cm.

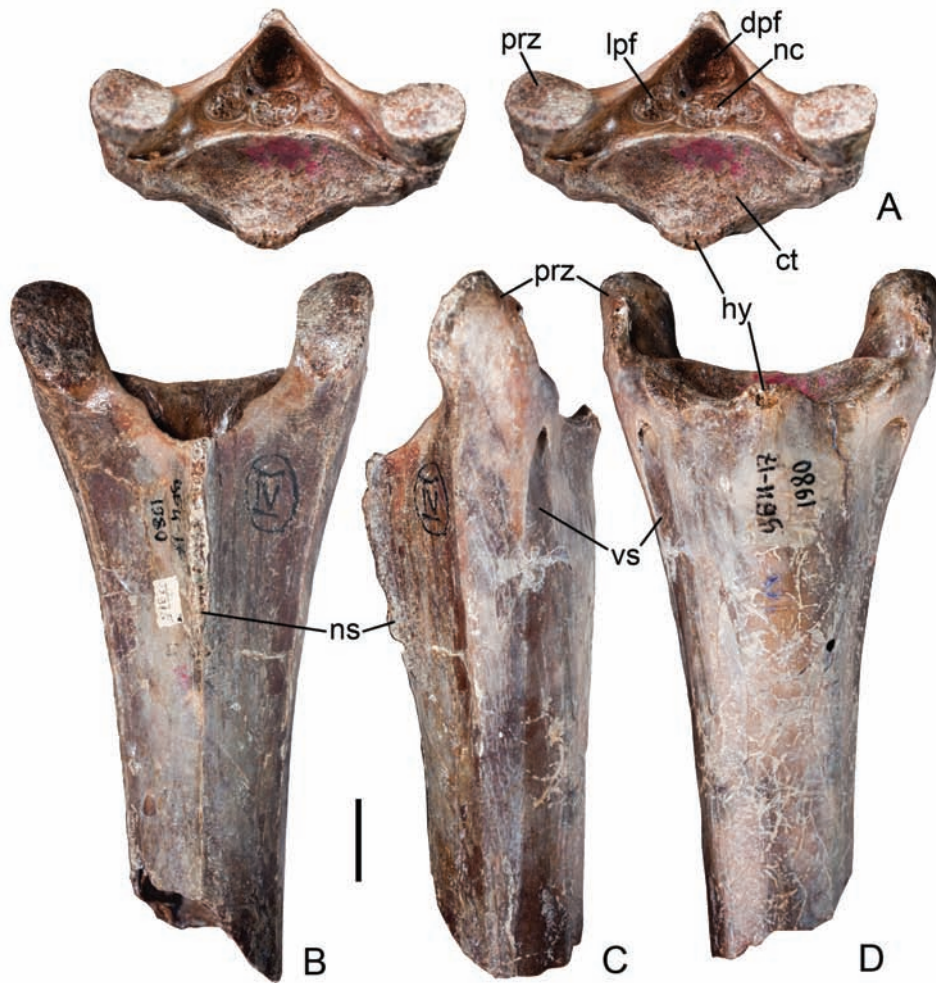


Fig. 11. CCMGE 1/11915, holotype, anterior fragment of cervical V of *Azhdarcho lancicollis*, in anterior (A, stereopair), dorsal (B), lateral (C), and ventral (D) views.

Abbreviations: ct – cotyle; dpf – dorsal pneumatic foramen; hy – hypapophysis; lpf – lateral pneumatic foramen; nc – neural canal; ns – neural spine; prz – prezygapophysis; vs – vertebrocostal sulcus. Scale bar = 1 cm.

foramina are smaller than the neural canal and placed closer to its dorsal border. In ZIN PH 147/44 the lateral pneumatic foramen is double on the right side. The maximum lateral constriction of the vertebra is at the base of postzygapophyses. ZIN PH 149/44 and 151/44 are possible anterior and posterior ends of the single specimen which is 1.5 times larger than ZIN PH 147/44.

ZIN PH 138/44 is the single known cervical VII (Fig. 14; CL = 50.0). The ventral side of the centrum is missing and the breakage reveals the ossified neural canal supported by tiny processes (Fig. 14C). Cervical VII is distinctly shorter and wider than cervical VI.

The dorsal surface of the neural arch is broken along the midline and the structure of the neural spine is unknown. The cotyle is dorsoventrally shallow, but the hypapophysis is still apparently large. On anterior side the neural canal is round and smaller than lateral and dorsal pneumatic foramina. The dorsal pneumatic foramen is proportionally larger than in any other cervical vertebra. In ZIN PH 138/44 there is a remnant of the fused cervical rib between the cotyle and base of the prezygapophyses (places for reduced parapophysis and diapophysis). It is thick and the foramen for the vertebral artery is minute. The posterior side of vertebra VII is markedly dif-

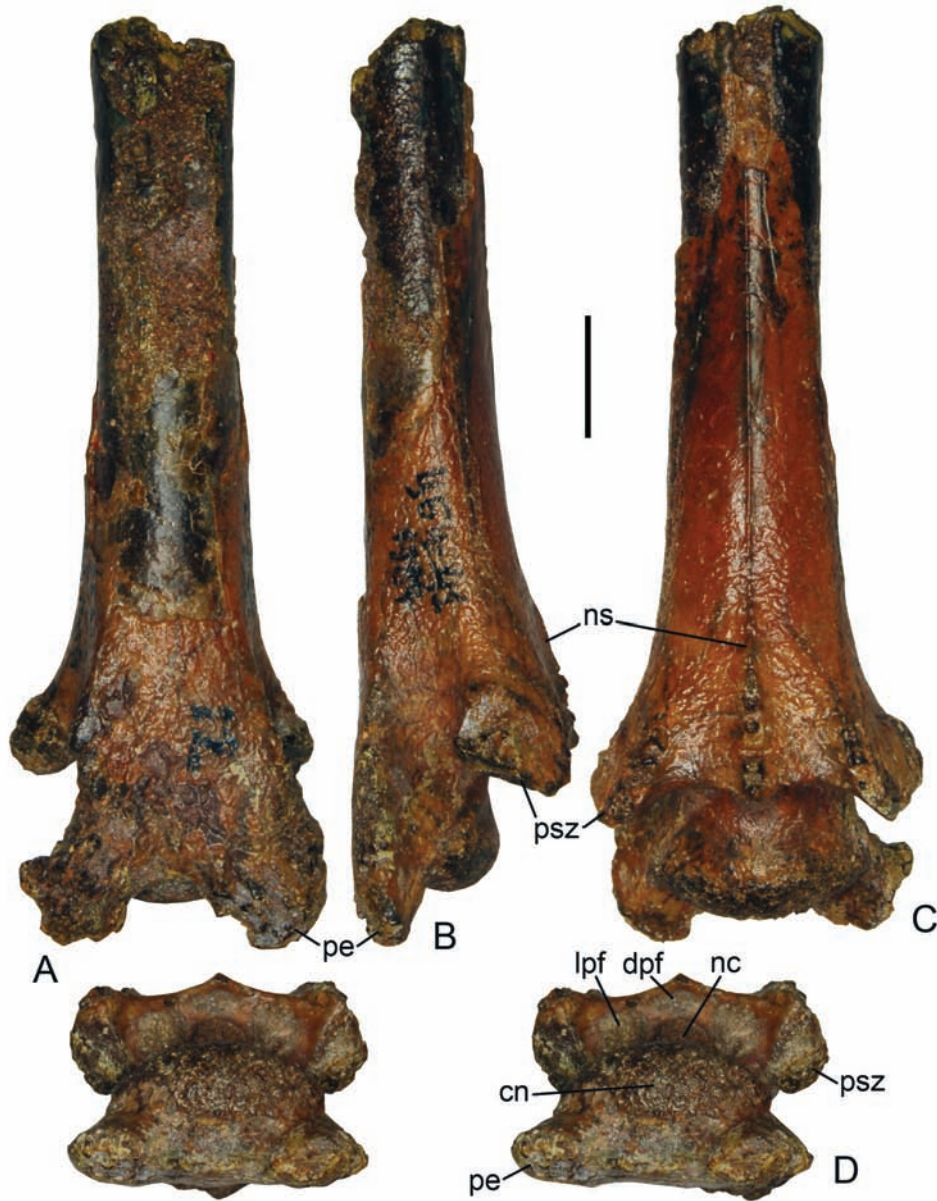


Fig. 12. ZIN PH 139/44, posterior fragment of cervical V of *Azhdarcho lancicollis*, in ventral (A), lateral (B), dorsal (C), and posterior (D, stereopair) views.

Abbreviations: cn – condyle; dpf – dorsal pneumatic foramen; lpf – lateral pneumatic foramen; nc – neural canal; ns – neural spine; pe – postexapophysis; psz – postzygapophysis. Scale bar = 1 cm.

ferent from the previous cervicals by having lateral pneumatic foramina that are distinctly larger than the neural canal, and a dorsal pneumatic foramen, not present on the posterior side in other cervicals (unknown for cervical VIII). The condyle is as shallow dorsoventrally as in cervical VI, but its dorsal margin

is convex (concave in cervical VI). The maximum lateral constriction of the vertebra is approximately at the middle. ZIN PH 138/44 was identified as “sixth (or possibly seven) cervical” and figured in ventral view (Unwin and Bakhurina 2000: 428, fig. 21.8C; mislabeled as dorsal view).

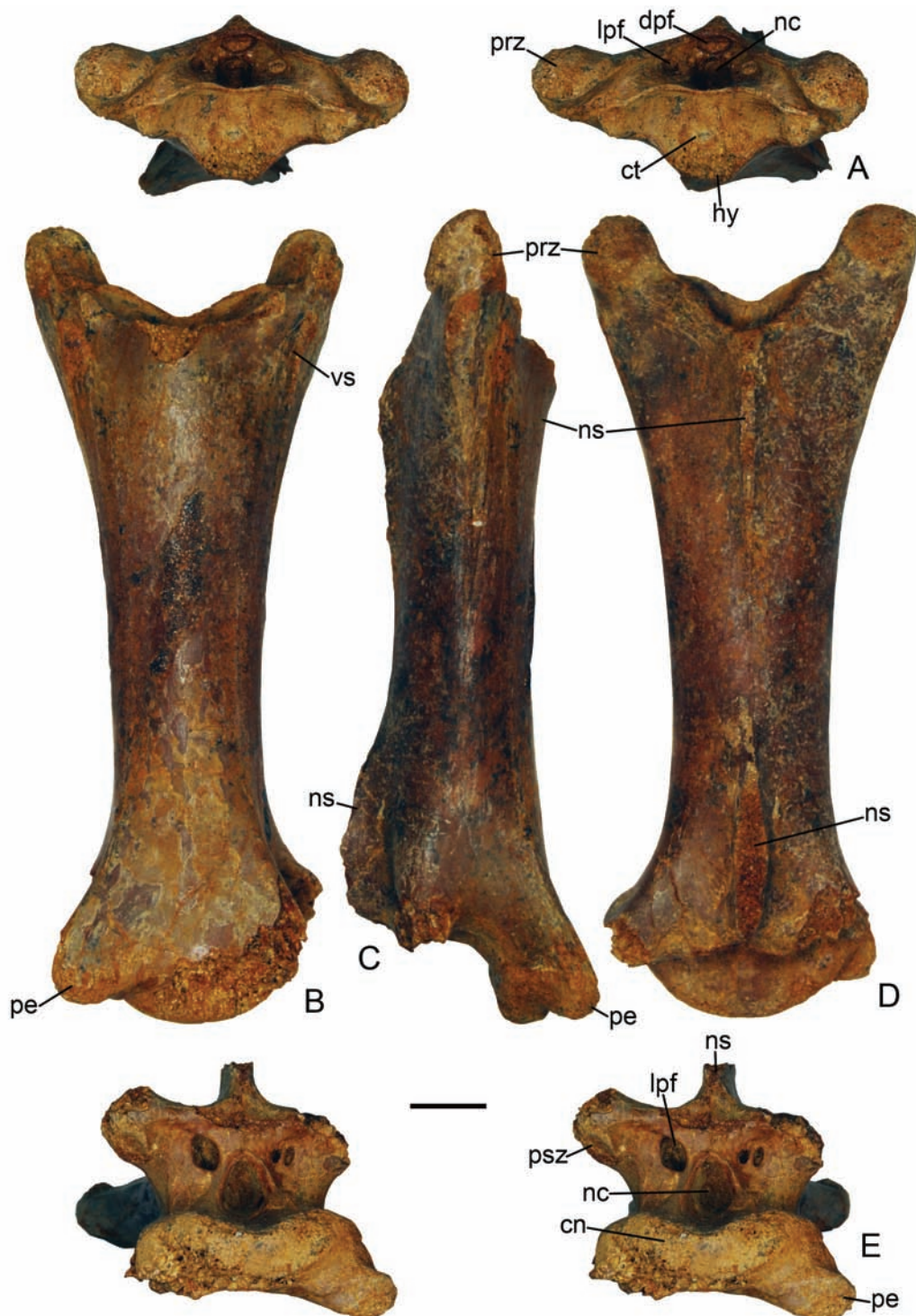


Fig. 13. ZIN PH 147/44, cervical VI of *Azhdarcho lancicollis*, in anterior (A, stereopair), ventral (B), lateral (C), dorsal (D), and posterior (E, stereopair) views.

Abbreviations: cn – condyle; ct – cotyle; dpf – dorsal pneumatic foramen; hy – hypapophysis; lpf – lateral pneumatic foramen; nc – neural canal; ns – neural spine; pe – postexapophysis; prz – prezygapophysis; psz – postzygapophysis; vs – vertebrocostal sulcus. Scale bar = 1 cm.

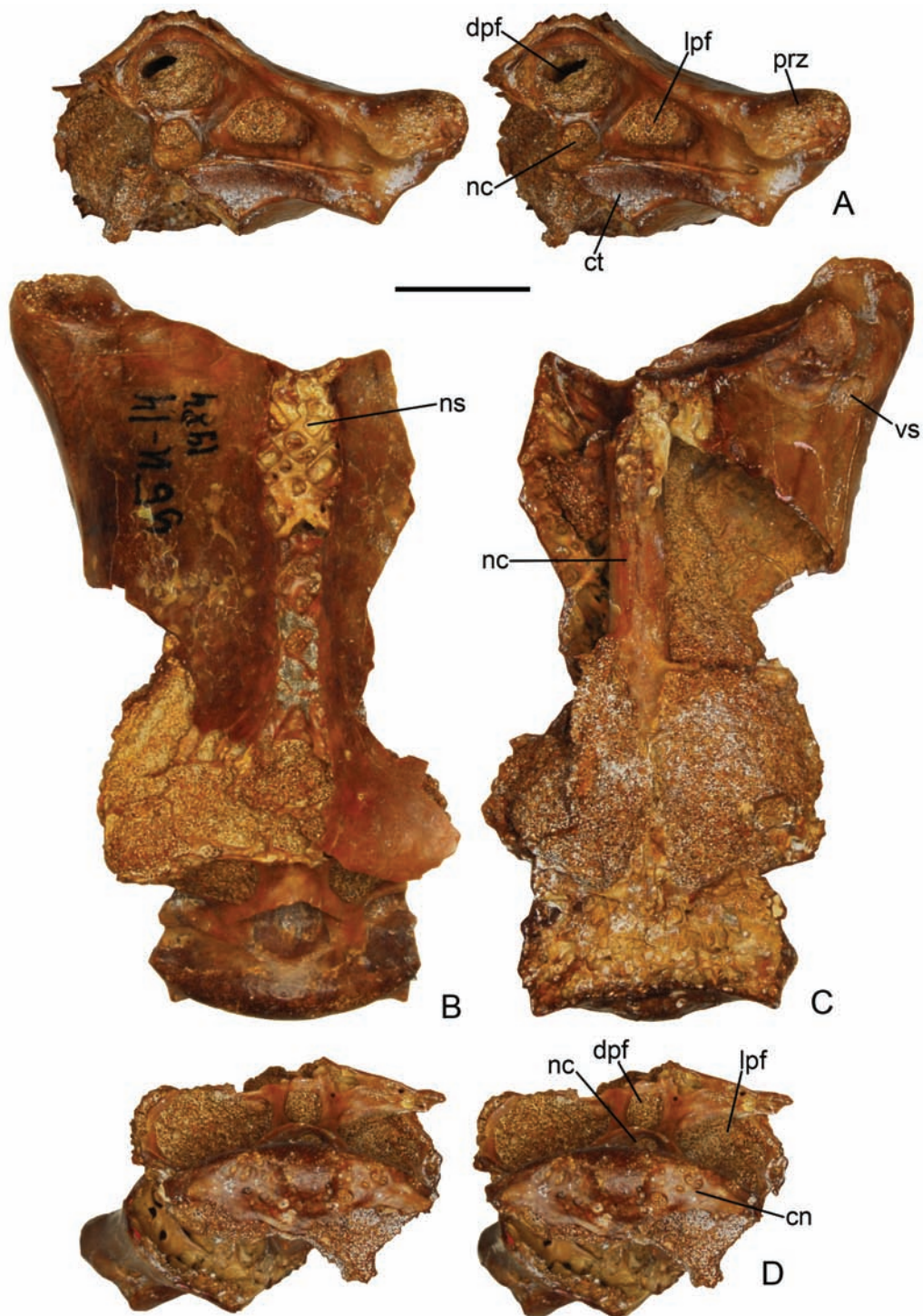


Fig. 14. ZIN PH 138/44, cervical VII of *Azhdarcho lancicollis*, in anterior (A, stereopair), dorsal (B), ventral (C), and posterior (D, stereopair) views.

Abbreviations: cn – condyle; ct – cotyle; dpf – dorsal pneumatic foramen; lpf – lateral pneumatic foramen; nc – neural canal; ns – neural spine; prz – prezygapophysis; vs – vertebrocostal sulcus. Scale bar = 1 cm.

Cervical VIII is known from single specimen ZIN PH 137/44 missing most of the neural arch (Fig. 15; ACH = 7.6; ACW = 27.0; CL = 43.0; PCH = 12.3; PCW = 29.5). It is shorter and wider than cervical VII, almost squarish in dorsal/ventral view. The cotyle is dorsoventrally shallow, as in cervical VII, but lacks the hypapophysis. The lateral pneumatic foramina are large and well separated from the neural canal. The cotyle is similar to that of cervical VII, dorsoventrally narrow and with convex dorsal margin. On posterior side, the lateral pneumatic foramina are larger than the neural canal. The ventral side of the centrum is convex; between the postexapophyses it is flat. Cervical VIII is unique among cervicals in having a pneumatic foramen on the lateral side of the centrum.

Cervical IX is represented by several centra and ZIN 122/44 with most of the neural arch preserved (Fig. 16). Cervical IX is similar with the atlas-axis in having a short centrum and high neural arch, but the centrum is much shorter, less than half of the centrum width. The cotyle is similar to that of cervical VIII: it is dorsoventrally narrow and transversely wide, with distinct hypapophysis (not preserved in all specimens because of abrasion), and concave dorsal margin. The peculiar feature of cervical IX is the extension of the preexapophyseal surfaces beneath the cotyle towards the hypapophysis. In ZIN PH 125/44 there is a distinct tubercle on the ventral centrum side posterior to the hypapophysis that delimits posteriorly this extended preexapophyseal

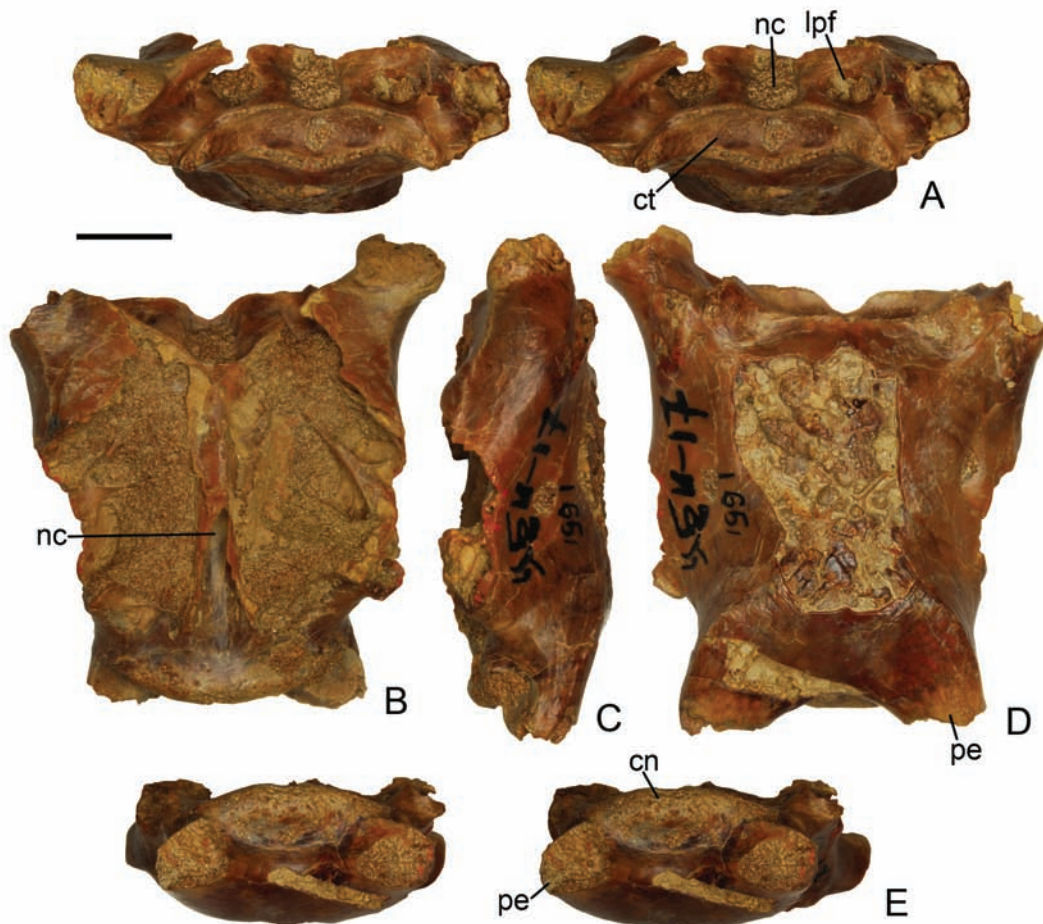


Fig. 15. ZIN PH 137/44, cervical VIII of *Azhdarcho lancicollis*, in anterior (A, stereopair), dorsal (B), lateral (C), ventral (C), and posterior (D, stereopair) views.

Abbreviations: cn – condyle; ct – cotyle; lpf – lateral pneumatic foramen; nc – neural canal; pe – postexapophysis; prz – prezygapophysis. Scale bar = 1 cm.

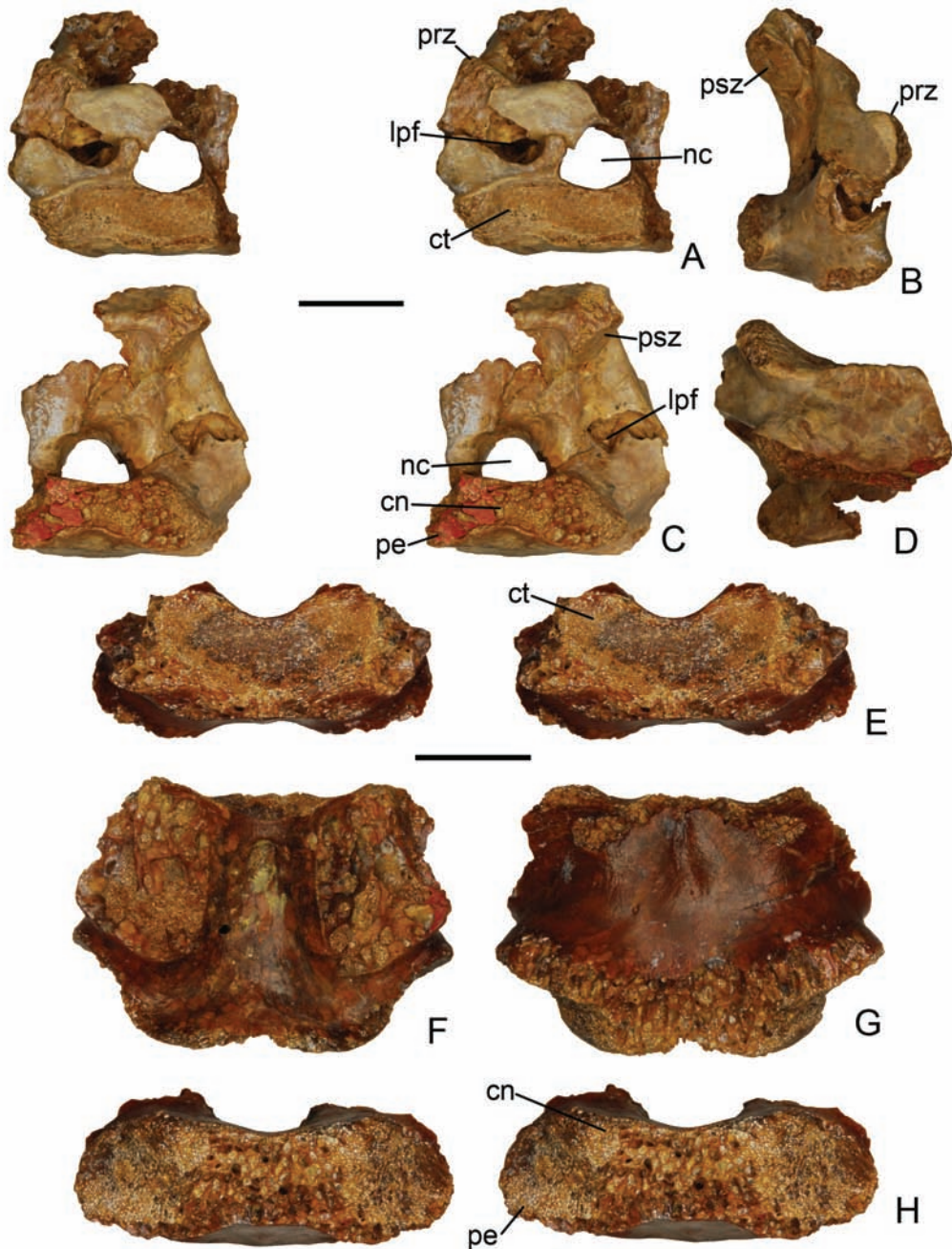


Fig. 16. Cervical IX of *Azhdarcho lancicollis*: A–D – ZIN PH 122/44, in anterior (A, stereopair), lateral (B), posterior (C, stereopair), and ventral (D) views; E–H – ZIN PH 123/44, centrum in anterior (E, stereopair), dorsal (F), ventral (G), and posterior (H, stereopair) views. *Abbreviations:* cn – condyle; ct – cotyle; lpf – lateral pneumatic foramen; nc – neural canal; pe – postexapophysis; prz – prezygapophysis; psz – postzygapophysis. Scale bars = 1 cm.

surface. The ventral surface of the centrum is flat and slightly concave between the postexapophyses. The postexapophyses are large, each of about one third of the total posterior width of the centrum. The condyle is relatively narrow dorsoventrally and has a convex dorsal margin. There are two lateral pneumatic foramina on both anterior and posterior sides of the neural arch. The dorsal pneumatic foramen was likely lacking. The neural canal is relatively large. The zygapophyses are very short, not distinct processes as in other postaxial cervicals. The postzygapophyseal articular surfaces are oval and facing ventrolaterally rather than posteroventrally as in the preceding cervicals. The postzygapophyses are connected by a distinct transverse ridge on the posterior side of the neural arch dorsal to the neural canal. A diapophysis could be present at the junction of the centrum and neural arch but this is not certain because this area in ZIN 122/44 is destroyed.

Comparison. The structure of the cervical vertebrae in *Azhdarcho* is basically similar to that of other pterodactyloids. The distinctive azhdarchid characters are elongation of middle cervicals IV, V, and VI, tubular middle cervicals with confluent centrum and neural arch and with low vestigial or absent neural spines, and lack of a pneumatic foramen on lateral sides in postaxial cervicals (Nessov 1984, 1991a; Padian 1984, 1986; Howse 1986; Bennett 1989, 1994; Padian et al. 1995; Unwin and Lü 1997; Company et al. 1999; Ikegami et al. 2000; Kellner 2003; Unwin 2003; Watabe et al. 2009). In *Azhdarcho* the longest cervical vertebra is the cervical V, anterior and posterior to it the length of vertebrae decreases: $I + II < III < IV < V > VI > VII > VIII > IX$. The same cervical formula was likely characteristic for all azhdarchids (Steel et al. 1997; Pereda Suberbiola et al. 2003), as well as for other pterodactyloids with not isometric postaxial cervicals (Bennett 2001). A similar formula has been reported for the azhdarchoid *Tupuxuara* with short cervicals: $III < IV = V > VI > VII$ (Kellner 1995).

In *Quetzalcoatlus* the cervical V is 5.6 times longer than wide (anteriorly) and in *Arambourgiania* this ratio might be as high as 6.9 (Frey and Martill 1996). In other azhdarchids the cervical V seems to be less elongated with CL/ANW ratio around 4 (Pereda Suberbiola et al. 2003). In *Azhdarcho* this ratio is reconstructed as 4.2. Other characters of cervical vertebrae considered sometimes to be diagnostic for the group, like vertebrocostal sulcus and prezygapophyseal tubercle (see review in Pereda Suberbiola et

al. 2003), are variably developed in the known sample of *Azhdarcho* and other azhdarchids.

All cervicals of *Azhdarcho* have ossified neural canal as in other azhdarchids. This was established as early as in the original description of the genus (Nessov 1984: 49). An idea that azhdarchids lack an ossified neural canal in cervical vertebrae, or this canal is confluent with the vertebral centrum (Currie and Russell 1982; Padian 1984, 1986; Bennett 1989, 1994; Kellner 2003), was based on inadequately preserved specimens (Martill et al. 1998; Unwin and Bakhurina 2000; Unwin 2003).

Among azhdarchids the most complete cervical series is known for *Quetzalcoatlus* sp. but only the longest cervical V has been figured so far (Lawson 1975: fig. 1; Howse 1986: fig. 7; Wellnhofer 1991b: fig. on p. 144; Frey and Martill 1996: fig. 9b, d).

The well preserved cervical III is known for *Volgadraco* from the Campanian of Saratov Province, Russia (Averianov et al. 2008: pl. 5, fig. 2). It is relatively shorter and more robust than smaller known specimens of that vertebra in *Azhdarcho* and has a strongly flexed ventral profile. The neural spine is high and robust and occupies all space between the anterior and posterior margins of the neural arch. There is a dorsal pneumatic foramen on the anterior side (absent in *Azhdarcho*). The lateral pneumatic foramina on the posterior side are compatible in size with the neural canal. These are distinctly smaller in *Azhdarcho* but development of the lateral pneumatic foramina in the cervicals of Azhdarchidae is size related (Godfrey and Currie 2005). The centrum beneath the condyle is distinctly higher in *Volgadraco* compared with *Azhdarcho*.

An almost complete azhdarchid cervical III was found in association with atlas-axis and posterior fragment of possible cervical V in the Cenomanian-Santonian of Mongolia (Watabe et al. 2009: figs 7–8). It has the blade-like neural spine along the whole neural arch and differs from the cervical III in *Azhdarcho* only in minor details: the dorsal margin of the cotyle is convex; the ventral side of the centrum is slightly concave in lateral profile anteriorly and posteriorly, with a transitional point in the center.

A short cervical with a high neural spine of a large pterodactyloid from the Campanian of Delaware, USA (Baird and Galton 1981: fig. 2) may belong to the Azhdarchidae. It is more robust and has larger postexapophyses but otherwise is similar to the cervical III of *Azhdarcho*.

Anterior and posterior fragments of a pterodactyloid cervical (parts of the single specimen?) from the Coniacian of England (Martill et al. 2008; figs 3–6) with a high neural spine extending along the whole neural arch may also be an azhdarchid cervical III rather than mid-cervical of a “non-azhdarchid azhdarchoid” pterosaur as the authors suggested. It has the pneumatic foramina lateral to the neural canal on both anterior and posterior ends and poorly developed multiple dorsal pneumatic foramina anteriorly.

The isolated cervical IV from the Cenomanian-Santonian of Mongolia (Watabe et al. 2009; figs 3–4) is virtually identical to that vertebra in *Azhdarcho*.

The isolated cervical vertebrae of *Bakonydraco* are identified here as the cervical IV (Ősi et al. 2005: fig. 4A), the cervical VI (Ősi et al. 2005: fig. 4B), and the cervical VII (Ősi et al. 2005: fig. 5A). The anterior fragment of a middle cervical (Ősi et al. 2005: fig. 5B) cannot be positively identified. These vertebrae are poorly preserved and the remaining morphology is the same as in *Azhdarcho*. The cervical VII has a higher neural spine along the whole neural arch, as in *Azhdarcho*.

The isolated azhdarchid mid-cervicals from the Campanian of Alberta, Canada are identified here as cervical IV (Godfrey and Currie 2005: figs 16.1 and 16.2) and cervical V (Godfrey and Currie 2005: fig. 16.3; juvenile). Both cervicals IV differ in proportions; the larger and more elongated specimen is possible from an older individual. These vertebrae are clearly different from the cervical IV in *Azhdarcho* by presence of an additional pneumatic foramen dorsal to the neural canal (anteriorly), dorsoventrally narrower lateral “wings” of the centrum cotyle, and relatively more robust and expanded postexpophyses. Otherwise the vertebrae are similar in both taxa. The most elongated cervical V of the Canadian form is also similar to that vertebra in *Azhdarcho* except much larger and ventrolaterally projecting postexpophyses. Earlier Currie and Russell (1982: fig. 2) published an anterior fragment of a mid-cervical azhdarchid vertebrae from the same locality. In proportions it is similar to the cervical IV but markedly different in having large confluent foramen for the neural canal and dorsal pneumatic foramen and apparent lack of lateral pneumatic foramina on anterior side of the neural arch. This specimen is small, with ANW of about 2 cm, and at least some of these differences may be related to its younger individual age.

A posterior fragment of a vertebra from the Maastrichtian of Spain (Company et al. 1999: fig. 3) with vertical postzygapophyseal articulation surfaces is most likely the cervical IV (identified as possible cervical VI in the cited paper). It has lateral pneumatic foramina larger than the neural canal. It differs from middle cervicals in *Azhdarcho* by extreme development of postexpophyses.

The posterior fragment of a cervical of “*Bogolubovia*” from the Campanian of Penza Province, Russia (Bogolubov 1914: figs 1 and 2; Bakhurina and Unwin 1995: fig. 14) is possible the cervical V (Averianov et al. 2005). It differs from other azhdarchids by a more pronounced arcuate transverse ridge dorsal to the neural canal and lateral pneumatic foramina and a relatively high vertical wall of the neural arch dorsal to this ridge. The postexpophyses are large and well expanded. In these features it resembles to some extent the cervical III of *Volgadraco* but absence of a high neural spine suggests that it is not the third cervical.

A long azhdarchid vertebra from the Campanian-Maastrichtian of Senegal, unfortunately not figured from the most informative anterior and posterior sides (Monteillet et al. 1982: pl. 1), is most likely the cervical V. It does not differ from the known specimens of *Azhdarcho*.

A distorted posterior fragment of an azhdarchid vertebra from the Coniacian-Santonian (earlier assigned to the Cenomanian-Turonian) of Japan (Ikegami et al. 2000: fig. 3) is likely cervical IV or V. Authors noted that this specimen differs from all known azhdarchids by having a well developed ridge parallel to the neural spine, but such ridges are actually present, although variably developed in *Azhdarcho* and other azhdarchids. According to Lawson (1975) in *Quetzalcoatlus* there are no any ridges on the dorsal surface of the neural arch in middle cervical vertebrae. If this correct, absence of the ridge-like neural spine would differentiate *Quetzalcoatlus* from other azhdarchid taxa.

A large poorly preserved cervical V of Azhdarchidae indet. with estimated length of about 55 cm is known from the Maastrichtian of France (Buffetaut et al. 1997: fig. 2). A rather complete but crushed cervical V with the length of about 37 mm has been recently described from the Maastrichtian of Montana, USA (Henderson and Peterson 2006: fig. 1). It was identified as belonging to cf. *Quetzalcoatlus* sp. A long azhdarchid vertebra lacking the posterior end from the Maastrichtian of Wyoming, USA (Estes 1964: fig. 70) is also likely to be the cervical V.

The single known vertebrae of *Arambourgiania* is possible the cervical V (Frey and Martill 1999; Martill et al. 1998). It differs from the cervical V in other azhdarchids by being extremely elongated (the total length ~62 cm), by laterally compressed centrum with cotyle and condyle higher than wide, by lack of the vertebrocostal sulcus at the anterior end, and by strong ventral crest posterior to the hypapophysis. The lateral pneumatic foramina are much larger than the neural canal but this may be correlated with large size of the specimen. It additionally differs from *Azhdarcho* in lack of an additional anterior pneumatic foramen dorsal to the neural canal.

A rather complete cervical VI of Azhdarchidae indet. has been described from the Campanian-Maastrichtian of Spain (Buffetaut 1999: fig. 1b, c).

Posterior cervicals are poorly known for Azhdarchidae. This region is best preserved and described in *Phosphatodraco* (Pereda Suberbiola et al. 2003). The cervical VIII in *Phosphatodraco* is unusually long being more than 50% of the length of the cervical V (~30% in *Azhdarcho* and ~20% in *Quetzalcoatlus*; Pereda Suberbiola et al. 2003). In *Phosphatodraco* and *Quetzalcoatlus* the cervical VIII has a high rectangular neural spine; in the former taxon it is placed at the posterior end of the vertebra (Pereda Suberbiola et al. 2003: fig. 3d). In *Azhdarcho* the neural arch is not preserved in the single known cervical VIII but it also might had a high posteriorly positioned neural spine, equal in height to the adjacent cervical IX. Among azhdarchids the cervical IX has been described previously only for *Phosphatodraco* (Pereda Suberbiola et al. 2003: fig. 3e) and *Volgadraco* (Averianov 2007: pl. 5, fig. 3). Both taxa are similar in having a large oval depression on the posterior side of the neural arch some distance dorsal to the neural canal (this region is inadequately preserved in known specimens of *Azhdarcho*). A similar depression between the postzygapophyses of the cervical IX is present also in *Pteranodon* (Bennett 2001: fig. 42B). The hypapophysis is very small or absent in *Azhdarcho* but relatively large in *Volgadraco* (unknown for *Phosphatodraco*). The pneumatic openings lateral to the neural are present on both anterior and posterior sides of the cervical IX in *Azhdarcho*. These openings were probably present anteriorly in *Volgadraco*. In *Phosphatodraco* the anterior side of the cervical IX is not prepared and these foramina are absent on the posterior side.

Dorsal vertebrae

Material. Notarium fragments: CCMGE 7/11915 (VBI-14, 1980); ZIN PH 5/44 (CBI-14, 1989); ZIN PH 153/44 (CBI-16, 1989); ZIN PH 6/44 (CBI-14, 1980). Free dorsals: ZIN 7/44, two fused dorsals (CBI-14, 1984); ZIN PH 154/44 (CBI-4, 2003); ZIN PH 155/44 (CBI-14, 1998); ZIN PH 156/44 (CBI-4, 2003); ZIN PH 157/44, centrum (CBI-14, 1997); ZIN PH 158/44, centrum (CBI-4, 1989); ZIN PH 159/44, centrum (CBI-14, 1984); ZIN PH 160/44, centrum (CBI-14, 1984).

Description. All dorsal vertebrae are procoelous as in other pterosaurs. Notarium is known from several fragments of fused vertebrae and fragmentary centra of small unfused notarial vertebrae (the latter are not catalogued). The anterior end of notarium is represented by two fragments missing neural arches of juvenile individuals, among which CCMGE 7/11915 is larger and more complete (Fig. 17: ACH = 12.5; ACW = 39.0). Both specimens consist of only two fused vertebrae. ZIN PH 153/44 is a much larger notarium fragment representing incomplete fused centra of three anterior dorsal vertebrae with PCW around 60 mm (not figured). The anterior notarial vertebrae differ from posterior notarial vertebrae and free dorsals in having distinctly wider centrum with flattened ventral surface. The centrum cotyle of the first notarial vertebra is similar to that of cervical IX in being transversely wide and dorsoventrally narrow and in having the preexapophyseal articulation surfaces. But these surfaces do not meet at the midline and in anterior view there is a concavity between them. The hypapophysis is absent. The dorsal margin of the cotyle is concave at the floor of the neural canal. The prezygapophyses are not developed as processes and the prezygapophyseal articulation surfaces are placed close to the neural canal. These surfaces are facing dorsomedially. The transverse process of the first vertebra is a short, robust and laterally directed process which is placed at the junction of the centrum and neural arch. On the second vertebra the transverse process was apparently placed higher on the neural arch and it is not preserved on the known fragments. The centrum of the second vertebrae is somewhat smaller than that of the first vertebra, with transversely narrower condyle. The lateral surface of the centrum of first vertebra has a pseudopleurocoel-like concavity. The ventral centrum surface is slightly concave in the first vertebra and slightly convex in

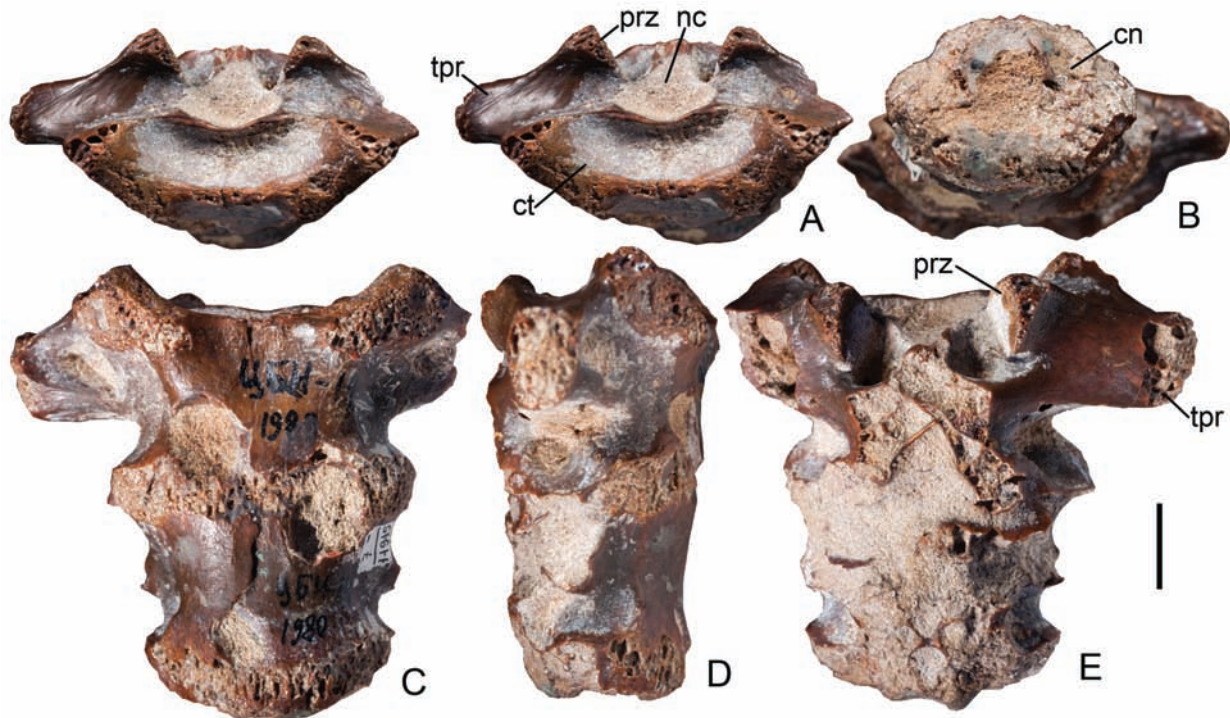


Fig. 17. CCMGE 7/11915, anterior notarium fragment of *Azhdarcho lancicollis*, in anterior (A, stereopair), posterior (B), ventral (C), lateral (D), and dorsal (E) views.

Abbreviations: cn – condyle; ct – cotyle; nc – neural canal; prz – prezygapophysis; tpr – transverse process. Scale bar = 1 cm.

the second vertebra. The centrum condyle of the second vertebra is of rhomboid shape with a concavity in the middle.

Two poorly preserved fused dorsals ZIN PH 6/44 represent the posterior end of the notarium (Fig. 18A, B; the first of these vertebrae was apparently fused to the preceding vertebra; CL = 17.3 for the last vertebra). The centra are transversely narrow as in free dorsals, with round cross-section. The condyle of the last vertebra is deeply incised by the neural canal. The neural arches and neural spines are vertical and placed centrally on the vertebrae. The postzygapophyseal articulation surfaces are small, placed close to the midline, and facing ventrolaterally. There is a deep vertical groove dorsal to the postzygapophyses on the posterior side of neural arch. Neural arches of two adjacent vertebrae are completely fused. The free space between the neural spines is similar in size with the neural spine. The neural spines were apparently low and broken at the contact with the supraneural plate.

Two fused vertebrae ZIN PH 7/44 (Fig. 18C–F; CL = 17.7 for the last vertebra) have free anterior and posterior ends. Most possible these vertebrae are fused free dorsals that do not belong to notarium or synsacrum, like in some specimens of *Pteranodon* (Bennett 2001: fig. 46A). The centra are similar to those of ZIN PH 6/44, but the neural arches are markedly inclined anteriorly so the prezygapophyses project much anterior to the centrum. The intervertebral foramen is narrow and oval. The structure of these vertebrae is similar to that of free dorsals (Fig. 19). The vertebra gradually expands transversely in dorsal direction without a clear boundary between the centrum and neural arch. The dorsal margins of cotyle and condyle are usually deeply incised by the neural canal. The ventral floor of the neural canal could be even deeper and reach the middle of the centrum height. The ventral surface of the centrum is round in cross-section and smooth. The neural arch is inclined anteriorly at various extents so the prezygapophyses project anterior to the centrum and postzygapophyses are placed

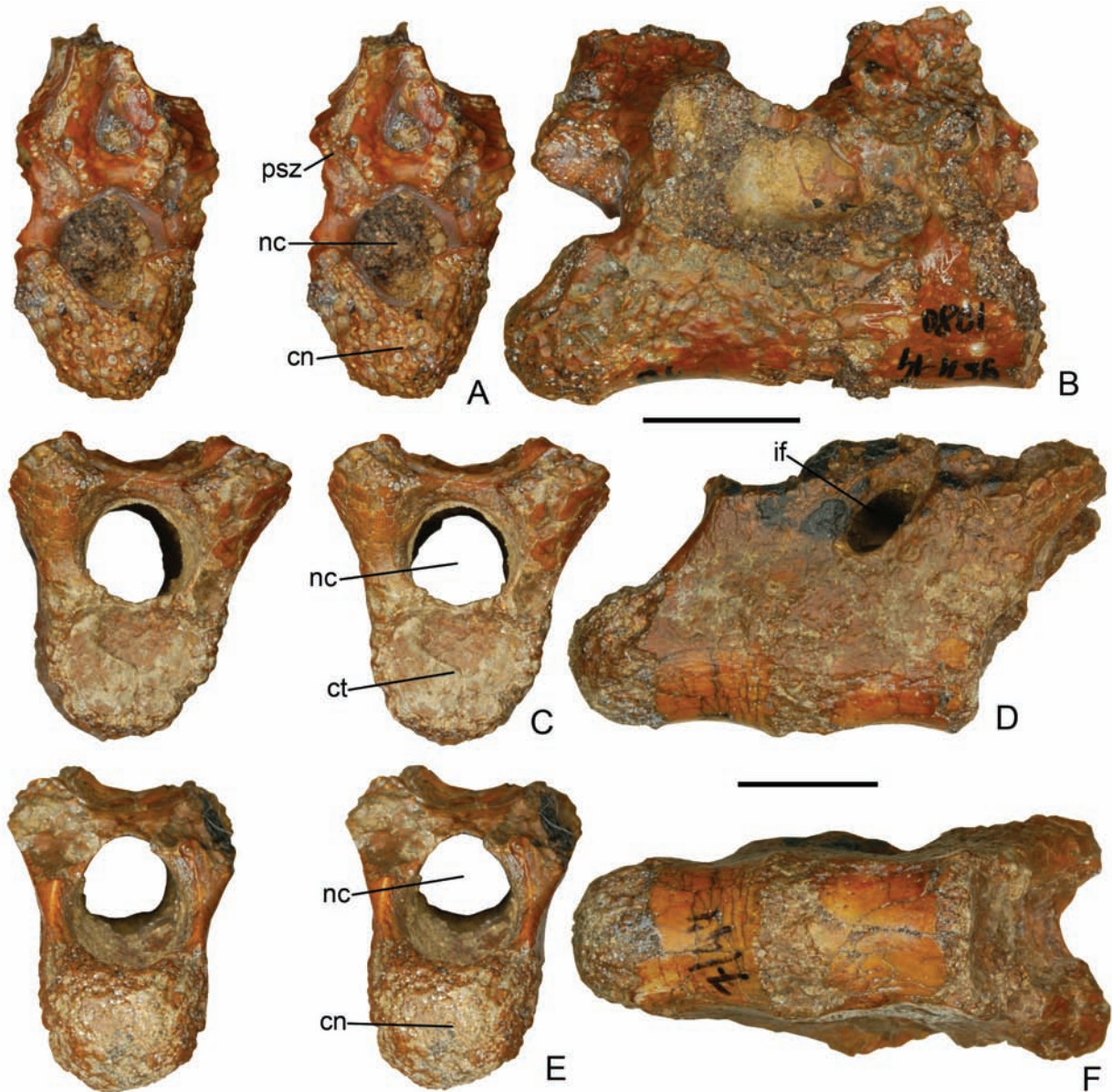


Fig. 18. Posterior notarium fragment (A, B; ZIN PH 6/44) and fused dorsals (C–F; ZIN PH 7/44) of *Azhdarcho lancicollis*, in anterior (A, C, stereopairs), lateral (B, D), posterior (E, stereopair), and ventral (F) views.

Abbreviations: cn – condyle; ct – cotyle; if – intervertebral foramen; nc – neural canal; psz – postzygapophysis. Scale bars = 1 cm.

anterior to the condyle end. The neural canal is relatively large and oval (long diameter vertical). The neural arch is poorly preserved in known specimens. The postzygapophyses are well separated with a deep groove between them. There is a small pneumatic foramen lateral to the base of the postzygapophyseal

articulation surface. In juvenile specimen ZIN PH 155/44 there is a considerable depression between the prezygapophyses and the missing neural spine bordered anteriorly by a distinct ridge (this region is not preserved in other specimens). In this specimen there is also a complex depression on the anterior side

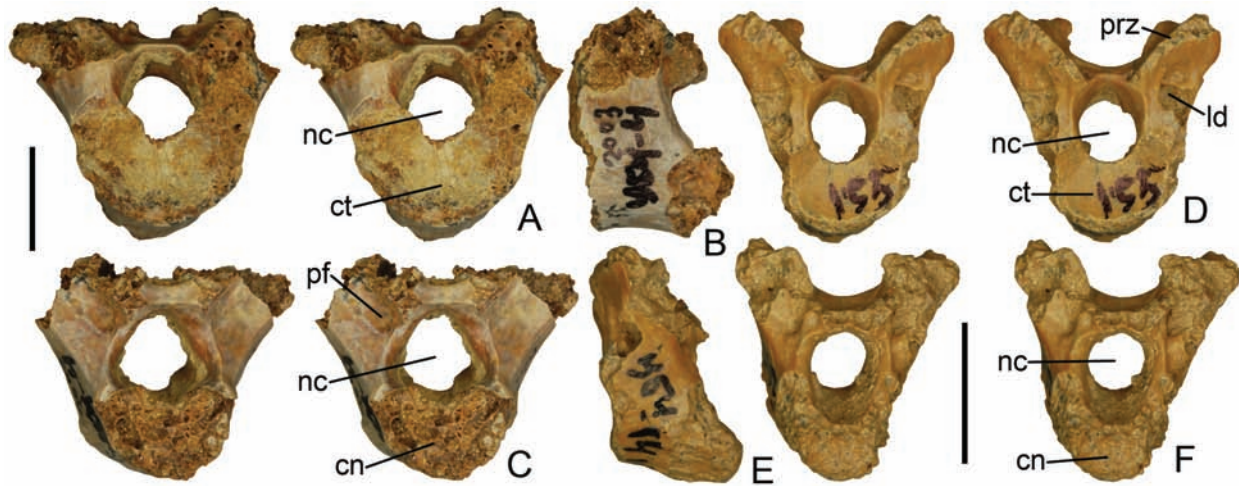


Fig. 19. Free dorsals of *Azhdarcho lancicollis*: A–C, ZIN PH 154/44, in anterior (A, stereopair), lateral (B), and posterior (C, stereopair) views; D–F, ZIN PH 155/44, in anterior (D, stereopair), lateral (E), and posterior (F, stereopair) views.

Abbreviations: cn – condyle; ct – cotyle; ld – lateral depression; nc – neural canal; pf – pneumatic foramen; prz – prezygapophysis. Scale bars = 1 cm.

of the neural arch lateral the neural canal and beneath the prezygapophyses (Fig. 19D). The prezygapophysal articulation surfaces are transversely wide and short anteroposteriorly.

Comparison. Notarium is present in all large pterodactyloids and consists of four-six fused vertebrae (Bennett 2001). For *Azhdarcho* the notarium is known only from immature specimens with two fused vertebrae and a larger fragment with three fused vertebrae (ZIN PH 153/44). In this specimen the last preserved vertebra show coossification with the subsequent vertebra which gives minimum count four for the notarial vertebrae.

An azhdarchid notarium fragment consisting of four fused vertebrae is known from the Campanian-Maastrichtian of Spain (Astibia et al. 1991: fig. 5; Buffetaut 1999: 291). It preserves completely fused supraneural plate and has triangular foramina between the neural spines and the supraneural plate. In ZIN PH 6/44 these foramina seems to be more round.

Bennettazhia has two fused dorsal vertebrae with free anterior and posterior ends (Gilmore 1928: fig. 2). Like ZIN PH 7/44 of *Azhdarcho* these vertebrae are likely not part of the notarium or synsacrum. These specimens are similar except in *Azhdarcho* the neural arches are more anteriorly inclined. These two anterior “free” dorsals were apparently fused to the notarium in *Volgadraco* (Averianov et al. 2008: pl. 6, fig. 1).

Bennett (2001: 52) noted that centra of dorsal vertebrae of *Azhdarcho* are relatively broader than in *Pteranodon*, with width to height ratio about 1.6. This observation seems to be correct although he did not specify on what material it is based. In few known dorsals of *Azhdarcho* with partially preserved neural arch it is anteriorly inclined at various extend, while in dorsals of *Pteranodon* the neural arch is vertical.

An isolated free dorsal almost identical to the vertebrae of *Azhdarcho* was reported from the Turonian-Coniacian of Kazakhstan (Averianov 2007: fig. 1).

Dorsal ribs

Material. Proximal end: ZIN PH 161/44 (CBI-4). Distal ends: ZIN PH 162/44 (CBI-14, 1984); ZIN PH 163/44 (CBI-14); ZIN PH 164/44 (CBI-14, 2004); ZIN PH 165/44 (CBI-14); ZIN PH 166/44 (CBI-); ZIN PH 167/44 (CBI-17); ZIN PH 168/44 (CBI-); ZIN PH 169/44 (CBI-).

Description. ZIN PH 161/44 is a proximal fragment of free dorsal rib with preserved capitulum and tuberculum (Fig. 20A–C). The capitulum is near globular with the well developed articulation surfaces divided into two parts meeting at a wide angle. There is no distinct neck of the capitulum. The tuberculum is ridge-like and approximately as long as the capitu-



Fig. 20. Dorsal ribs of *Azhdarcho lancicollis*: A–C, ZIN PH 161/44, proximal fragment, in posterior (A), anterior (B), and proximal (C) views; D–G, ZIN PH 168/44, ventral fragment in four different views; H–K, ZIN PH 169/44, ventral fragment in four different views.

Abbreviations: ca – capitulum; pf – pneumatic foramen; tu – tuberculum. Scale bars = 5 mm.

lum. It is oriented perpendicular to the shaft which is antero-posteriorly flattened. The shaft is hollow. A small pneumatic foramen is just distal to the capitulum on the posterior side. On this side there is also an oval depression distal to the tuberculum bordered

medially by a short ridge. This depression possible served for insertion of the external intercostal muscle elevating the rib.

In collection there are several peculiar fragments which Nessov (1991a: 21) considered to be distal ends of the dorsal ribs (Fig. 20D–K). This interpretation is followed here. These evidently distal ends of the notarial ribs articulating with the sternum (in *Pteranodon* distal ends of free dorsal ribs were possible not ossifying [Bennett 2001]). The distal end has three processes: the middle process with globular articulation surface on a distinct neck and two lateral processes. One lateral process is small and spine-like (not complete on either specimen), the opposite process is large, plate-like, and spirally curved. Along the rib shaft there is a marked ridge disappearing before the distal end. The shaft is hollow and triangular in cross-section when the ridge is present.

Comparison. The distal rib fragments described above are similar with distal ends of notarial ribs of *Pteranodon* (Bennett 2001: fig. 56) in curvature and in having a longitudinal ridge and more or less globular distal articulation surface. However, they are markedly different in having two additional lateral processes. Nothing similar has been described for pterosaurs, but the structure of the dorsal ribs is imperfectly known for these animals (Bennett 2001).

Sternum

Material. Anterior fragments: ZIN PH 170/44 (CBI-5, 2006); ZIN PH 171/44 (CBI-5a, 1989).

Description. The sternum of *Azhdarcho* is known from two fragments, ZIN PH 170/44 and 171/44, one of which is more complete but covered by the matrix and other with better visible coracoid facets (Fig. 21). The cristospine is a massive hook-like process which is completely ventral to the sternal plate (assuming that the sternal plate was horizontally oriented). The cristospine does not project anteriorly beyond the coracoid facets. The coracoid facets are asymmetrical and alternating, one in front of the other, with saddle-shaped anterolaterally facing articulation surfaces. The ventral keel of the cristospine is relatively high and robust. The dorsal side of the sternal plate is deeply concave with a depression in the middle of the preserved portion (presence of pneumatic foramen within this depression cannot be established because this area is covered by the matrix).

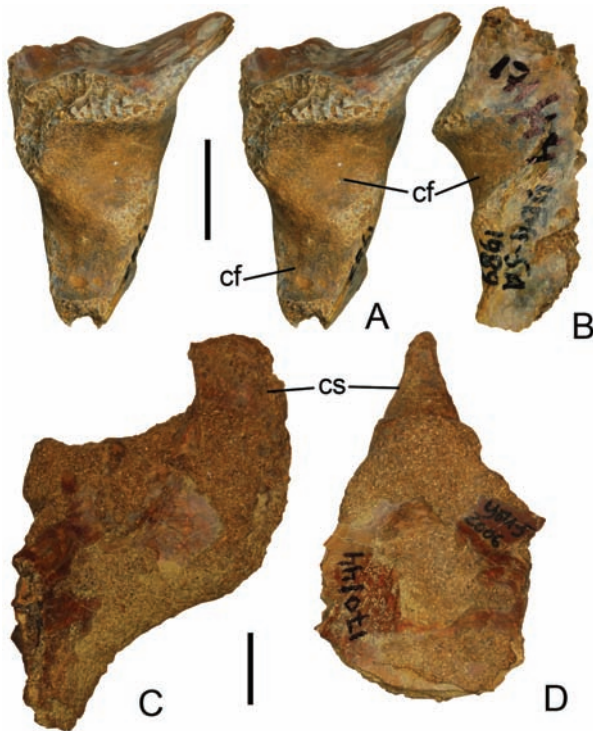


Fig. 21. Sternum fragments of *Azhdarcho lancicollis*: A, B – ZIN PH 171/44, in anterior (A, stereopair) and lateral (B) views; C, D – ZIN PH 170/44, in lateral (C) and dorsal (D) views.

Abbreviations: cf – coracoid facet; cs – cristospine. Scale bars = 1 cm.

Comparison. Azhdarchids have a primitive morphology of the cristospine with asymmetrical (alternating) position of coracoid facets, shared also by “rhamphorhynchoids,” *Dsungaripterus*, *Tupuxuara*, and some other pterodactyloids (Kellner 1995; Bennett 2001; Frey et al. 2003). In ornithocheiroids position of the sternocoracoid joints is symmetrical, side by side (Bennett 2001). The structure of the cristospine is markedly different in *Azhdarcho* and *Pteranodon*. In *Pteranodon* it is placed anterior to the sternal plate, coracoid facets are facing dorsolaterally, and the cristospine projects much anterior to the coracoid facets. In *Azhdarcho* it is short and hook-like, ventral to the sternal plate, coracoid facets are facing anterolaterally, and it is not protruding anteriorly beyond the sternocoracoid joints.

Scapulocoracoid

Material. Fragments with glenoid fossa: ZIN PH 173/44, right (CBI-5a, 1984); ZIN PH 174/44,

right (CBI-14, 1987); ZIN PH 175/44, right (CBI-14, 1984). Fragmentary juvenile coracoids unfused with scapula: ZIN PH 176/44, left (CBI-); ZIN PH 177/44, right (CBI-4, 1989); ZIN PH 178/44, right (CBI-14, 1987); ZIN PH 182/44, left (CBI-14). Distal coracoid fragments: ZIN PH 179/44, left (CBI-14); ZIN PH 180/44, right (CBI-14); ZIN PH 181/44, right (CBI-14, 1989).

Description. The scapulocoracoid is known from three fragments representing glenoid fossa (Fig. 22A–C), several juvenile unfused fragmentary coracoids (Fig. 22D–H), and distal coracoid fragments, and several pieces that could be parts of the scapula. The latter suggest that the distal scapula facet for articulation with the notarium was narrow and slightly concave, but identification of these specimens is not certain.

The glenoid fossa has a complex saddle-shaped articulation surface which is complementary to the saddle-shaped humeral head. It is divided into two unequal parts by a vertical ridge, anterior and posterior if the ridge is lateral (orientation of the glenoid is not certain). The anterior part is about three times larger than posterior part and extends more ventrally compared with the latter. The boundary between fused scapula and coracoid is marked by a distinct groove. The scapular part of the glenoid fossa is distinctly larger than the coracoid part. The glenoid fossa is bordered by prominent supra- and infraglenoid buttresses. The infraglenoid buttress is hook-like wrapping around a smooth depressed area. At the ventral area of the anterior articulation surface of the glenoid there is a large foramen leading to the canal directing posteromedially. Possibly this canal is connecting with a deep furrow along the anterior margin of proximal coracoid seen in other specimens. The lateral edge of the scapula dorsal to the glenoid fossa is a sharp ridge flanked anteromedially by a distinct groove.

The coracoid was likely oriented almost horizontally. The proximal part of the posterior surface is occupied by a prominent coracoid flange with heavy sculpture on dorsal surface for insertion of m. sternocoracoideus. The coracoid shaft in the middle has a rhomboid cross-section with a prominent dorsal ridge that border anteriorly the m. sternocoracoideus attachment area. More distally the coracoid becomes more flattened and expands at the end. In this region there is a deep and wide groove on the dorsal coracoid surface along its anterior margin. The distal end of coracoid is concave with saddle-shaped articulation facet for the sternum.



Fig. 22. Scapulocoracoid fragments of *Azhdarcho lancicollis*: A–C – ZIN PH 175/44, right fragment with glenoid fossa, in posterior (A), lateral (B, stereopair), and anterior (C) views; D–F – ZIN PH 179/44, distal fragment of left coracoid, in ventral (D), dorsal (E), and distal (F) views; G, H – ZIN PH 176/44, left juvenile coracoid fragment unfused with scapula, in dorsal (G) and posterior (H) views.

Abbreviations: cfl – coracoid flange; f – foramen; gl – glenoid; gr – groove; igb – infraglenoid buttress; sgb – supraglenoid buttress; sta – sternal articulation. Scale bars = 1 cm.

Comparison. The coracoid of *Azhdarcho* is similar to the coracoid of *Quetzalcoatlus* (Wellnhofer 1991b: fig. on p. 144; Frey et al. 2003: fig. 1b) in having a prominent coracoid flange and a deep vertical groove on scapula dorsal to the glenoid. An expanded coracoid flange occupying more than half the total shaft length of the coracoid is a possible synapomorphy

for the Azhdarchidae (Kellner and Langston 1996; Unwin and Lü 1997). McGowen et al. (2002) and Godfrey and Currie (2005) described a large pneumatic foramen anteromedial to the glenoid fossa. This corresponds in position to the large canal opening described above for *Azhdarcho*. Nessov (1991a) thought that this canal was housing the supracora-

coid ligament lifting the wing. The profile of the glenoid fossa in *Azhdarcho* is more deeply concave than in *Montanazhdarcho* (McGowen et al. 2002: fig. 3C).

A juvenile coracoid unfused with scapula very similar to that of *Azhdarcho* is known from the Cenomanian of Uzbekistan (Averianov 2007: pl. 8, fig. 1).

The scapulocoracoid fragment of an azhdarchid from the Campanian of Alberta, Canada figured by Godfrey and Currie (2005: fig. 16.6A) in one unspecified view is difficult to compare with that bone in *Azhdarcho*.

Humerus

Material. ZIN PH 12/44, left humerus lacking distal end (CBI-4v). ZIN PH 26/44, left proximal fragment (CBI-14, 1984). ZIN PH 89/44, left proximal fragment (CBI-5, 2006). ZIN PH 24/44, right proximal fragment lacking humeral head (CBI-41, 1984). ZIN PH 25/44, left proximal fragment lacking humeral head (CBI-4, 1989). ZIN PH 27/44, left proximal fragment lacking humeral head (CBI-4, 1987). ZIN PH 13/44, left humeral head (CBI-4, 2003). ZIN PH 29/44, left humeral head (CBI-14, 1987). ZIN PH 90/44, right humeral head (CBI-4). CCMGE 8/12454, right distal fragment (CBI-41, 1985). ZIN PH 8/44, left distal fragment (CBI-56, 1989). ZIN PH 9/44, right distal fragment (CBI-4g). ZIN PH 10/44, right distal fragment (CBI-41, 1987). ZIN PH 11/44, left distal fragment (CBI-4, 2003). ZIN PH 91/44, right distal fragment (CBI-14). ZIN PH 92/44, left distal fragment (CBI-, 2006). ZIN PH 93/44, right juvenile humerus (CBI-14, 2006). ZIN PO 6472, left juvenile humerus lacking proximal and distal ends (CBI-14).

Description. The humerus is represented by several proximal and distal fragments, ZIN PH 12/44 having nearly completely preserved shaft (Fig. 23A E), and ZIN PH 93/44, complete juvenile specimen. The humeral head is not complete on either specimen. It is largest in ZIN PH 90/44 with PW more than 43.0. The humeral head is broad and crescentic in proximal view, with saddle shaped articular surface, convex anteroposteriorly and concave dorsoventrally. The articular surface is asymmetrical, with the widest point closer to the ventral side than to the dorsal side. The humeral neck is inclined posteriorly to the long axis of the shaft at an angle of $\sim 38^\circ$. The anterior side of the neck is variously depressed, with a small cleft-like pneumatic foramen at the base of the delto-

pectoral crest (this area is best preserved in ZIN PH 26/44; Fig. 23I). In ZIN PH 12/44 this pneumatic foramen is revealed as a large hollow space between the dense trabecular bone tissue of the humeral neck and the deltopectoral crest (Fig. 23D). The articular surface of the humeral head overhangs the neck along the posterior side, so it is exposed posteriorly at much greater extent than anteriorly.

The deltopectoral crest is placed along the dorsal border of the bone close to the proximal head and directed anteriorly. The angle between the deltopectoral crest and the long axis of humeral head is $\sim 80^\circ$. The deltopectoral crest is curved in dorsoventral plane, with convex dorsal and concave ventral sides. Its entire length is preserved only in ZIN PH 24/44 (Fig. 23F–H). Its width gradually decreases distally, with the end about 1.5 times narrower than the base. The distal end of the deltopectoral crest has no bulbous expansion. The ulnar crest is destroyed in all specimens, except the juvenile ZIN PH 93/44.

The shaft of the humerus is best preserved in ZIN PH 12/44 (Fig. 23A–E). The shaft is relatively short, slightly convex posteriorly, and subtriangular in cross-section, with flat or concave anterior side, and convex posteroventral and dorsal sides. The dorsal side of the shaft is divided into two surfaces by a line between the deltopectoral crest and the supracondylar tubercle: the proximal part of this surface is facing posterodorsally and the distal part is facing anterodorsally. On this distal surface, close to the line described above, there is an oval scar impression possible for m. triceps (Fig. 23B; Bennett 2003: fig. 3B). The minimum constriction of the shaft is little more proximal relative to the bone center. On posterodorsal side, opposite and distal to the deltopectoral crest, there is a prominent longitudinal muscle scar, possible for m. teres major and m. latissimus dorsi (Fig. 23B; Bennett 2003: fig. 3C). A similar muscle scar is preserved in ZIN PH 26/44. The shaft is gradually expanding distally towards the distal epiphysis.

The distal end of humerus is known from several fragments, among which CCMGE 8/12454 is the best preserved (DW = 48.6; Fig. 24). The largest specimen in the sample is ZIN PH 8/44 with DW ~ 61.0 . The epiphysis is D-shaped in distal view, with flat anterior side and convex posterior, dorsal, and ventral sides. The border between the anterior and ventral side is rounded and indistinct while between the anterior and dorsal sides there is a sharp ridge extending distally towards the ectepicondyle. On this ridge,

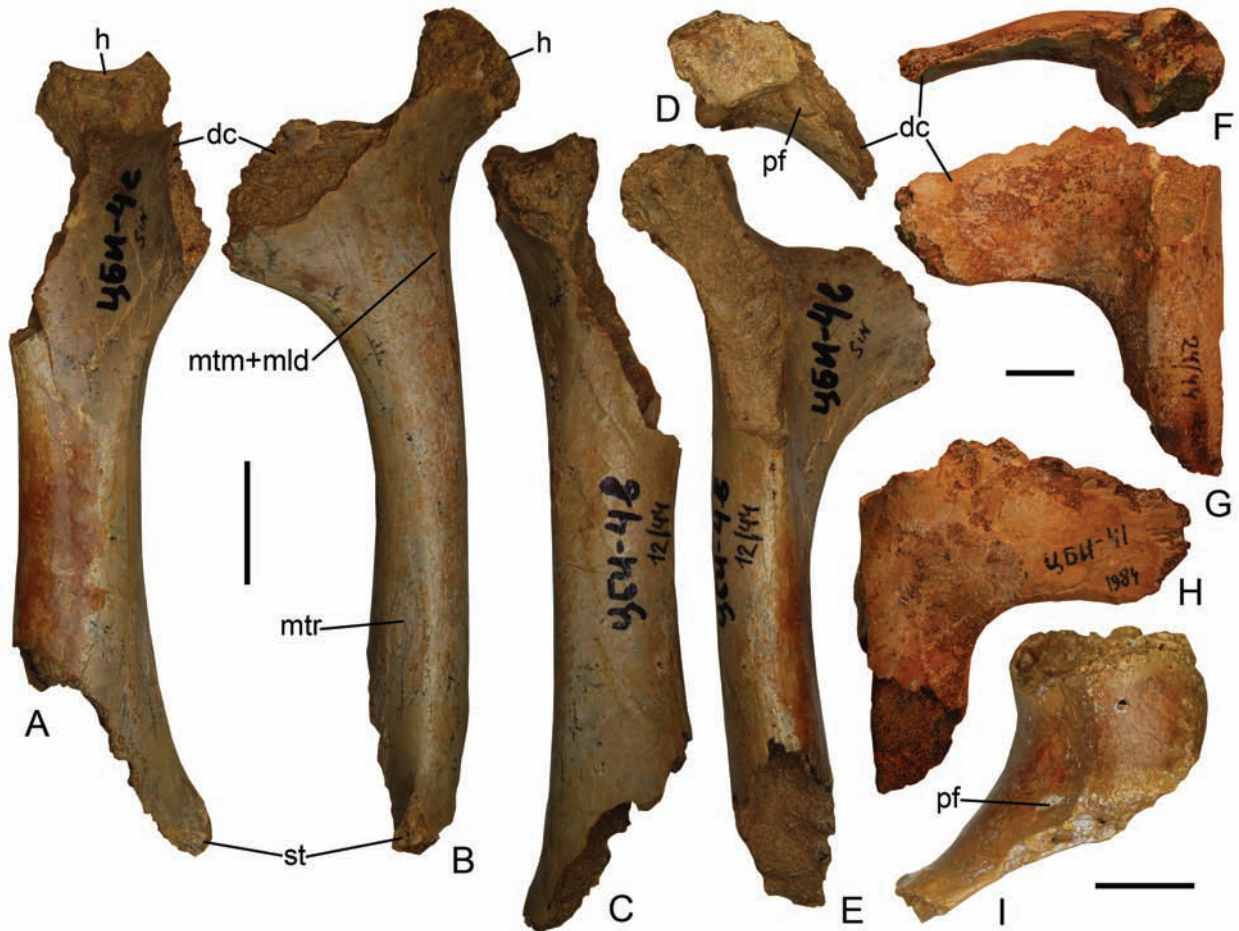


Fig. 23. Humerus fragments of *Azhdarcho lancicollis*: A–E – ZIN PH 12/44, left humerus lacking distal end, in anterior (A), dorsal (B), posterior (C), proximal (D), and ventral (E) views; F–H – ZIN PH 24/44, right proximal fragment, in proximal (F), ventral (G), and dorsal (H) views; I – ZIN PH 26/44, left proximal fragment, in proximal view.

Abbreviations: dc – deltopectoral crest; h – head; mtm+mld – scar for m. teres major and m. latissimus dorsi; mtr – scar for m. triceps; pf – pneumatic foramen; st – supracondylar tubercle. Scale bars = 2 cm (A–E) and 1 cm (F–I).

about 2 cm proximal from the ectepicondyle, there is a prominent supracondylar tubercle for the insertion of the flexors of the carpus and digits (Bennett 1989: fig. 1; 2003: fig. 3D).

The anterior side of the epiphysis is dominated by the capitulum, an oblique semicircular condyle for articulation with the radius and the dorsal (capitular) cotyle of ulna. The trochlea, a smaller and less rounded condyle for articulation with the ventral (trochlear) cotyle of ulna, is placed at the anteroventral corner of the epiphysis. In all relevant specimens there is a prominent groove on the trochlea possible housed a thick layer of articulation cartilage. The

capitulum and trochlea are separated by a deep intertrochlear sulcus. The articular surfaces of capitulum and trochlea extend on both anterior and distal sides of the epiphysis. The long axis of the capitulum is oriented at an angle of $\sim 60^\circ$ to the anterior side (in distal view). On anterior side, the capitulum is placed in the center of the epiphysis and surrounded by a depressed area ventrally and deep narrow groove (fovea supratrochlearis ventralis) dorsally. On the distal side, the capitulum extends towards the posterodorsal corner of the epiphysis. At the posterior margin of the distal side of the epiphysis there is a prominent ulnar tubercle continuing posterodorsally

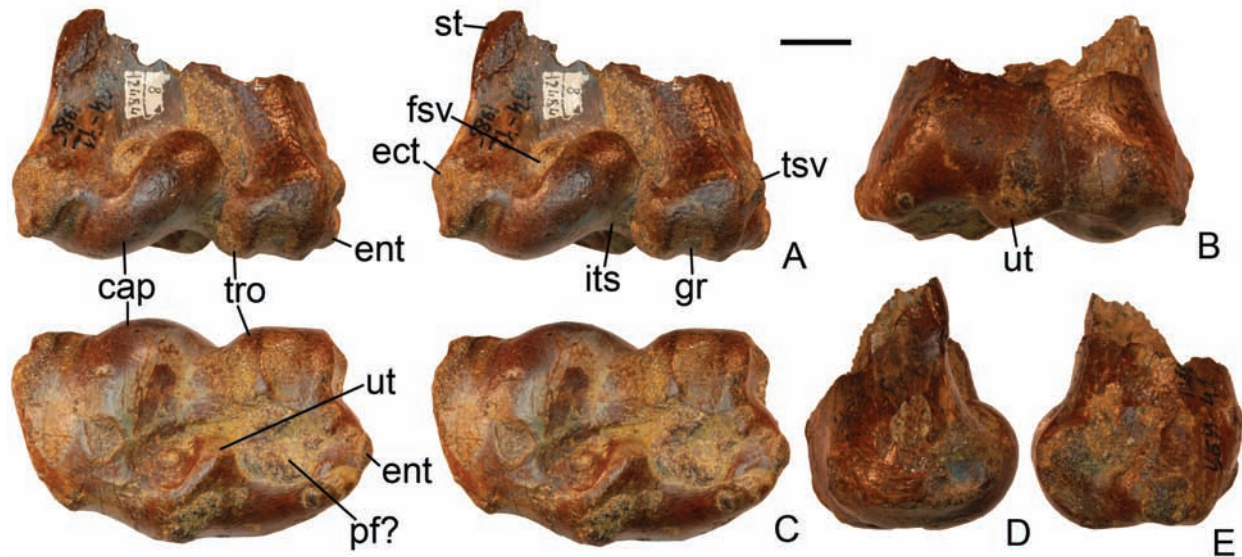


Fig. 24. CCMGE 8/12454, distal fragment of right humerus of *Azhdarcho lancicollis*, in anterior (A, stereopair), posterior (B), distal (C, stereopair), dorsal (D), and ventral (E) views.

Abbreviations: cap – capitulum; ect – ectepicondyle; ent – entepicondyle; fsv – fovea supratrochlearis ventralis; gr – groove; its – intertrochlear sulcus; pf – pneumatic foramen; st – supracondylar tubercle; tro – trochlea; tsv – tuberculum supracondyloideum ventralis; ut – ulnar condyle. Scale bar = 1 cm.

into a short ridge. The ulnar tubercle is placed at the level between the capitulum and trochlea and separated from the articular surfaces of these condyles by a crescentic depression. The ventral half of this depression, opposite to the trochlea, bears numerous small foramina and apparently corresponds to the pneumatic foramen present in this place in *Montana-azhdarcho* (McGowen et al. 2002: p. 6) and in *Quetzalcoatlus* (according to coding of this taxon in Andres and Ji 2008). This area is best preserved in ZIN PH 8/44 where the bone breakage just proximal to this depression does not reveal any hole that would be expected for a pneumatic foramen.

The ectepicondyle is separated from the capitulum by a shallow groove and has a small round depression. The entepicondyle is a bump-like eminence at the posteroventral corner of the epiphysis separated from the trochlea by a wide ventral groove. Just ventral to the trochlea there is a small tubercle, tuberculum supracondyloideum ventralis.

ZIN PH 93/44 is a tiny complete humerus without fused distal epiphysis and with total L = 12.6 (not figured here because it is covered by a thick layer of sandstone preventing it from damage). This bone may come from an embryo or recently hatched

animal. In proportions it is almost identical to more adult specimens. ZIN PO 6472 is about twice larger specimen with missing proximal and distal ends.

Comparison. Azhdarchidae retain a primitive pterodactyloid construction of the humerus with flat deltopectoral crest (Bennett 1989, 2001; Padian and Smith 1992). According to Padian and Smith (1992) and Unwin and Lü (1997) the following construction of the deltopectoral crest is diagnostic for Azhdarchidae: it is displaced distally from the humeral head, elongate, and lacks a distal expansion. All these features are found in *Azhdarcho*. McGowen et al. (2002) also considered lack of distal expansion of the deltopectoral crest to be diagnostic for the Azhdarchidae. In all adequately preserved humeri of Azhdarchidae there is a pneumatic foramen on the anterior side between the humeral neck and the base of the deltopectoral crest, and there is no proximal pneumatic on the dorsal side. The same pattern of proximal pneumatization of the humerus is found also in non-azhdarchid azhdarchoids and in lonchodectids; in dsungaripterids the proximal pneumatic foramen is on the dorsal side (Kellner 1995; Witton et al. 2009). The anterior proximal pneumatic foramen is found also in *Pteranodon* whereas the other ornithocheir-

oids have the dorsal proximal pneumatic foramen on the humerus (e.g., Weishampel 1985; Kellner and Tomida 2000; Bennett 2001).

The humerus of *Bennettazhia* is very similar to that of *Azhdarcho*. The differences in the humerus morphology noted in the diagnosis of the former genus by Nessov (1991a: 20–21) are not confirmed by this study; possibly they were based on not adequate drawings published by Gilmore (1928: fig. 1). I had an opportunity to study the type material of *B. oregonensis* Gilmore, 1928 in the National Museum of Natural History, Washington. The humerus of that species has a somewhat hatchet-shaped deltopectoral crest, while in *Azhdarcho* it is gradually tapering towards the end. Another difference is in the shape of the distal epiphysis in distal view, but this region is poorly preserved in the type humerus of *B. oregonensis* which precludes a more detailed comparison. An isolated humerus similar to that bone in *Azhdarcho* and *Bennettazhia* has been described from Aptian-Albian of Texas, USA (Murry et al. 1991: figs 1–2).

The humerus of *Azhdarcho* is very similar to the azhdarchid humeri from the Campanian of Alberta, Canada (Godfrey and Currie 2005: fig. 16.6B–G) except it has a ridge for the muscle attachment instead of trough-like depressions in Canadian specimens. *Azhdarcho* differs from *Montanazhdarcho* by lack of a distinct pneumatic foramen on the distal surface of the distal epiphysis of humerus.

In *Quetzalcoatlus* (Lawson 1975: fig. 1b–d; Langston 1981: fig. on p. 102), the humerus is more robust than in *Azhdarcho* and has hypertrophied deltopectoral crest and supracondylar tubercle. The humerus of a large azhdarchid from the Maastrichtian of Montana, USA (Padian and Smith 1992: fig. 1A–F) is known from fragments.

Ulna

Material. ZIN PH 86/44, left ulna lacking distal end and with mostly destroyed proximal end (CBI-14, 2006). ZIN PH 41/44, left proximal fragment (CBI-). ZIN PH 14/44, right distal end (CBI-41, 1984). ZIN PH 15/44, left distal end (CBI-4v).

Description. ZIN PH 86/44 is the largest specimen with essentially complete shaft but with proximal end mostly destroyed and distal end missing (PW is more than 53.5; not figured here). ZIN PH 41/44 is a better preserved and twice smaller proximal fragment (PW = 26.9; Fig. 25A–E). The olecranon process on

the posterior side for insertion of m. triceps brachii is destroyed in this specimen. The articulation surfaces of the dorsal (capitular) and ventral (trochlear) cotyles are partially preserved. What is preserved from the articular surfaces is slightly convex for the ventral cotyle and saddle-shaped for the dorsal cotyle. The articular surfaces are faced anteroproximally (in life the ulna was placed at an obtuse angle to the humerus and these surfaces could be facing strictly medially). There is a large oval pneumatic foramen on the anterior side just distal to and between the cotyles. A much smaller pneumatic foramen is adjacent to the dorsal border of the larger foramen. In ZIN PH 41/44 there is a remnant of a proportionally smaller pneumatic foramen between the cotyles. A distinct short crest for insertion of collateral ligaments is developed along the ventral edge of the bone beneath the ventral cotyle. A low biceps tubercle with an oblique groove for insertion of m. biceps brachii is present anteroventral to the large pneumatic foramen. Distally to the biceps tubercle there is a conspicuous linear scar extending up to the preserved distal end of the fragment. This scar is probably for insertion of an interosseus membrane between the ulna and radius. In ZIN PH 86/44 the biceps tubercle is very weak and the scar for the interosseus membrane is absent.

The shaft is oval in cross-section. The minimum shaft width is about twice less than the width at the proximal end.

The distal end of ulna is known from two specimens of similar size, ZIN PH 14/44 and 15/44. The first specimen has a better preserved distal end (DW = 41.0; Fig. 25F–J), while in the second specimen the longer part of the shaft is preserved. The distal end is about 1.7 times expanded dorsoventrally compared with the shaft some distance proximal to the end. The ventral side of the end is expanded in a distinctly larger extend compared with the dorsal side. The articular surface contacting the proximal syncarpal occupies all the distal end of the bone, with a tongue-like extension of the dorsal articular surface onto the posterior side. The dorsal articular surface is nearly flat or only slightly convex. The large tuberculum is positioned closer to the ventral side. Its articular surface is destroyed. The ventral fovea is mostly destroyed but still recognizable as a round depression (Fig. 25J). On the ventral side there are remnants of the rugose area for attachment of the ulnar collateral ligaments. On the posterior side a distinct depression is between the dorsal articular surface and the tuberculum. Within

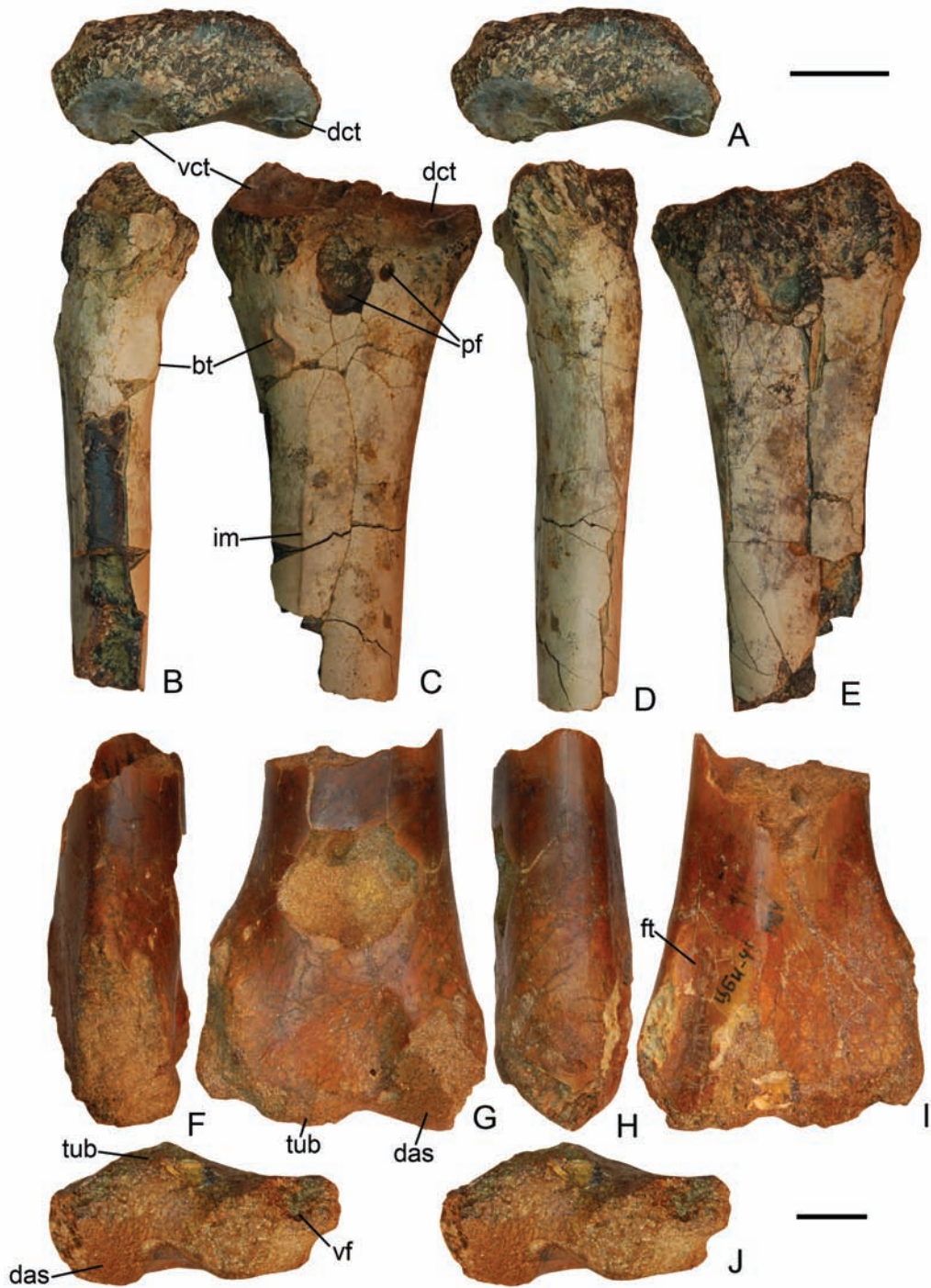


Fig. 25. Ulna fragments of *Azhdarcho lancicollis*: A–E – ZIN PH 41/44, left proximal fragment, in proximal (A, stereopair), ventral (B), anterior (C), dorsal (D), and posterior (E) views; F–J – ZIN PH 14/44, right distal fragment, in ventral (F), posterior (G), dorsal (H), anterior (I), and distal (J, stereopair).

Abbreviations: bt – biceps tubercle; das – dorsal articular surface; dct – dorsal cotyle; ft – groove for flexor tendon; im – interosseus membrane scar; pf – pneumatic foramen; tub – tuberculum; vct – ventral cotyle; vf – ventral fovea. Scale bars = 1 cm.

this depression, close to the articular border, there are two minute openings representing the pneumatic foramen. A prominent groove for the flexor tendon is extending on the anterior side along the dorsal margin. It is flanked dorsally by a distinct ridge. Another longitudinal ridge is dissecting the anterior side of the distal end into two unequal parts: a narrower flat dorsal and a wider slightly concave ventral.

Comparison. Description of ulna in *Montanazhdarcho* (McGowen et al., 2002: figs 1, 2E, 3E) as having distal end divided into two large tubercles is different from the condition seen in *Azhdarcho*. Without firsthand study of the specimen it is not clear if this difference is real or caused by distortion of the bone.

Bennett (2001: 78–79) mentioned undescribed proximal ulna fragments of *Arambourgia* and *Quetzalcoatlus*. In *Arambourgia* the cotyles are proximally oriented and there are one or two rather small pneumatic foramina on the anterior side between the cotyles. *Quetzalcoatlus* entirely lacks this pneumatic foramen.

The large proximal ulna fragment of Azhdarchidae indet. from the Maastrichtian of Western Australia (Bennett and Long 1991: figs 2, 3) is very similar to that bone in *Azhdarcho*, except it has a series of small pneumatic foramina instead of one large foramen, and has not a longitudinal ridge distal to the biceps tubercle. A similar ridge is present in an azhdarchid ulna from the Campanian of Canada (Godfrey and Currie 2005: fig. 16.7). In that specimen the pneumatic foramen between the cotyles is proportionally smaller than in ZIN PH 41/44, but almost the same in size as in ZIN PH 86/44. The distal end of the Canadian specimen is also very similar in proportions to the distal end of ulna in *Azhdarcho*.

The distal ulna fragment of Azhdarchidae indet. from the Campanian-Maastrichtian of New Zealand (Wiffen and Molnar 1988: figs 1, 2J) is also similar to the ulna of *Azhdarcho*, differing mainly in a relatively more massive end in distal view.

A poorly preserved possible azhdarchid ulna fragment is known from the Turonian of Armenia (Averianov and Atabekyan 2005; in that paper the specimen was misidentified as radius).

Radius

Material. CCMGE 8/11915, right proximal fragment (CBI-7a, 1980). ZIN PH 88/44, right proximal fragment (CBI-14, 1989). ZIN PH 199/44,

right proximal fragment (CBI-14, 2006). CCMGE 10/11915, right distal fragment (CBI-5a, 1980). ZIN PH 1/44, right distal fragment (CBI-14v, 1984). ZIN PH 28/44, right distal fragment (CBI-5, 2003). ZIN PH 87/44, right distal fragment (CBI-).

Description. The proximal end of the radius is best preserved in CCMGE 8/11915 (PW = 22.2; Fig. 26C–G). The proximal side is occupied by a tear-drop shaped concave cotyle, the articular surface contacting the capitulum of the humerus. The tubercle is a dorsal projection of the proximal end, which is as long as the maximum shaft diameter. Anterior side of the tubercle is occupied by a second articular surface which is compatible in size with the articular surface of the cotyle. The width of proximal radius narrows rapidly to a relatively slender parallel-sided shaft. The shaft is oval in cross-section, with the dorsoventral long axis. The proximal part of the shaft is better preserved in ZIN PH 199/44 (Fig. 26A, B). Proximally it has a ridge along the dorsal edge with prominent muscle scars (the proximal scar is possible for m. biceps).

There are four distal radius fragments, with DW = 13.2 in the smallest (ZIN PH 87/44) and 28.0 in the largest (ZIN PH 1/44). The distal end is about twice expanded dorsoventrally compared with the shaft diameter. The anterior side of the distal end is dominated by the large anterior tuberosity, a prominent ridge extending close and parallel to the ventral margin. Opposite to this ridge, at the distoventral end of the posterior side there is a large tubercle with ventral articular surface for the proximal syncarpal. In distal view, the line formed by this tubercle and anterior tuberosity is inclined at an angle of ~80° to the dorsoventral axis of the distal end. The distal articular surface is broadly convex and extends to the anterior tuberosity. The highest point of this convexity is at the middle of the distal end. There is no distinct pneumatic foramen at the distal end, but in all four specimens there are characteristic fields along the dorsal and ventral margins where the bone wall is eroded and a cancellar osseous structure with large spaces separated by thin bone lamellae is revealed. These two fields were possible functioning as pneumatic foramina.

Comparison. *Azhdarcho* differs from *Montanazhdarcho* by having no distinct pneumatic foramen at the distal end of radius. This foramen is also lacking in *Quetzalcoatlus* (Bennett 2001: p. 80) and in a large azhdarchid from the Maastrichtian of Montana, USA



Fig. 26. Radius fragments of *Azhdarcho lancicollis*: A, B – ZIN PH 199/44, right radius lacking distal end, in anterior (A) and posterior (B) views; C–G – CCMGE 8/11915, right proximal fragment, in proximal (C), ventral (D), anterior (E), dorsal (F), and posterior (G) views; H–L – CCMGE 10/11915, right distal fragment, in distal (H), anterior (I), ventral (J), posterior (K), and dorsal (L) views.

Abbreviations: at – anterior tuberosity; saf – second articular surface; tu – tubercle. Scale bars = 2 cm (A, B) and 1 cm (C–L).

(Padian 1984: fig. 1E–G; Padian and Smith 1992: fig. 2). The distal epiphysis of the latter specimens is similar to that of *Azhdarcho*.

The distal end of radius of an azhdarchid from the Campanian of Saratov Province, Russia (Averianov et al. 2005: fig. 2) is different from that bone

in *Azhdarcho* in having the ventral side protruding considerably more distally compared with the dorsal end.

The proximal and distal ends of the radius of *Bakonydraco* (Ösi et al. 2005: fig. 6A, B) are virtually the same as in *Azhdarcho*.

Carpus

Material. Proximal syncarpal: ZIN PH 94/44 (CBI-14, 1980), right; ZIN PH 95/44 (CBI-, 1978), right; ZIN PH 96/44 (CBI-17, 1980), right; ZIN PH 97/44 (CBI-14, 1987), left; ZIN PH 98/44 (CBI-4v), left. Distal syncarpal: ZIN PH 99/44 (CBI-14, 2004), right; ZIN PH 100/44 (CBI-5a, 1989), right; ZIN PH 101/44 (CBI-17, 1984), right; ZIN PH 102/44 (CBI-4, 1989), right; ZIN PH 103/44 (CBI-14), left; ZIN PH 104/44 (CBI-14, 1989), left fragment. Preaxial carpal: ZIN PH 183/44 (CBI-14, 1987).

Description. The proximal syncarpal is triangular in proximal/distal view (Fig. 27). On the proximal side the center is occupied by a large and deeply concave circular fovea for articulating with the tubercle of ulna. Anterodorsally and anteroventrally it is flanked by two strap-like and less concave articular surfaces. The dorsal facet is for the dorsal articulating facet of the ulna and ventral facet is for the dorsal articulation surface of the radius. Dorsal facet for the

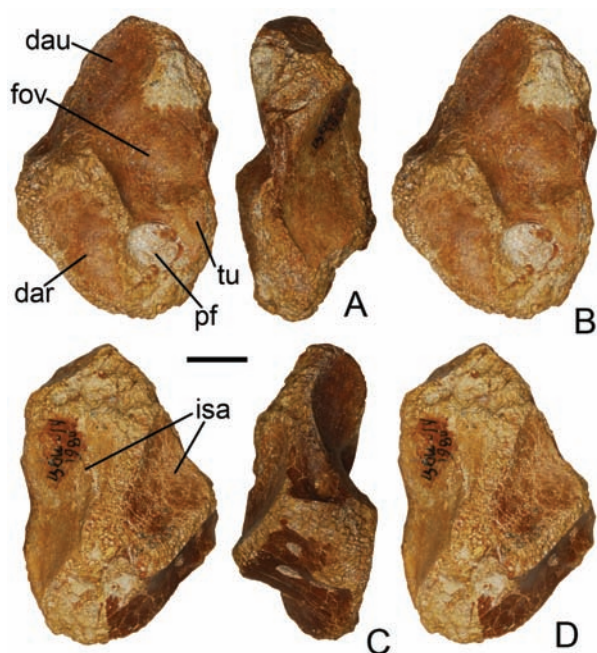


Fig. 27. ZIN PH 94/44, right proximal syncarpal of *Azhdarcho lancicollis*, in posterior (A), proximal (B, stereopair), anterior (C), and distal (D, stereopair) views.

Abbreviations: dar – facet for dorsal articular surface of radius; dau – facet for dorsal articular surface of ulna; fov – fovea; isa – intersyncarpal articular surface; pf – pneumatic foramen; tu – tuberculum. Scale bar = 1 cm.

ulna and the fovea are confluent, while ventral facet for the radius is separated from both surfaces by a high ridge. Posterior to the radius facet and ventral to the fovea there is a large circular pneumatic foramen. On the posterior margin of the bone between the fovea and this pneumatic foramen there is a tubercle. The distal side of the bone is largely occupied by the intersyncarpal articulation facet which is separated by an oblique ridge into larger posterior and smaller anterior parts. There is a small pneumatic foramen just ventral to the intersyncarpal facet and opposite to the pneumatic foramen of the proximal side (it is best preserved in ZIN PH 96/44). The free surface ventral to the intersyncarpal facet bears three large neurovascular openings.

The proximal side of the distal syncarpal mirrors the distal side of the proximal side with which it articulates (Fig. 28). The intersyncarpal facet is composed of two ridges separated by a deep oblique groove. The ridges taper in opposite directions: anterior towards dorsal side and posterior towards ventral side. Ventral to the anterior ridge there is a pneumatic foramen in ZIN PH 99/44 (it seems to be absent in ZIN PH 101/44). Along the ventral there is a short process with prominent tear-shaped convex facet for the preaxial carpal (in flight this side of the bone would be directed anteriorly). On the distal side of the bone there are large flat dorsal articulation surface and depressed about twice smaller ventral articulation surfaces (in flight orientation according to Bennett, 2001; these would be anterior and posterior surfaces in the orientation used here). Between these surfaces and the process for the preaxial carpal there is a large and deep circular fovea for articulation with the proximal tuberculum of metacarpal IV, with a pneumatic foramen inside. This foramen is opposite to the foramen on the proximal side of the bone.

The preaxial carpal is known from several very incomplete specimens among which ZIN PH 183/44 is the most complete (Fig. 29). In the preserved part it is almost identical to the element of *Bakonydraco* identified as “second? phalanx? of the wing finger” (Ősi et al. 2005: 785, fig. 6C). On the proximal end there is large oval cotyle for articulating with the distal syncarpal. There is no longitudinal groove preserved in this fragment.

Comparison. *Azhdarcho* is similar with *Quetzalcoatlus* and *Dsungaripterus* in having the dorsal articulating surface of distal syncarpal for articulating with the fourth metacarpal considerable smaller than

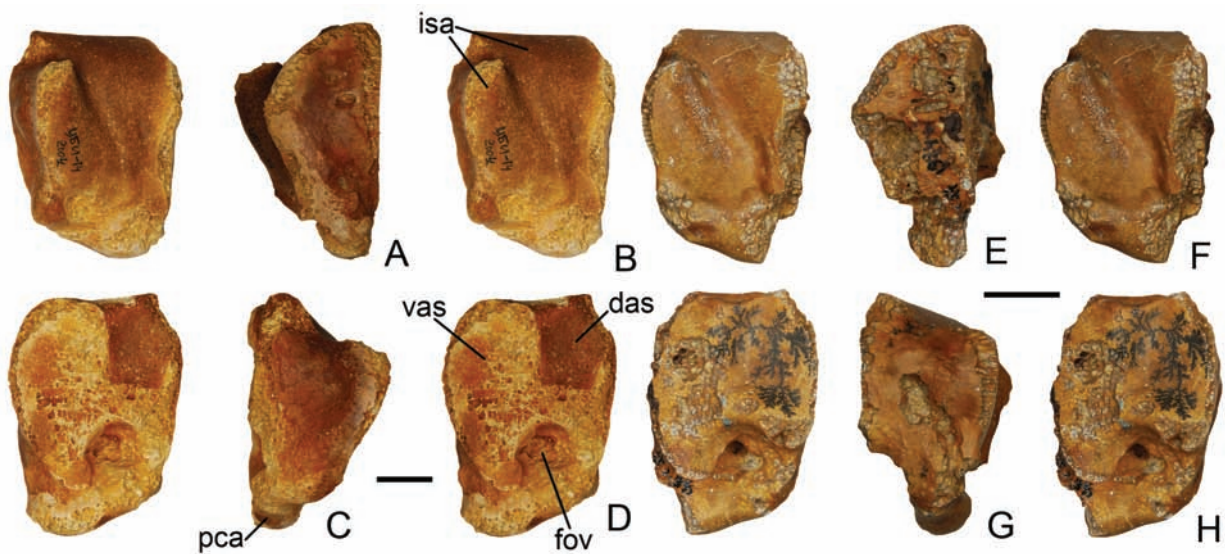


Fig. 28. Right distal syncarpals of *Azhdarcho lancicollis* (A–D – ZIN PH 99/44; E–H – ZIN PH 101/44), in anterior (A, E), proximal (B, F, stereopairs), posterior (C, G), and distal (D, H, stereopairs) views.

Abbreviations: das – dorsal articular surface; fov – fovea; isa – intersyncarpal articular surface; pca – facet for preaxial carpal; vas – ventral articular surface. Scale bars = 1 cm.

the ventral surface while in *Pteranodon* and *Nyctosaurus* both surfaces are subequal in size. Bennett (2001) discussed also difference between these taxa in the length of the preaxial carpal process resulting in the shape of the distal syncarpal. This observation was possible based on the previously figured specimen ZIN PH 101/44 (Nessov and Yarkov 1989: fig. 2-2; Nessov 1997: pl. 16, fig. 2), where the preaxial carpal process is not complete. The newly collected specimen ZIN PH 99/44 (Fig. 28A–D) show no considerable difference in shape or length of the preaxial process with that bone in *Pteranodon* (Bennett 2001: fig. 79A, B).

McGowen et al. (2002) described the proximal syncarpal of *Montanazhdarcho* as damaged and broken into two separate pieces. However, it is difficult to expect this short and stout bone to be broken when the surrounding long and hollow bones are not broken. More likely these are two proximal carpals that are still not fused ontogenetically as can be seen in some immature ornithocheiroid individuals (Wellnhofer 1985: fig. 38; Wellnhofer 1991a: fig. 19; Kellner and Tomida 2000: figs 36–41). If so this would contradict the alleged mature age of the holotype specimen of *Montanazhdarcho* (Padian et al. 2005). On the proximal side of the proximal syncarpal in *Montanazhdar-*

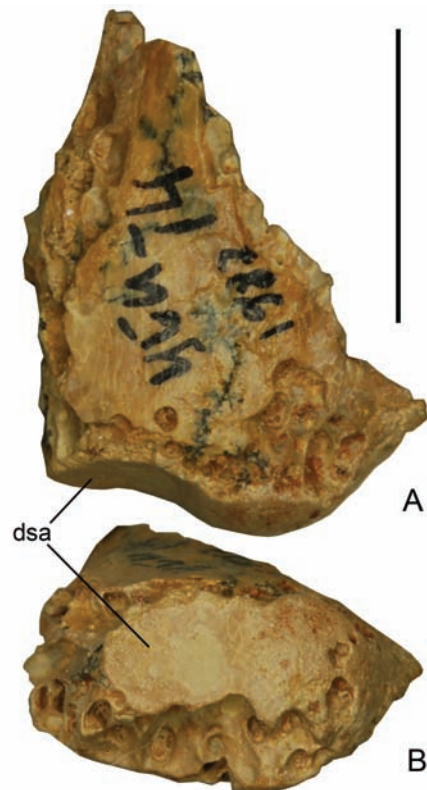


Fig. 29. ZIN PH 183/44, preaxial carpal of *Azhdarcho lancicollis*, in dorsal or ventral (A) and proximal (B) views.

Abbreviation: dsa – facet for distal syncarpal. Scale bar = 1 cm.

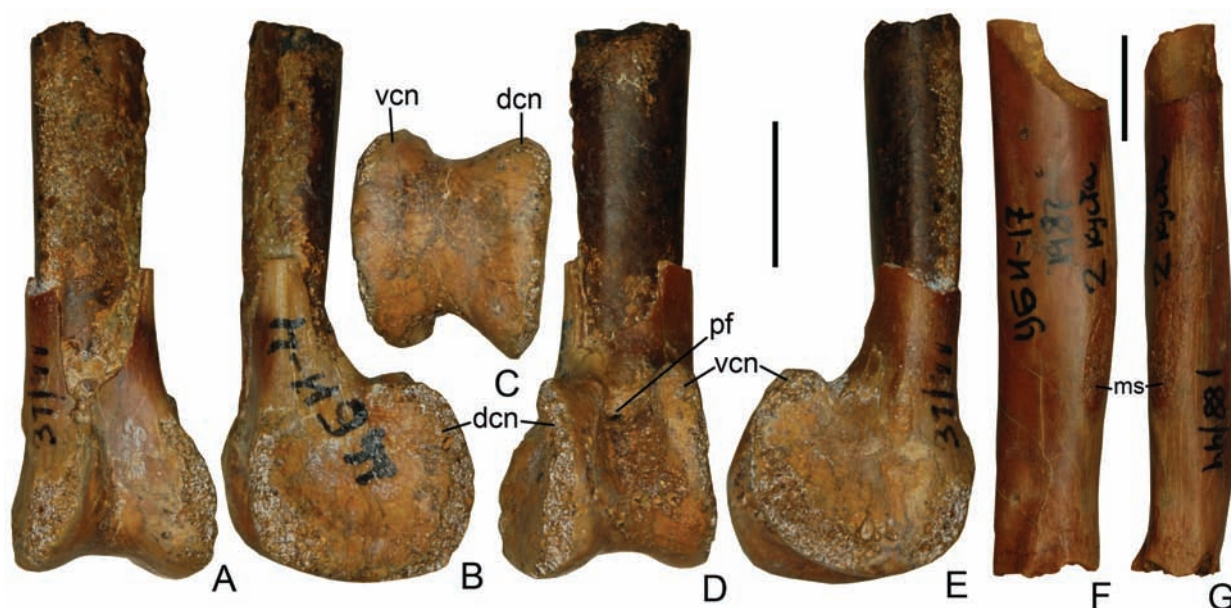


Fig. 30. Wing metacarpal fragments of *Azhdarcho lancicollis*: A–E – ZIN PH 31/44, left fragment with distal epiphysis, in anterior (A), dorsal (B), distal (C), posterior (D), and ventral (E) views; F, G – ZIN PH 188/44, right shaft fragment near distal epiphysis, in posterior (F) and dorsal (G) views.

Abbreviations: dcn – dorsal condyle; ms – muscle scar; pf – pneumatic foramen; vcn – ventral condyle. Scale bars = 1 cm.

cho there are two pneumatic foramina (McGowen et al. 2002: fig. 3F), while only one in *Azhdarcho*. The double pneumatic foramen in this place is also known for *Pteranodon* (Bennett 2001: fig. 79C).

A well preserved distal syncarpal of a large azhdarchid from the Maastrichtian of Montana, USA (Padian 1984: fig. 2A–F; Padian and Smith 1992: fig. 3) is almost identical to that bone in *Azhdarcho*.

Wing metacarpal

Material. Metacarpal IV distal fragments with epiphysis: ZIN PH 30/44, left (CBI-14, 2003); ZIN PH 31/44, left (CBI-4); ZIN PH 32/44, left (CBI-14, 1989); ZIN PH 34/44, right (CBI-4, 1987); ZIN PH 42/44, right (CBI-14); ZIN PH 43/44, right (CBI-17, 1980). Metacarpal IV distal shaft fragments: ZIN PH 33/44, left (CBI-14); ZIN PH 35/44, right (CBI-14, 1987); ZIN PH 187/44, left (CBI-5a); ZIN PH 188/44, right (CBI-17, 1987); ZIN PH 189/44, right (CBI-17, 1989).

Description. The wing metacarpal is known from shaft and distal fragments (Fig. 30). The shaft is oval in cross-section with the long axis dorsoventral. Just proximal to the distal epiphysis there is a characteris-

tic waist of the diaphysis. Proximal to this waist there is an extensive muscle scar along the dorsal edge of the shaft (Fig. 30F, G). This scar is oval with rugose sculpture distally and linear proximally. The largest specimen with preserved distal epiphysis has DW = 23.8 (ZIN PH 30/44). The distal epiphysis is pulley-like with round and subequal in size dorsal and ventral condyles. The distal end of the metacarpal is dorsally deflected and because of this the posterior edge of the dorsal condyle is visible from the anterior side. The posterior lip of the dorsal condyle is more expanded at the proximal end compared with the ventral condyle. On the posterior side in the cleft-like groove between the condyles there is a pneumatic foramen.

Comparison. A wing metacarpal fragment of a large azhdarchid has been described from the Campanian of Penza Province, Russia (Averianov 2007: pl. 8, fig. 4). It differs from that bone in *Azhdarcho* by marked depressions between proximal ends of dorsal and ventral condyles on both anterior and posterior sides; on the posterior side this depression is pierced by a net of pneumatic foramina.

A wing metacarpal from the Campanian of Alberta, Canada (Godfrey and Currie 2005: fig. 16.9) has more asymmetrical dorsal and ventral condyles

and a deep better delimited depression between their proximal ends on the posterior side. The shaft is more bent before the distal epiphysis than in *Azhdarcho*.

In some pterodactyloids there is a median ridge between the dorsal and ventral condyles of the wing metacarpal (Owen 1859: pl. 4, figs 9–11; Wellnhofer 1985: fig. 21a–d). This ridge is present also in a wing metacarpal distal fragment from the Campanian of Canada identified originally as a distal end of tibia (Currie and Padian 1983: fig. 1). In *Azhdarcho*, *Montanazhdarcho* (McGowen et al. 2002), other azhdarchids and pterodactyloids (Bennett 2001) this median ridge is absent.

Wing finger phalanges

Material. Proximal fragments of phalanx IV-1: ZIN PH 36/44, left (CBI-); ZIN PH 37/44, left (CBI-14, 1984); ZIN PH 38/44, right (CBI-52, 1989); ZIN PH 39/44, left (CBI-4); ZIN PH 201/44, left (CBI-); ZIN PH 202/44, left (CBI-14). Proximal fragments of phalanx IV-2: ZIN PH 203/44, left (CBI-14, 1984); ZIN PH 204/44, left (CBI-4, 1989); ZIN PH 205/44, left (CBI-5a, 1989); ZIN PH 206/44, left (CBI-14); ZIN PH 207/44, left (CBI-14, 1989); ZIN PH 208/44, left (CBI-14, 1987); ZIN PH 209/44, left (CBI-14); ZIN PH 210/44, right (CBI-5a, 1989); ZIN PH 211/44, right (CBI-14, 1980); ZIN PH 212/44, right (CBI-14, 1987). Proximal fragments of phalanx IV-3: ZIN PH 213/44, left (CBI-5a); ZIN PH 214/44, left (CBI-14); ZIN PH 215/44, right (CBI-14). Fragments of phalanx IV-4: ZIN PH 216/44, (CBI-14, 2003); ZIN PH 217/44, (CBI-14, 1989); ZIN PH 218/44, (CBI-4, 1987); ZIN PH 219/44, (CBI-14).

Description. The proximal wing finger phalanx IV-1 is known from several fragments (Fig. 31). In the largest specimen ZIN PH 36/44 PW = 43.6. The proximal end is anteroposteriorly expanded and bears two cotyles for articulation with the wing metacarpal. The cotyles extend on the hook-like extensor tendon projects and separated by a strong ridge which has a semicircular profile in dorsoventral profile fitting into the intercondylar sulcus of the pulley-shaped distal condyle of the wing metacarpal. The dorsal cotyle extends posteriorly into the prominent posterior process and thus it is about twice wider anteroposteriorly than the ventral cotyle. The articulation surface of the ventral cotyle is more convex than that of the dorsal cotyle. The extensor tendon process is

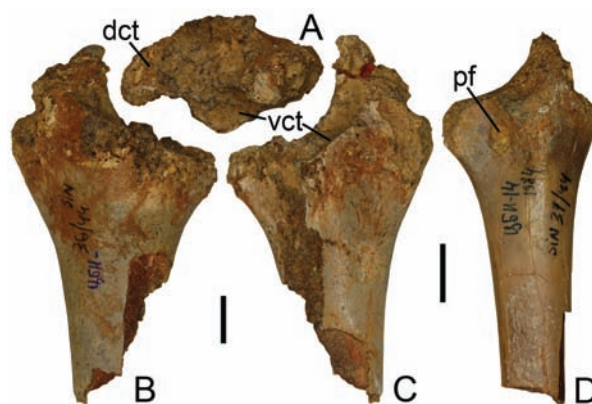


Fig. 31. Proximal fragments of proximal wing finger phalanges of *Azhdarcho lancicollis*: A–C – ZIN PH 36/44, left fragment, in proximal (A), dorsal (B), and ventral (C) views; D – ZIN PH 37/44, left fragment, in ventral view.

Abbreviations: dct – dorsal cotyle; pf – pneumatic foramen; vct – ventral cotyle. Scale bars = 1 cm.

dissected by a deep groove on anterior side. On the posteroventral side between the cotyles there is a large pneumatic foramen (Fig. 31D). Distal to this foramen there is a spacious sculptured area for muscle attachment. The shaft is gradually tapering distally. It is hollow but the bone walls are thicker than in other limb bones. The shaft is triangular in cross-section near the proximal end. Distally the cross-section becomes oval and dorsoventrally compressed.

More distal wing finger phalanges are represented by several specimens with preserved proximal end and numerous less complete fragments. These phalanges are more flattened dorsoventrally compared with the proximal wing finger phalanx and bear a prominent longitudinal ridge on the ventral side. ZIN PH 203/44 is the best preserved proximal part of the second phalanx (Fig. 32A, B). The proximal end projects posteriorly beyond the shaft. The proximal articulation surface is slightly concave and of tear-drop shape (long axis anteroposterior, pointed anteriorly). The ventral median ridge is closer to the posterior margin proximally and becomes more central distally. The dorsal surface is flat or slightly concave. The phalanx has a slight anterior curvature in the middle. The proximal articulation surface of the third phalanx is relatively shorter anteroposteriorly and more round (Fig. 32C–E). The fourth phalanx is rod-like and triangular in cross-section with golf-club like distal end (Fig. 32F, G).



Fig. 32. Fragments of distal wing finger phalanges of *Azhdarcho lancicollis*: A, B – ZIN PH 203/44, left proximal fragment of phalanx IV-2, in dorsal (A) and ventral (B) views; C–E – ZIN PH 215/44, right proximal fragment of phalanx IV-3, in dorsal (C), proximal (D), and ventral (E) views. F, G – ZIN PH 216/44, distal fragment of phalanx IV-4, in dorsal (F) and ventral (G) views.

Abbreviation: vr – ventral ridge. Scale bars = 1 cm.

Comparison. In pterodactyloids there is no much variation in the structure of the proximal wing finger phalanx. Russell (1972: fig. 1) described a poorly preserved possible azhdarchid proximal wing finger phalanx from the Campanian of Alberta, Canada. Another specimen from this locality was described but not figured by Godfrey and Currie (2005). The preserved morphology of the figured specimen is identical to that of *Azhdarcho*. The same is true for the proximal wing finger phalanx fragment of a large azhdarchid from the Campanian of Saratov Province, Russia (Averianov 2007: pl. 8, fig. 5).

A T-shaped cross-section of wing finger phalanges II and III is considered to be unique for Azhdarchidae (Unwin and Lü 1997). In *Azhdarcho* a T-shaped cross-section have all wing finger phalanges distal to the first phalanx (II, III, and IV). In distal wing finger phalanges of an azhdarchid from the Aptian of Brazil and in *Quetzalcoatlus* the ventral ridge is closer to one side of the phalanx (anterior for *Quetzalcoatlus*; Martill and Frey 1999: fig. 3B, C). In *Azhdarcho* it is closer to the posterior end near the proximal end and almost central along the most length of the phalanx.

Manual phalanges of digits I–III

Material. Proximal phalanges: ZIN PH 220/44 (CBI-5a, 1989); ZIN PH 221/44 (CBI-4, 1987);

ZIN PH 222/44, proximal fragment (CBI-14, 1987); ZIN PH 223/44, proximal fragment (CBI-14); ZIN PH 224/44, proximal fragment (CBI-5, 2006); ZIN PH 225/44, proximal fragment (CBI-17); ZIN PH 226/44, distal fragment (CBI-4); ZIN PH 227/44, distal fragment (CBI-14, 2004); ZIN PH 228/44, distal fragment (CBI-14); ZIN PH 229/44, distal fragment (CBI-14, 2006). Distal phalanges: ZIN PH 231/44 (CBI-14); ZIN PH 232/44 (CBI-14); ZIN PH 233/44 (CBI-17, 1980); ZIN PH 234/44 (CBI-14); ZIN PH 235/44 (CBI-14, 2004); ZIN PH 236/44 (CBI-); ZIN PH 237/44 (CBI-4a, 2006); ZIN PH 239/44 (CBI-); ZIN PH 230/44, proximal fragment (CBI-14); ZIN PH 238/44, proximal fragment (CBI-, 1989).

Description. The proximal manual phalanges of non-wing digits are known from two complete but poorly preserved specimens and several proximal and distal fragments (Fig. 33A–J). These phalanges are curved and have massive laterally expanded proximal end. The proximal articulation surface is oval and concave. The proximal part of the phalanx is rhomboid in cross-section with ridges on anterior, posterior, lateral, and medial sides. One of the side ridges (not clear if it is medial or lateral) is usually more prominent, flange-like. On the posterior side near the proximal end and close to these ridges there are two well delimited oval depressions with smaller pneumatic openings inside. The smaller of these depressions is at the flange-like ridge. The shaft is not

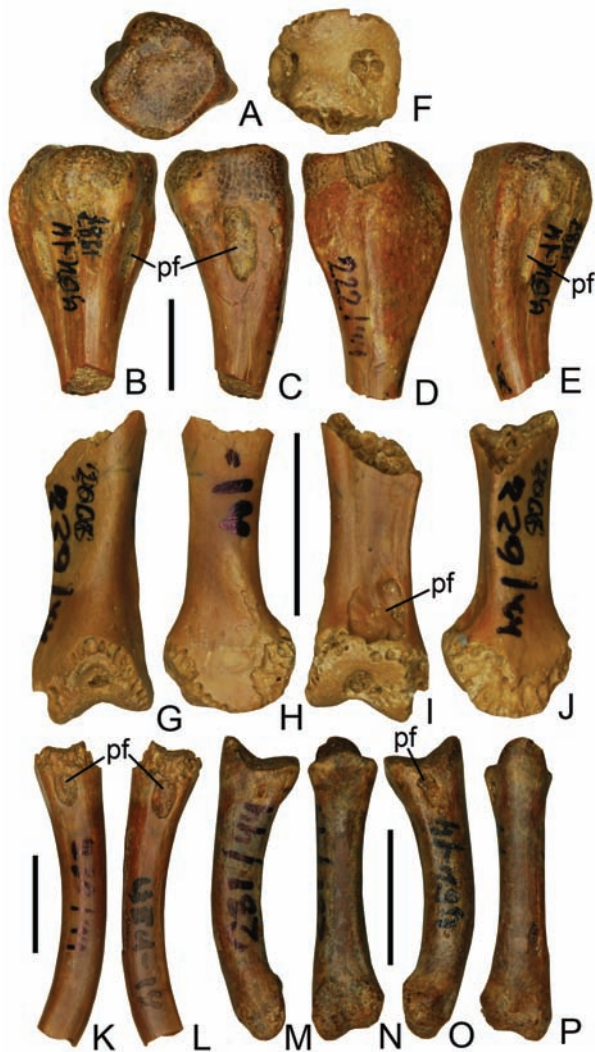


Fig. 33. Manual phalanges of *Azhdarcho lancicollis*: A–E – ZIN PH 222/44, proximal fragment of proximal phalanx, in proximal (A), posterior (B), anterior (D), and side (C, E) views; F–J – ZIN PH 229/44, distal fragment of proximal phalanx, in distal (F), anterior (G), posterior (I), and side (H, J) views; K, L – ZIN PH 230/44, proximal fragment of distal phalanx in side views; M–P – ZIN PH 231/44, distal phalanx, in side (M, O), posterior (N), and anterior (P) views.

Abbreviation: pf – pneumatic foramen. Scale bars = 1 cm.

hollow but highly porous. Closer to the distal end the shaft is more or less triangular in cross-section, with flat posterior side and ridge along anterior side. On posterior side near the distal end there is another depression with small pneumatic openings inside. The distal epiphysis is little expanded compared with the shaft and semicircular in side view, with 180° exten-

sion of the distal articulation surface. On the articulation surface there are a deep median sulcus and two variable developed foramina.

Distal phalanges vary in length and curvature. ZIN PH 230/44 is the fragment of the longest distal phalanx (Fig. 33K, L). It is subrectangular in cross-section near the proximal end with flattened ventral side and convex dorsal side. The shaft near the distal end is oval in cross-section. The bone is hollow. On medial and proximal sides near the proximal end there are large oval pneumatic foramina. The specimen ZIN PH 231/44 (Fig. 33M–P) represents the more common type. It is shorter and has the proximal end subtriangular in cross-section and with much smaller pneumatic foramina. The distal condyle is more or less oblique.

Comparison. A similar curved proximal fragment of the proximal manual phalanx is known from the Cenomanian of Uzbekistan (ZIN PH 44/44; misidentified in Averianov 2007 as pedal phalanx). It has only one pneumatic foramen.

Femur

Material. Proximal fragments: CCMGE 9/11915, left (CBI-17, 1980); ZIN PH 16/44, right (CBI-5a, 1991); ZIN PH 18/44, left (CBI-5a, 1987); ZIN PH 19/44, right (CBI-14); ZIN PH 192/44, right (CBI-14); ZIN PH 193/44, right (CBI-14, 1985); ZIN PH 194/44, right (CBI-14); ZIN PH 195/44, left (CBI-14, 1985); ZIN PH 196/44, left (CBI-17, 2004); ZIN PH 197/44, right (CBI-); ZIN PH 198/44, left (CBI-4e, 2006). Shaft fragment: ZIN PH 17/44, left (CBI-14, 1980). Distal fragments: ZIN PH 20/44, right (CBI-5a, 1989); ZIN PH 21/44, left (CBI-14, 1987); ZIN PH 22/44, right (CBI-5a, 1987); ZIN PH 23/44, left (CBI-).

Description. The femur of *Azhdarcho* is represented by several proximal and distal fragments (Fig. 34), some of which come from very small, maybe recently hatching individuals (e.g. ZIN PH 197/44). The largest specimen has DW=34.2 (ZIN PH 20/44). The femoral head is globular with anteroposterior diameter greater than the mediolateral diameter. It is placed on a relatively long neck which is subtriangular in cross-section. The neck is oriented at an angle of 30–50° to the longitudinal axis of the shaft (the angle increases with the size of the specimen). The greater trochanter is not complete on either specimen. On the posterior side between the greater trochanter and

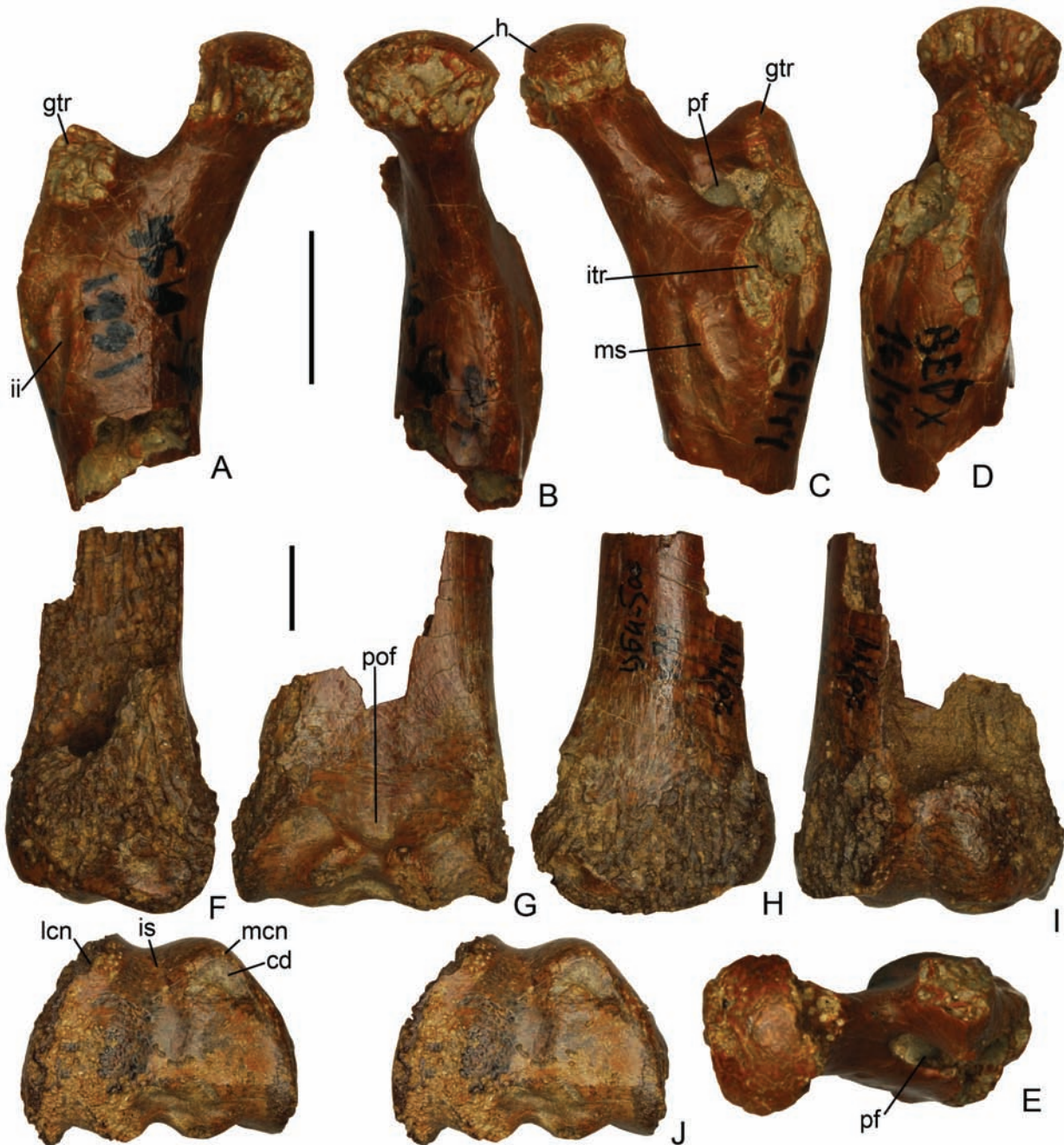


Fig. 34. Femur fragments of *Azhdarcho lancicollis*: A–E – ZIN PH 16/44, right proximal fragment, in anterior (A), medial (B), posterior (C), distal (D), and proximal (E) views; F–J – ZIN PH 20/44, right distal fragment, in medial (F), posterior (G), lateral (H), anterior (I), and distal (J, stereopair) views.

Abbreviations: cd – circular depression; gtr – greater trochanter; h – head; ii – scar for m. iliofemoralis internus; is – intercondylar sulcus; itr – internal trochanter; lcn – lateral condyle; mcn – medial condyle; ms – muscle scar; pf – pneumatic foramen; pof – popliteal fossa. Scale bars = 1 cm.

the femoral neck there is intertrochanteric depression with a large pneumatic foramen in the center. Laterally this depression is bordered by a low ridge which extends between the greater trochanter and internal trochanter, a prominent rugose area served for insertion of *m. puboischiofemoralis externus*. On the posterior side medial to the internal trochanter there is another prominent ridge-like muscle scar. A similar scar is present on the anterior side distal to the greater trochanter (“lesser trochanter” for insertion of *m. iliofemoralis internus*).

The shaft is slightly sigmoidally bent and bears distinct and long linear muscle scars along the posterior and medial sides. The shaft is oval in cross-section with long axis mediolateral. The shaft is slightly expanding towards the distal end. In lateral view the distal epiphysis is less than twice wider than the shaft.

The distal epiphysis of the femur is D-shaped in proximal view, straight posteriorly and convex anteriorly. The medial and lateral condyles are almost symmetrical and separated by shallow and narrow intercondylar sulcus. A small posterior part of this intercondylar sulcus is separated by a short transverse ridge. This part is more depressed compared with the rest of the intercondylar sulcus. On the medial condyle near anterior end there is a small circular depression. The articulation surface of the condyles is flat or slightly concave on the proximal side and becomes more concave on the extension of this surface on the posterior side. These lateral concavities and the median intercondylar sulcus make up three grooves along the posterior side of the distal epiphysis in proximal view. On the posterior side just proximal to the epiphysis there is a large and shallow popliteal fossa bordered proximally by a transverse muscle scar.

Comparison. The femur of an azhdarchid from the Campanian of Alberta, Canada (Godfrey and Currie 2005: fig. 16.10B–C) is little less symmetrical in distal view compared with that bone in *Azhdarcho*.

Nessov (1991a: 19) thought that two isolated proximal femur fragments, one from the Albian of England and other from the Hauterivian-Barremian of Argentina, might belong to Azhdarchidae. The Argentinean specimen (Montanelli 1987: fig. 1A–C) apparently lacks a proximal pneumatic foramen on the posterior side and thus do not belong to Azhdarchidae. The British specimen (Seeley 1870: pl. 7, figs 7–9) is indeed very similar to the femur of *Azhdarcho* and may come from an unknown azhdarchid. It has the same proximal pneumatic foramen and

the neck is oriented to the shaft at an angle of $\sim 55^\circ$ ($30\text{--}50^\circ$ in *Azhdarcho*).

Buffetaut (1999: 291) mentioned a proximal femur fragment similar to that bone in *Azhdarcho* from the Campanian-Maastrichtian of Spain. It also has a deep foramen at the base of the great trochanter.

Tibiotarsus

Material. Distal fragments: ZIN PH 190/44, left (CBI-5a, 1991); ZIN PH 191/44, right (CBI-14, 1985).

Description. The tibiotarsus is known from two fragments of the distal epiphysis (Fig. 35). Both condyles are subequal in size but the lateral condyle is protruding little farther posteriorly. The intercondylar sulcus is narrow and shallow. In this sulcus there is small circular fossa on the anterior side apparently for the origin of intertarsal ligaments (Bennett 2001: 106). The articulation surface extends proximally on the posterior surface approximately as much as on

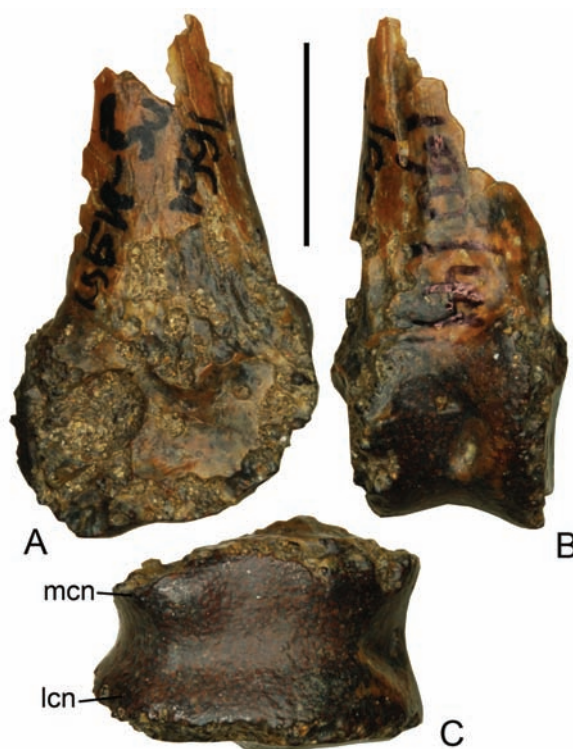


Fig. 35. ZIN PH 190/44, distal fragment of left tibiotarsus of *Azhdarcho lancicollis*, in medial (A), anterior (B), and distal (C) views. Abbreviations: lcn – lateral condyle; mcn – medial condyle. Scale bar = 1 cm.

the anterior surface. The shaft is oval in cross-section with long axis anteroposterior. In ZIN PH 190/44 there is a partially preserved medial epicondyle.

Comparison. The azhdarchid tibiotarsus is known from the Campanian of Alberta, Canada (Currie and Jacobsen 1995; Godfrey and Currie 2005), but not described in detail.

The tibiotarsus in *Azhdarcho* is similar to that bone in *Pteranodon* (Bennett 2001: fig. 108) except the articulation surface of the condyles extends more proximally on the posterior side in the former taxon.

The bone fragment from the Campanian of Alberta described as distal end of a pterodactyloid tibia (Currie and Padian 1983: fig. 1) is more likely the distal fragment of the wing metacarpal of a non-azhdarchid pterosaur (see McGowen et al. 2002: 8).

Metatarsus

Material. ZIN PH 200/44, proximal fragment of right second or third metatarsal (CBI-5a, 1989).

Description. ZIN PH 200/44 is possible the second or third metatarsal compared the metatarsals in *Pteranodon* (Bennett 2001: figs 115 and 115). The specimen preserves the proximal end and the most of the diaphysis (Fig. 36). The proximal articulation surface is subtriangular, pointing posteriorly. It is flat and laterally slanting. The anterior side of the proximal end is convex while medial and lateral sides are concave. The shaft is laterally bent and slender, about three times less in diameter than the anteroposterior diameter of the proximal end. Near the proximal end there are small oval pneumatic foramina on anterior and lateral sides and a larger depression with the net of small pneumatic foramina on the medial side. Distal to the latter there is a prominent ligament bump. The shaft is circular in cross-section and hollow with thin walls except the thickened anterior wall.

Comparison. The detailed structure of the metatarsals is poorly known for Pterosauria. ZIN PH 200/44 is similar with the middle metatarsal in *Pteranodon* in general structure and having a prominent ligament bump, but different in more triangular and anteroposteriorly shorter proximal articulation surface and having three instead of one proximal pneumatic foramina. Godfrey and Currie (2005: fig. 16.11) described a third or fourth metatarsal of an azhdarchid from the Campanian of Alberta, Canada. It is more robust than ZIN PH 200/44 and lacks any pneumatic foramina.



Fig. 36. ZIN PH 200/44, proximal fragment of right metatarsal II or III of *Azhdarcho lancicollis*, in proximal (A), lateral (B), posterior (C), medial (D), and anterior (E) views.

Abbreviations: lb – ligament bump; pf – pneumatic foramen. Scale bar = 1 cm.

Pedal phalanges

Material. Proximal phalanx: ZIN PH 240/44 (CBI-14). Distal phalanges: CCMGE 52/11915 (CBI-17); ZIN PH 241/44 (CBI-); ZIN PO 6442 (CBI-14, 1999).

Description. Pedal phalanges of *Azhdarcho* are far less common at Dzharakuduk compared with manual phalanges. They differ by straight shaft and less developed pneumatization. ZIN PH 240/44 with not divided triangular proximal articulation surface

is the proximal phalanx (Fig. 37A–E). The proximal end is massive. The distal epiphysis is much smaller and projects dorsally well beyond the shaft. The shaft is triangular in cross-section. The ventral side is flat and depressed between sharp lateral and medial edges. This phalanx lacks any pneumatic foramina.

In collection there are several distal phalanges with proximal articulation surface subdivided into two parts (Fig. 37F–O). In ZIN PH 241/44 the proximal epiphysis is transversely expanded with a peculiar outgrowth on one side. On the opposite side near the proximal end there is an oval pneumatic foramen. The shaft is triangular in cross-section, with a sulcus along the ventral side. The distal epiphysis is not much expanded beyond the shaft. In CCMGE 52/11915 the proximal articulation surface is more symmetrical and saddle-shaped. Otherwise it is similar to ZIN PH 241/44 except it lacks a pneumatic foramen.

PHYLOGENETIC POSITION OF AZHDARCHO

The new materials of *Azhdarcho* described herein significantly expand our knowledge on this taxon. Here I shall concentrate on the phylogenetic position of *Azhdarcho* within the Azhdarchidae; implications of these materials for the functional morphology and paleoecology of this pterosaur will be discussed in a separate paper.

The phylogenetic interrelationships within Pterosauria were a subject of several cladistic analyses starting with the manually produced cladogram by Howse (1986). In the majority of the published analyses only three azhdarchid taxa has been used (*Azhdarcho*, *Zhejiangopterus*, and *Quetzalcoatlus*) and on all resulting trees the phylogenetic relationships within these three taxa are not resolved (Kellner 2003, 2004; Wang et al. 2005, 2009; Lü et al. 2008, 2010). The only exception is the analysis by Andres and Ji (2008) which employed also the fourth azhdarchid taxon (*Bakonydraco*) and produced at least some resolution within the Azhdarchidae (*Bakonydraco* is the sister taxon to the remaining unresolved taxa).

The new materials on *Azhdarcho* allow coding of this taxon by the following additional characters from the matrix by Andres and Ji (2008): 4(0), 6(0), 45(0), 46(0), 69(0), 76(0), 77(1), 78(0), 79(0), 80(1), 84(1), 88(1), 91(0), 93(1), 97(0), 98(0), 108(0), and 109(0/1). I changed coding of the character 43 for *Zhejiangopterus* from 1 to 0 because the position of the mandibular symphysis relative to the mandibular rami

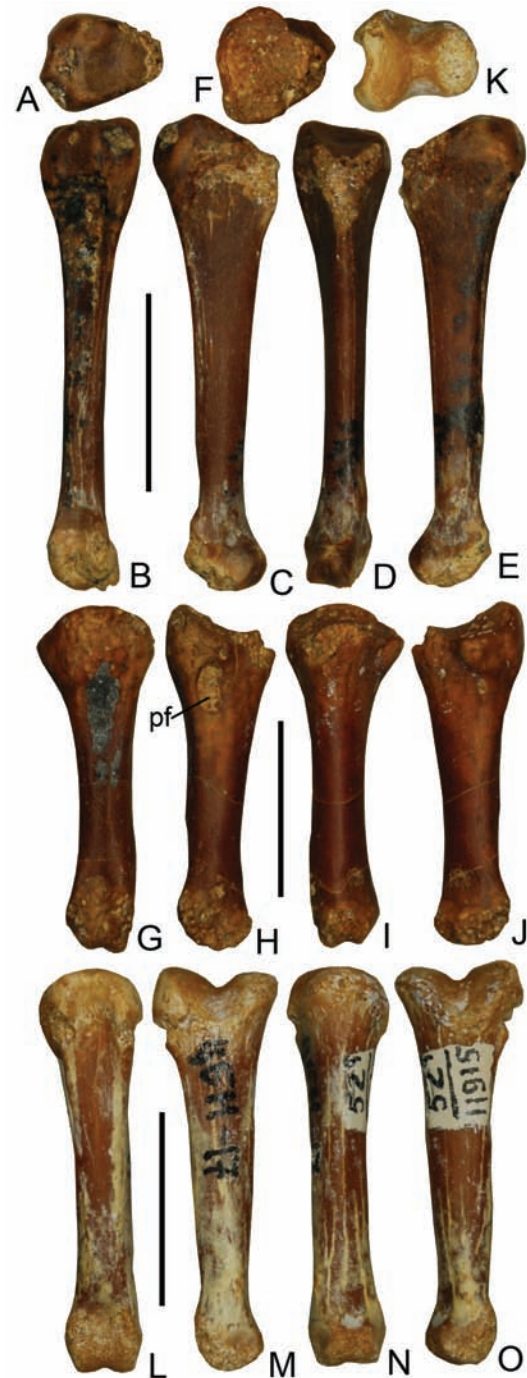


Fig. 37. Pedal phalanges of *Azhdarcho lancicollis*: A–E – ZIN PH 240/44, proximal phalanx, in proximal (A), posterior (B), side (C, E), and anterior (D) views; F–J – ZIN PH 241/44, distal phalanx, in proximal (F), posterior (G), side (H, J), and anterior (I) views; K–O – CCMGE 52/11915, distal phalanx, in proximal (K), posterior (L), side (M, O), and anterior (N) views.

Abbreviation: pf – pneumatic foramen. Scale bars = 1 cm.

in this taxon is not much different from that of *Quetzalcoatlus* and not as ventral as in *Pteranodon*. I also coded *Bakonydraco* as having the medial carpal longer than wide (character state 98[0]) following my reinterpretation of the supposed phalanx fragment (Ósi et al. 2005: fig. 6C) as the preaxial (=medial) carpal. *Bakonydraco* was coded by Andres and Ji (2008) as having dentary bony sagittal crest (character 46[1]) but I see no reasons for this. It was subsequently recoded by the character state 46[0]. Andres and Ji (2008) also coded *Bakonydraco* as having low neural spine of middle cervical vertebrae (character 67[1]) while other azhdarchids were coded as having extremely reduced or absent neural spine on these vertebrae (character 67[2]). But actually, *Bakonydraco* does not differ from other azhdarchids in the state of reduction of neural spines in middle cervicals. It is coded here accordingly by the character state 67[2].

The dataset of Andres and Ji (2008) modified as described above was analyzed using NONA version 2.0 (Goloboff 1999) run with Winclada version 1.00.08 interface (Nixon 1999). All characters were equally weighted and treated as unordered except characters 65 and 67 ordered by Andres and Ji (2009). Ten thousands repetitions of the parsimony ratchet (island hopper) algorithm with random constraint level 15 produced six most parsimonious trees with a length of 327 steps with a consistency index of 0.48 and a retention index of 0.80. These trees are 11 steps shorter than the two most parsimonious trees obtained by Andres and Ji (2008). On the strict consensus tree (Fig. 38) the monophyletic Azhdarchidae is supported by four unambiguous synapomorphies:

65(2): middle cervical vertebrae extremely elongated;

67(2): neural spines of middle cervical vertebrae extremely reduced or absent;

86(1): deltopectoral crest positioned further down on humerus;

106(1): T-shaped cross-section of second and third wing finger phalanges.

The Azhdarchidae consists of the clade comprising *Quetzalcoatlus* and *Zhejiangopterus* and more basal *Bakonydraco* and *Azhdarcho* forming polytomy to this clade. However, there are no unambiguous synapomorphies for the clade *Quetzalcoatlus* + *Zhejiangopterus*. The analysis revealed also two autapomorphies for *Quetzalcoatlus*:

15(1): premaxillary sagittal crest;

75(0): sternum semi-circular.



Fig. 38. Fragment of the strict consensus tree produced by NONA 2.0 used a modified dataset by Andres and Ji (2008) showing interrelationships within the Azhdarchidae. Only unambiguously optimized characters are shown (black circles are nonhomoplasies and white circles are homoplasies). The numbers at the circles are characters (above) and states (below) which correspond to those in Andres and Ji (2008).

The presence of a premaxillary crest cannot be established for *Azhdarcho* and *Bakonydraco* because of lack of the relevant cranial material. It is absent in *Zhejiangopterus* but the known skulls likely come from immature individuals (Unwin and Lü 1997) and the crest may appear at a later ontogenetic stage. Additionally could be a sexual variation in the cranial crest development in pterosaurs (Bennett 1992). The second character is difficult to evaluate when description of actual fossils is lacking.

The analysis performed herein suggests that the Turonian *Azhdarcho* and the Santonian *Bakonydraco* occupy a phylogenetic position basal to the Campanian *Zhejiangopterus* and the Maastrichtian *Quetzalcoatlus*, which makes a sense at least from the geochronological point of view. A hall-mark between these two groups of taxa might be elongation of the jaws, particularly the symphyseal part of dentary which was obviously short in *Bakonydraco* and *Azhdarcho*. More fossils are needed for better understanding of the phylogenetic interrelationships within the Azhdarchidae.

ACKNOWLEDGMENTS

The field work at Dzharakuduk in 1997–2006 was funded by the National Geographic Society (5901-97 and 6281-98) and the National Science Foundation (EAR-9804771 and 0207004). The laboratory work was supported by the Civilian Research and Development Foundation (RU-G1-2571-ST-04 and RUB1-2860-ST-07) and the Russian Foundation for Basic Research (07-04-91110-AFGIR and 09-04-00222). I am grateful to Dmitry Grigor'ev (Saint Petersburg State University) for taking photos of some specimens in CCMGE collection (Figs 11, 17, and 26H–L)

and to Chris King (University of Greenwich, Chatham Maritime) for his kind permission to use stratigraphic chart and geologic section from his unpublished work (Fig. 1A, B). I am grateful to Eberhard Frey (Staatliches Museum für Naturkunde, Karlsruhe) and Natasha Bakhurina (University of Bristol) for reviewing the paper and useful comments.

REFERENCES

- Andres B.B. and Ji Q. 2008.** A new pterosaur from the Liaoning Province of China, the phylogeny of the Pterodactyloidea, and convergence in their cervical vertebrae. *Palaeontology*, **51**: 453–469.
- Arambourg C. 1954.** Sur la présence d'un Ptérosaure gigantesque dans les Phosphates de Jordanie. *Comptes Rendus Hebdomadaires des Séances de l'Académie des Sciences*, **238**: 133–134.
- Arambourg C. 1959.** *Titanopteryx philadelphiae* nov. gen., nov. sp. Ptérosaure géant. *Notes et Mémoires sur le Moyen-Orient*, **7**: 229–234.
- Archibald J.D. and Averianov A.O. 2005.** Mammalian faunal succession in the Cretaceous of the Kyzylkum Desert. *Journal of Mammalian Evolution*, **12**: 9–22.
- Archibald J.D., Sues H.-D., Averianov A.O., King C., Ward D.J., Tsaruk O.I., Danilov I.G., Rezvyi A.S., Veretennikov B.G. and Khodjaev A. 1998.** Précis of the Cretaceous paleontology, biostratigraphy and sedimentology at Dzharakuduk (Turonian?-Santonian), Kyzylkum Desert, Uzbekistan. In: S.G. Lucas, J.I. Kirkland and J.W. Estep (Eds.). Lower to Middle Cretaceous Terrestrial Ecosystems. *Bulletin of the New Mexico Museum of Natural History and Science*, **14**: 21–28.
- Astibia H., Buffetaut E., Buscalioni A.D., Cappetta H., Corral J.C., Estes R.D., Garcia-Garmilla F., Jaeger J.-J., Jimenez-Fuentes E., Le Loeuff J., Mazin J.-M., Orue-Etxebarria X., Pereda Suberbiola X., Powell J.E., Rage J.-C., Rodriguez-Lazaro J., Sanz J.L. and Tong H. 1991.** The fossil vertebrates from Laño (Basque Country, Spain); new evidence on the composition and affinities of the Late Cretaceous of continental Europe. *Terra Nova. Official Journal of the European Union of Geosciences*, **2**: 460–466.
- Averianov A.O. 2004.** New data on Cretaceous flying reptiles (Pterosauria) from Russia, Kazakhstan, and Kyrgyzstan. *Paleontological Journal*, **38**: 426–436.
- Averianov A.O. 2007.** New records of azhdarchids (Pterosauria, Azhdarchidae) from the Late Cretaceous of Russia, Kazakhstan, and Central Asia. *Paleontological Journal*, **41**: 189–197.
- Averianov A.O. 2008.** [Superorder Pterosauria]. In: M.F. Ivakhnenko and E.N. Kurochkin (Eds.). Fossil Vertebrates of Russia and Adjacent Territories. Fossil Reptiles and Birds. Part 1. Moscow, GEOS: 319–342. [In Russian]
- Averianov A.O. and Atabekyan A.A. 2005.** The first discovery of a flying reptile (Pterosauria) in Armenia. *Paleontological Journal*, **39**: 210–212.
- Averianov A.O. and Sues H.-D. 2007.** A new troodontid (Dinosauria: Theropoda) from the Cenomanian of Uzbekistan, with a review of troodontid records from the territories of the former Soviet Union. *Journal of Vertebrate Paleontology*, **27**: 87–98.
- Averianov A.O., Arkhangelsky M.S., Pervushov E.M. and Ivanov A.V. 2005.** A new record of an azhdarchid (Pterosauria: Azhdarchidae) from the Upper Cretaceous of the Volga Region. *Paleontological Journal*, **39**: 433–439.
- Averianov A.O., Arkhangelsky M.S. and Pervushov E.M. 2008.** A new Late Cretaceous azhdarchid (Pterosauria, Azhdarchidae) from the Volga Region. *Paleontological Journal*, **42**: 634–642.
- Baird D. and Galton P.M. 1981.** Pterosaur bones from the Upper Cretaceous of Delaware. *Journal of Vertebrate Paleontology*, **1**: 67–71.
- Bakhurina N.N. and Unwin D.M. 1995.** A survey of pterosaurs from the Jurassic and Cretaceous of the former Soviet Union and Mongolia. *Historical Biology*, **10**: 197–245.
- Barrett P.M., Butler R.J., Edwards N.P. and Milner A.R. 2008.** Pterosaur distribution in time and space: an atlas. *Zitteliana*, **B28**: 61–107.
- Bennett S.C. 1989.** A pteranodontid pterosaur from the Early Cretaceous of Peru, with comments on the relationships of Cretaceous pterosaurs. *Journal of Paleontology*, **63**: 669–677.
- Bennett S.C. 1992.** Sexual dimorphism of *Pteranodon* and other pterosaurs, with comments on cranial crests. *Journal of Vertebrate Paleontology*, **12**: 422–434.
- Bennett S.C. 1994.** Taxonomy and systematics of the Late Cretaceous pterosaur *Pteranodon* (Pterosauria, Pterodactyloidea). *Occasional Papers of the Museum of Natural History, the University of Kansas*, **169**: 1–70.
- Bennett S.C. 2001.** The osteology and functional morphology of the Late Cretaceous pterosaur *Pteranodon*. Part I. General description and osteology. *Palaeontographica, Abteilung A: Paläozoologie, Stratigraphie*, **260**: 1–112.
- Bennett S.C. 2003.** Morphological evolution of the pectoral girdle of pterosaurs: myology and function. In: E. Buffetaut and J.-M. Mazin (Eds.). Evolution and Palaeobiology of Pterosaurs. *Geological Society Special Publication*, **217**: 191–215.
- Bennett S.C. and Long J.A. 1991.** A large pterodactyloid pterosaur from the Late Cretaceous (Late Maastrichtian) of Western Australia. *Records of the Western Australian Museum*, **15**: 435–443.
- Bogolubov N.N. 1914.** [On the pterodactyl vertebra from the Upper Cretaceous deposits of Saratov Government]. *Ezhegodnik po Geologii i Mineralogii Rossii*, **16**: 1–7. [In Russian]

- Buffetaut E. 1999.** Pterosauria from the Upper Cretaceous of Laño (Iberian Peninsula): a preliminary comparative study. In: H. Astibia, J.C. Corral, X. Murelaga, X. Orue-Etxebarria and X. Pereda Suberbiola (Eds.). *Geology and Palaeontology of the Upper Cretaceous Vertebrate-Bearing Beds of the Laño Quarry (Basque-Cantabrian Region, Iberian Peninsula)*. *Estudios del Museo Ciencias Naturales de Alava*, **14**(Num. Espec. 1): 289–284.
- Buffetaut E. 2001.** An azhdarchid pterosaur from the Upper Cretaceous of Cruzy (Herauld, France). *Comptes Rendus de l'Academie des Sciences, Serie II, Fascicule A: Sciences de la Terre et des plantes*, **333**: 357–361.
- Buffetaut E., Laurent Y., Le Loeuff J. and Bilotte M. 1997.** A terminal Cretaceous giant pterosaur from the French Pyrenees. *Geological Magazine*, **134**: 553–556.
- Buffetaut E., Grigorescu D. and Csiki Z. 2002.** A new giant pterosaur with a robust skull from the latest Cretaceous of Romania. *Naturwissenschaften*, **89**: 180–184.
- Buffetaut E., Grigorescu D. and Csiki Z. 2003.** Giant azhdarchid pterosaurs from the terminal Cretaceous of Transylvania (western Romania). In: E. Buffetaut and J.-M. Mazin (Eds.). *Evolution and Palaeobiology of Pterosaurs*. *Geological Society Special Publication*, **217**: 91–104.
- Bunzel E. 1871.** Die Reptilienfauna der Gosauformation in der Neuen Welt bei Weiner-Neustadt. *Abhandlungen der kaiserlich-königliche geologischen Reichsanstalt*, **5**: 1–18.
- Cai Z. and Wei F. 1994.** On a new pterosaur (*Zhejiangopterus linhaiensis* gen. et sp. nov.) from Upper Cretaceous in Linhai, Zhejiang, China. *Vertebrata Palasiatica*, **32**: 181–194.
- Chitoku T. 1996.** Pterosaur bone from the Upper Cretaceous of Enbetsu, Hokkaido. *Bulletin of the Hobetsu Museum*, **12**: 17–24.
- Company J., Ruiz-Omenaca J.I. and Pereda Suberbiola X. 1999.** A long-necked pterosaur (Pterodactyloidea, Azhdarchidae) from the Upper Cretaceous of Valencia, Spain. *Geologie en Mijnbouw*, **78**: 319–333.
- Currie P.J. and Jacobsen A.R. 1995.** An azhdarchid pterosaur eaten by a velociraptorine theropod. *Canadian Journal of Earth Sciences*, **32**: 922–925.
- Currie P.J. and Padian K. 1983.** A new pterosaur record from the Judith River (Oldman) Formation of Alberta. *Journal of Paleontology*, **57**: 599–600.
- Currie P.J. and Russell D.A. 1982.** A giant pterosaur (Reptilia: Archosauria) from the Judith River (Oldman) Formation, Alberta. *Canadian Journal of Earth Sciences*, **19**: 894–897.
- Estes R.D. 1964.** Fossil vertebrates from the Late Cretaceous Lance Formation, Eastern Wyoming. *University of California Publications in Geological Sciences*, **49**: 1–180.
- Frey E. and Martill D.M. 1996.** A reappraisal of *Arambourgiania* (Pterosauria, Pterodactyloidea): One of the world's largest flying animals. *Neues Jahrbuch für Geologie und Paläontologie Abhandlungen*, **199**: 221–247.
- Frey E., Buchy M.-C. and Martill D.M. 2003.** Middle- and bottom-decker Cretaceous pterosaurs: unique designs in active flying vertebrates. In: E. Buffetaut and J.-M. Mazin (Eds.). *Evolution and Palaeobiology of Pterosaurs*. *Geological Society Special Publication*, **217**: 267–274.
- Fritsch A. 1881.** Ueber die Entdeckung von Vogelresten in der böhmischen Kreideformation. *Sitzungsberichte der königlich-böhmischen Gesellschaft der Wissenschaften in Prag*: 275–276.
- Fritsch A. 1883.** Studien im Gebiet der böhmischen Kreideformation. Palaeontologische Untersuchung der einzelnen Schichten. III Die Iserschichten. *Archiv der naturwissenschaftlichen Landesdurchforschung von Böhmen, Geologische Abteilung*, **5**: 1–140.
- Fritsch A. 1905.** Synopsis der Saurier der böhmischen Kreideformation. *Sitzungsberichte der königlich-boemischen Gesellschaft der Wissenschaften, mathematisch-naturwissenschaftlichen Klasse*, **8**: 1–7.
- Gilmore C.W. 1928.** A new pterosaurian reptile from the marine Cretaceous of Oregon. *Proceedings of the United States National Museum*, **73**: 1–5.
- Godfrey S.J. and Currie P.J. 2005.** Pterosaurs. In: P.J. Currie and E.B. Koppelhus (Eds.). *Dinosaur Provincial Park: A Spectacular Ancient Ecosystem Revealed*. Bloomington, Indianapolis, Indiana University Press: 292–311.
- Goloboff P. 1999.** NONA (ver. 1.9). Software published by the author, S.M. de Tucuman, Argentina. Available on-line at www.cladistics.org.
- Henderson M.D. and Peterson J.E. 2006.** An azhdarchid pterosaur cervical vertebra from the Hell Creek Formation (Maastrichtian) of southeastern Montana. *Journal of Vertebrate Paleontology*, **26**: 192–195.
- Howse S.C.B. 1986.** On the cervical vertebrae of the Pterodactyloidea (Reptilia: Archosauria). *Zoological Journal of the Linnean Society*, **88**: 307–328.
- Ikegami N., Kellner A.W.A. and Tomida Y. 2000.** The presence of an azhdarchid pterosaur in the Cretaceous of Japan. *Paleontological Research*, **4**: 165–170.
- Kellner A.W.A. 1995.** The relationships of the Tapejariidae (Pterodactyloidea) with comments on pterosaur phylogeny. In: A. Sun and Y.-Q. Wang (Eds.). *Sixth Symposium on Mesozoic Terrestrial Ecosystems and Biota*. Short Papers. Beijing, China Ocean Press: 73–77.
- Kellner A.W.A. 2003.** Pterosaur phylogeny and comments on the evolutionary history of the group. In: E. Buffetaut and J.-M. Mazin (Eds.). *Evolution and Palaeobiology of Pterosaurs*. *Geological Society Special Publication*, **217**: 105–137.

- Kellner A.W.A. 2004.** New information on the Tapejaridae (Pterosauria, Pterodactyloidea) and discussion of the relationships of this clade. *Ameghiniana*, **41**: 521–534.
- Kellner A.W.A. and Langston W., Jr. 1996.** Cranial remains of *Quetzalcoatlus* (Pterosauria, Azhdarchidae) from Late Cretaceous sediments of Big Bend National Park, Texas. *Journal of Vertebrate Paleontology*, **16**: 222–231.
- Kellner A.W.A. and Tomida Y. 2000.** Description of a new species of Anhangueridae (Pterodactyloidea) with comments on the pterosaur fauna from the Santana Formation (Aptian-Albian), northeastern Brazil. *National Sciences Museum Monographs*, **17**: 1–135.
- Langston W., Jr. 1981.** Pterosaurs. *Scientific American*, **244**: 92–102.
- Lawson D.A. 1975a.** A pterosaur from the latest Cretaceous of West Texas: discovery of the largest flying creature. *Science*, **187**: 947–948.
- Lawson D.A. 1975b.** Could pterosaurs fly? *Science*, **188**: 676–678.
- Lü J., Unwin D.M., Jin X., Liu Y. and Ji Q. 2010.** Evidence for modular evolution in a long-tailed pterosaur with a pterodactyloid skull. *Proceedings of the Royal Society B: Biological Sciences*, **277**: 383–389.
- Lü J., Unwin D.M. and Zhang X. 2008.** A new azhdarchoid pterosaur from the Lower Cretaceous of China and its implications for pterosaur phylogeny and evolution. *Naturwissenschaften*, **95**: 891–897.
- Martill D.M. and Frey E. 1999.** A possible azhdarchid pterosaur from the Crato Formation (Early Cretaceous, Aptian) of northeast Brazil. *Geologie en Mijnbouw*, **78**: 315–318.
- Martill D.M., Frey E., Sadaqah R.M. and Khoury H.N. 1998.** Discovery of the holotype of the giant pterosaur *Titanopteryx philadelphiae* Arambourg 1959, and the status of *Arambourgiania* and *Quetzalcoatlus*. *Neues Jahrbuch für Geologie und Paläontologie Abhandlungen*, **207**: 57–76.
- Martill D.M., Witton M.P. and Gale A.S. 2008.** Possible azhdarchoid pterosaur remains from the Coniacian (Late Cretaceous) of England. *Zitteliana*, **B28**: 209–218.
- Martinson G.G. 1969.** [Biostratigraphy and fauna of the Cretaceous continental deposits of Tajik Depression, Kyzylkum and circum-Tashkent Chuli]. In: G.G. Martinson (Ed.). [Continental deposits of the Eastern Regions of Middle Asia and Kazakhstan (Lithostratigraphy and Biostratigraphy)]. Nauka, Leningrad: 18–51. [In Russian]
- McGowen M.R., Padian K., De Sosa M.A. and Harmon R.J. 2002.** Description of *Montanazhdarcho minor*, an azhdarchid pterosaur from the Two Medicine Formation (Campanian) of Montana. *PaleoBios*, **22**: 1–9.
- Montanelli S.B. 1987.** Presencia de Pterosauria (Reptilia) en la Formacion La Amarga (Hauteriviano-Barremiano), Neuquen, Argentina. *Ameghiniana*, **24**: 109–113.
- Monteillet J., Lappartient J.R. and Taquet P. 1982.** Un Ptérosaure géant dans le Crétacé supérieur de Paki (Sénégal). *Comptes Rendus des Séances de l'Académie des Sciences, Serie II. Mécanique-Physique, Chimie, Sciences de l'Univers, Sciences de la Terre*, **295**: 409–414.
- Murry P.A., Winkler D.A. and Jacobs L.L. 1991.** An azhdarchid pterosaur humerus from the Lower Cretaceous Glen Rose Formation of Texas. *Journal of Paleontology*, **65**: 167–170.
- Nessov L.A. 1981.** [Amphibians and reptiles in Cretaceous ecosystems of Middle Asia]. In: I.S. Darevsky (Ed.). [Questions of Herpetology. Fifth All-Union Herpetological Conference. Abstracts of Reports]. Leningrad, Nauka: 91–92. [In Russian]
- Nessov L.A. 1984.** [Pterosaurs and birds from the Late Cretaceous of Middle Asia]. *Paleontologicheskii Zhurnal*, **1**: 47–57. [In Russian]
- Nessov L.A. 1986.** [The first finding of Late Cretaceous bird *Ichthyornis* in Old World and some other bird bones from Cretaceous and Paleogene of Soviet Middle Asia]. *Trudy Zoologicheskogo Instituta AN SSSR*, **147**: 31–38. [In Russian]
- Nessov L.A. 1988.** [New Cretaceous and Paleogene birds of Soviet Middle Asia and Kazakhstan and environments]. *Trudy Zoologicheskogo Instituta AN SSSR*, **182**: 116–123. [In Russian]
- Nessov L.A. 1990.** [Flying reptiles of the Jurassic and Cretaceous of the USSR and significance of their remains for the paleogeographic environmental reconstruction]. *Vestnik Leningradskogo Universiteta, Seriya 7: Geologiya, Geografiya*, **4**(28): 3–10. [In Russian]
- Nessov L.A. 1991a.** [Giant flying reptiles of the family Azhdarchidae. I. Morphology, systematics]. *Vestnik Leningradskogo Universiteta, Seriya 7: Geologiya, Geografiya*, **2**(14): 14–23. [In Russian]
- Nessov L.A. 1991b.** [Giant flying reptiles of the family Azhdarchidae. II. Paleoenvironment, sedimentological condition of burial]. *Vestnik Leningradskogo Universiteta, Seriya 7: Geologiya, Geografiya*, **3**(21): 16–24. [In Russian]
- Nessov L.A. 1991c.** [Flying reptiles above platan forests and brackish-water sea bays]. *Gerpetologicheskoe Issledovaniya*, **1**: 147–163. [In Russian]
- Nessov L.A. 1995.** [Dinosaurs of Northern Eurasia: New Data about Assemblages, Ecology and Paleobiogeography]. Izdatel'stvo Sankt-Peterburgskogo Universiteta, Saint Petersburg. 156 pp. [In Russian]
- Nessov L.A. 1997.** [Cretaceous Nonmarine Vertebrates of Northern Eurasia] (Posthumous edition by L.B. Golovneva and A.O. Averianov). Izdatel'stvo Sankt-Peterburgskogo Universiteta, Saint Petersburg. 218 pp. [In Russian]
- Nessov L.A. and Yarkov A.A. 1989.** [New Cretaceous-Paleogene birds of the USSR and some remarks on the

- origin and evolution of the class Aves]. *Trudy Zoologicheskogo Instituta AN SSSR*, **197**: 78–97. [In Russian]
- Nessov L.A., Archibald J.D. and Kielan-Jaworowska Z. 1998.** Ungulate-like mammals from the Late Cretaceous of Uzbekistan and a phylogenetic analysis of Ungulatomorpha. In: K.C. Beard and M.R. Dawson (Eds.). Dawn of the Age of Mammals in Asia. Bulletin of the Carnegie Museum of Natural History, **34**: 40–88.
- Nixon K.C. 1999.** Winclada (Beta) version 0.9.9. Software published by the author, Ithaca, NY. Available on-line at www.cladistics.org.
- Ósi A., Weishampel D.B. and Jianu C.-M. 2005.** First evidence of azhdarchid pterosaurs from the Late Cretaceous of Hungary. *Acta Palaeontologica Polonica*, **50**: 777–787.
- Owen R. 1859.** Supplement (No. I) to the Monograph on the Fossil Reptilia of the Cretaceous Formations. Order Pterosauria Owen, genus *Pterodactylus* Cuvier. *Monographs of the Palaeontological Society of London*: 1–19.
- Padian K. 1984.** A large pterodactyloid pterosaur from the Two Medicine Formation (Campanian) of Montana. *Journal of Vertebrate Paleontology*, **4**: 516–524.
- Padian K. 1986.** A taxonomic note on two pterodactyloid families. *Journal of Vertebrate Paleontology*, **6**: 289.
- Padian K., Ricqles A.J., de and Horner J.R. 1995.** Bone histology determines identification of a new fossil taxon of pterosaur (Reptilia, Archosauria). *Comptes Rendus de L'Academie des Sciences, Serie II*, **320**: 77–84.
- Padian K. and Smith M.B. 1992.** New light on Late Cretaceous pterosaur material from Montana. *Journal of Vertebrate Paleontology*, **12**: 87–92.
- Pereda Suberbiola X., Bardet N., Jouve S., Iarochene M., Bouya B. and Amaghaz M. 2003.** A new azhdarchid pterosaur from the Late Cretaceous phosphates of Morocco. In: E. Buffetaut and J.-M. Mazin (Eds.). Evolution and Palaeobiology of Pterosaurs. *Geological Society Special Publication*, **217**: 79–90.
- Pyatkov K.K., Pyanovskaya I.A., Bukharin A.K. and Bykovskii Yu.K. 1967.** [Geological Structure of Central Kyzylkum]. Fan, Tashkent. 177 p. [In Russian]
- Redman C.M. and Leighton L.R. 2009.** Multivariate faunal analysis of the Turonian Bissekty Formation: Variation in the degree of marine influence in temporally and spatially averaged fossil assemblages. *Palaios*, **24**: 18–26.
- Russell D.A. 1972.** A pterosaur from the Oldman Formation (Cretaceous) of Alberta. *Canadian Journal of Earth Sciences*, **9**: 1338–1340.
- Seeley H.G. 1870.** The Ornithosauria: An Elementary Study of the Bones of Pterodactyles, Made from Fossil Remains Found in the Cambridge Upper Greensand. Deighton, Bell, and Co., Cambridge. X+135 p.
- Seeley H.G. 1881.** The reptile fauna of the Gosau Formation preserved in the Geological Museum of the University of Vienna. *Quarterly Journal of the Geological Society of London*, **37**: 620–707.
- Sochava A.V. 1968.** [Red-colored Cretaceous Sediments of Middle Asia]. Nauka, Leningrad. 122 p. [In Russian]
- Steel L., Martill D.M., Kirk J.R.J., Anders A., Loveridge R.F., Frey E. and Martin J.G. 1997.** *Arambourgiania philadelphiae*: giant wings in small halls. *The Geological Curator*, **6**: 305–313.
- Unwin D.M. 2001.** An overview of the pterosaur assemblage from the Cambridge Greensand (Cretaceous) of Eastern England. *Mitteilungen aus dem Museum fuer Naturkunde in Berlin, Geowissenschaftliche Reihe*, **4**: 189–221.
- Unwin D.M. 2003.** On the phylogeny and evolutionary history of pterosaurs. In: E. Buffetaut and J.-M. Mazin (Eds.). Evolution and Palaeobiology of Pterosaurs. *Geological Society Special Publication*, **217**: 139–190.
- Unwin D.M. and Bakhurina N.N. 2000.** Pterosaurs from Russia, Middle Asia and Mongolia. In: M.J. Benton, M.A. Shishkin, D.M. Unwin and E.N. Kurochkin (Eds.). The Age of Dinosaurs in Russia and Mongolia. Cambridge, Cambridge University Press: 420–433.
- Unwin D.M. and Lü J.-C. 1997.** On *Zhejiangopterus* and the relationships of pterodactyloid pterosaurs. *Historical Biology*, **12**: 199–210.
- Unwin D.M., Bakhurina N.N., Lockley M.G., Manabe M. and Lü J.-C. 1997.** Pterosaurs from Asia. *Paleontological Society of Korea Special Publication*, **2**: 43–65.
- Wang X.-L., Kellner A.W.A., Zhou Z. and Campos D.A. 2005.** Pterosaur diversity and faunal turnover in Cretaceous terrestrial ecosystems in China. *Nature*, **437**: 875–879.
- Wang X., Kellner A.W.A., Jiang S. and Meng X. 2009.** An unusual long-tailed pterosaur with elongated neck from western Liaoning of China. *Anais da Academia Brasileira de Ciencias*, **81**: 793–812.
- Watabe M., Tsuihiji T., Suzuki D. and Tsogtbaatar K. 2009.** The first discovery of pterosaurs from the Upper Cretaceous of Mongolia. *Acta Palaeontologica Polonica*, **54**: 231–242.
- Wellnhofer P. 1970.** Die Pterodactyloidea (Pterosauria) der Oberjura-Plattenkalke Süddeutschlands. *Abhandlungen der Bayerische Akademie der Wissenschaften, Mathematisch-Naturwissenschaftliche Klasse, Neue Folge*, **141**: 1–135.
- Wellnhofer P. 1980.** Flugsaurierreste aus der Gosau-Kreide von Muthmannsdorf (Niederösterreich) – ein Beitrag zur Kierfermechanik der Pterosaurier. *Mitteilungen der Bayerischen Staatssammlung für Paläontologie und historische Geologie*, **20**: 95–112.
- Wellnhofer P. 1985.** Neue Pterosaurier aus der Santana-Formation (Apt) der Chapada do Araripe, Brasilien. *Palaeontographica, Abteilung A: Paläozoologie, Stratigraphie*, **187**: 105–182.

- Wellnhofer P. 1991a.** Weitere Pterosaurierfunde aus der Santana-Formation (Apt) der Chapada do Araripe, Brasilien. *Palaeontographica, Abteilung A: Paläozoologie, Stratigraphie*, **215**: 43–101.
- Wellnhofer P. 1991b.** The Illustrated Encyclopedia of Pterosaurs. Salamander Books, London. 192 p.
- Wellnhofer P. and Buffetaut E. 1999.** Pterosaur remains from the Cretaceous of Morocco. *Paläontologische Zeitschrift*, **73**: 133–142.
- Wiffen J. and Molnar R.E. 1988.** First pterosaur from New Zealand. *Alcheringa*, **12**: 53–59.
- Witton M.P. 2009.** A new species of *Tupuxuara* (Thalassodromidae, Azhdarchoidea) from the Lower Cretaceous Santana Formation of Brazil, with a note on the nomenclature of Thalassodromidae. *Cretaceous Research*, **30**: 1293–1300.
- Witton M.P., Martill D.M. and Green M. 2009.** On pterodactyloid diversity in the British Wealden (Lower Cretaceous) and a reappraisal of “*Palaeornis*” *cliftii* Mantell, 1844. *Cretaceous Research*, **30**: 676–686.
- Witton M.P. and Naish D. 2008.** A reappraisal of azhdarchoid pterosaur functional morphology and paleoecology. *PLoS ONE*, **3**: e2271.

Submitted June 3, 2010; accepted September 10, 2010.